Available online at www.sciencedirect.com

ScienceDirect

Procedia Engineering 00 (2017) 000–000

Procedia Engineering

www.elsevier.com/locate/procedia

Sustainable Civil Engineering Structures and Construction Materials, SCESCM 2016

Next generation wireless smart sensors toward sustainable civil infrastructure

B.F. Spencer, Jr.[a,*], J-W. Park[a], K.A. Mechitov,[b] H. Jo[c], G. Agha[b]

[a]*Department of Civil and Environmental Engineering, University of Illinois at Urbana-Champaign, Urbana, IL, 61801, USA*
[b]*Department of Computer Science, University of Illinois at Urbana-Champaign, Urbana, IL, 61801, USA*
[c]*Department of Civil Engineering and Engineering Mechanics, University of Arizona, Tucson, AZ, 85721, USA*

Abstract

This paper presents the recent development of a next-generation wireless smart sensor (WSS) platform to enable a more accurate, inexpensive, and greatly simplified method of instrumenting structures for structural health monitoring. The modular hardware platform features a 24-bit high-precision, analog-to-digital converter with eight differential channels of analog input, and programmable antialiasing filters. The node can measure: (i) three-axes of acceleration for global response monitoring (ii) strain for local response monitoring, (iii) temperature, and (iv) high-level voltage signals from external sensors, providing the multi-scale sensed information needed for advanced structural health monitoring (SHM). Communication with a power-optimized ZigBee radio can be achieved at distances of up to 1 km. An extensible, actor-based software framework facilitates the creation of distributed SHM applications. The framework employs a service-oriented architecture (SOA) approach and provides a suite of modular, reusable, and extensible middleware services suitable for WSS applications. This platform addresses critical SHM needs, enabling tightly synchronized sensing, addressing data loss, and efficiently implementing the demanding numerical algorithms required for system identification and damage detection on sensor nodes with limited resources.

Peer-review under responsibility of the organizing committee of SCESCM 2016.

Keywords: wireless sensor; smart sensor; xnode; structural health monitoring

1. Introduction

Structural health monitoring (SHM), combining various sensing technologies with data acquisition and processing capability, plays a pivotal role in assessing the condition of structures. The ability to continuously monitor the integrity

* Corresponding author. Tel.: +1-217-333-8630.
E-mail address: bfs@illlinois.edu

Peer-review under responsibility of the organizing committee of SCESCM 2016.

of structures in real-time can provide for increased safety to the public, particularly for the aging structures in widespread use today. The ability to detect damage at an early stage can reduce the costs and down-time associated with repair of critical damage. Observing and/or predicting the onset of dangerous structural behavior, such as flutter in bridges, can allow for advance warning of such behavior and commencement of mitigating control or removal of the structure from service for the protection of human life. In addition to monitoring long-term degradation, assessment of structural integrity after catastrophic events, such as earthquakes, hurricanes, tornados, or fires, is vital. These assessments can be a significant expense (both in time and money), as was seen after the 1994 Northridge earthquake with the sheer number of buildings that needed to have the moment-resisting connections inspected. Additionally, structures internally, but not obviously, damaged in an earthquake may be in great danger of collapse during aftershocks; structural integrity assessment can help to identify such structures to enable evacuation of building occupants and contents prior to aftershocks. Furthermore, after natural disasters, it is imperative that emergency facilities and evacuation routes, including bridges and highways, be assessed for safety. Addressing these issues is the goal of SHM.

Visual inspection has been the common practice in inspecting and monitoring the condition of civil infrastructures. However, cost often prohibits the use of visual inspection to infrequent occurrences. Wired sensor-based monitoring systems have long been the most common supplement to inspections; however, realizations of such wired systems are limited by the high cost of instrumentation and maintenance due to cabling; scalability is the main issues that limits the use of wired based system in larger and more complex structures. For instance, the total cost of the monitoring system on the Bill Emerson Memorial Bridge in Cape Girardeau, Missouri was approximately $1.3 million for 86 accelerometers, which makes the average installed cost per sensor a little more than $15,000; this cost is not atypical of today's wired SHM systems [1].

Wireless smart sensors are an attractive alternative, differing from traditional wired sensors in a number of significant ways. For example, each WSS node communicates wirelessly, eliminating the need for costly cabling. Moreover, each node has an on-board microprocessor that can be used for digital signal processing, self-diagnosis, self-calibration, self-identification, and self-adaptation functions. Sensor can be easily deployed, moved, and replaced after initial instrumentation of the system.

Researchers have made continuous efforts to develop a series of wireless or smart sensor platforms to facilitate structural health monitoring [2]. Wireless sensors have been commercially available for over a decade; however, only a limited number of full-scale implementations have been realized, primarily due to the lack of critical hardware and software elements. One example of full-scale deployment was a wireless sensor network implemented on the Golden Gate Bridge in 2008, which had issues with scalability of the network; it took approximately 10 hours to collect 80 seconds of data (sampled at 1000 Hz) from 56 sensor nodes to a central location [3]. On the hardware side, the developed sensor node was only able to measure acceleration data out of available measurands such as strain and wind data that are necessary for integrated structural health monitoring of the bridge. To address these issues, researchers at the University of Illinois built upon the Imote2 platform, overcoming numerous hardware and software hurdles. These developments were showcased in a US-Korea-Japan collaboration that deployed the world's largest wireless smart sensor network to monitor the 2nd Jindo Bridge in South Korea [4, 5]. Unfortunately, the Imote2 is no longer in production.

This paper presents the recent development of the Xnode, a next-generation wireless smart sensor (WSS) platform to enable a more accurate, inexpensive, and greatly simplified method of instrumenting structures for structural health monitoring. This platform addresses critical SHM needs, enabling tightly synchronized sensing, addressing data loss, and efficiently implementing the demanding numerical algorithms required for system identification and damage detection on sensor nodes with limited resources.

2. Experience and lessons learned from the 2nd Jindo Bridge deployment

This section briefly summarizes the 2nd Jindo Bridge deployment and discusses the key lessons learned from that experience. First the necessary hardware and software developments are discussed. Subsequently, the full-scale deployment and results are presented. In-depth reports of the deployment and the design of the hardware and software framework are found in Refs. [4, 5].

2.1. Hardware Development

A wireless sensor platform designed for data-intensive applications, Intel's Imote2, was selected for this effort, due to its high-performance Xscale processor (PXA27x) ranging from 13 to 416 MHz and relatively large memory size of 32 MB FLASH, and 32 MB SDRAM; such large RAM enables the on-board computations and serves as storage of long-term measurements. Sensing with the Imote2 is facilitated by sensor board(s) stacked on the Imote2 via two board-to-board connectors. To measure various responses such as acceleration, strain and wind speed to accurately identify structural condition of the bridge, several types of sensor boards were developed (see Fig. 1); the SHM-A board and SHM-H boards were developed to measure acceleration and high-precision acceleration response of the bridge; SHM-S board was developed to measure strain response; SHM-DAQ board was developed to measure analog sensor signal and connected to anemometer to acquire wind information at the bridge site.

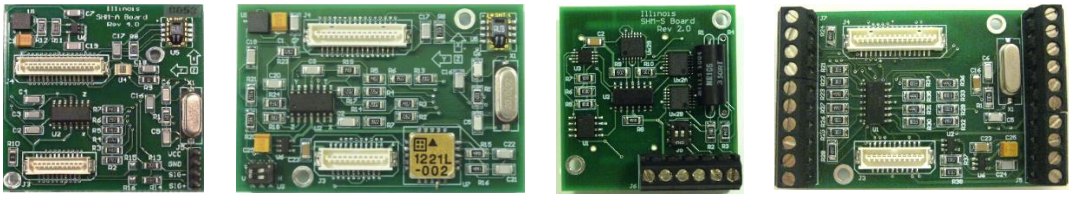

(a) SHM-A (b) SHM-H (c) SHM-S (d) SHM-DAQ

Fig. 1. Developed sensor boards: (a) 3-axis acceleration, (b) high-precision acceleration, (c) strain, (d) analog data acquisition.

2.2. Software Development

The Illinois Structural Health Monitoring Project (ISHMP) Services Toolsuite, developed through collaboration between researchers in Smart Structures Technology Laboratory and Open Systems Laboratory at University of Illinois at Urbana-Champaign, is the software foundation for the Imote2-based remote sensing functionality deployed at the 2nd Jindo Bridge. With the Toolsuite, these powerful nodes can achieve highly-synchronized data collection, aggregation, synthesis, and decision-making in real time. The distributed application coordinated scheduled and event-triggered data acquisition, power management, and network monitoring and maintenance functionalities. Because SHM applications for WSSNs require complex programming, ranging from network functionality to embedded algorithm implementation, software development in this environment is very difficult, exacerbated by the fact that many different sensor platforms exist with their own special-purpose operating systems and applications. The service-oriented architecture of the Illinois SHM Toolsuite is based on the actor model [9] to support concurrency and distribution. This facilitates application development by enabling the composition of middleware services and application code to be selected to fulfill the specific requirements of a particular deployment.

2.3. Full-scale Deployment and Results

The first autonomous, full-scale wireless bridge monitoring system was initially installed on the second Jindo Bridge in South Korea in 2009 through a joint effort among the University of Illinois at Urbana-Champaign, the Korea Advanced Institute of Science and Technology (KAIST), and the University of Tokyo. The 2nd Jindo Bridge is a cable-stayed bridge connecting the Korean peninsula and the Jindo Island. The bridge consists of steel box girder with a center span of 344 m and 60 parallel wire strand cables (see Fig. 2).

The monitoring system comprised 113 WSS nodes measuring a total of 659 channels of data by 2010, resulting in the world's largest wireless smart sensor network for dynamic bridge SHM. The SHM-A sensor board was used on 100 nodes. A SHM-H board, which enables measurement of accelerations as low as 0.05mg, was used for 10 nodes. The remaining three nodes were connected to 3D ultrasonic anemometers to measure and collect wirelessly the speed and direction of wind on the bridge. Wireless strain measurements were also available using the SHM-S sensor board. All 113 nodes were self–powered using solar or wind energy harvesting. Should any anomalies in the measured data

be detected during the autonomous system operation, the base-station computers automatically email the research team so that appropriate action can be taken.

Fig. 2. Jindo Bridge, Jindo, South Korea.

The monitoring system can estimate the bridge's various physical states. For example, as depicted in Fig. 3, the modal properties such as natural frequencies, mode shapes, and modal damping ratios can be extracted from the measured accelerations and used to refine the numerical model to determine structural performance and find possible damage locations. Cable tension force, one of the most important integrity measures for cable-stayed bridges, is estimated automatically using a vibration-based method.

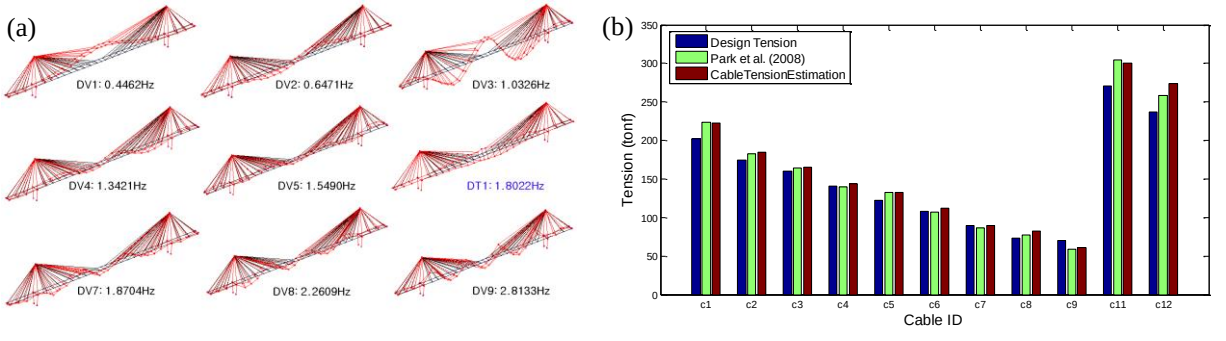

Fig. 3. Monitoring results: (a) mode shapes and natural frequencies; (b) cable tension estimation.

The Imote2 wireless sensor platform, coupled with the various SHM sensor boards developed at the University of Illinois and powered by the Illinois SHM Toolsuite software, has been a significant enabler of research on wireless sensor-based structural health monitoring. The hardware and software platforms, developed in part for the 2nd Jindo Bridge deployment, have been later utilized by over 70 research groups in 15 countries.

2.4. Lessons Learned

The experience of deploying a large network of wireless sensor for monitoring cable-stayed bridge taught the research team several important lessons:

1. *Fidelity of data acquisition.* The data acquisition capability is limited by the analog-to-digital converter's (ADC) minimum resolution, available sampling rate, and measurement synchronization. Measuring low-level ambient vibrations using existing wireless smart sensors can be particularly challenging, so a high-resolution ADC is required (e.g., 24-bit). Another issue is sampling rate. SHM can often be categorized in to consist of

two types of responses: static and dynamic. Static responses vary slowly in time, requiring low-sampling rates (e.g.,1 Hz); temperature, humidity, light, crack depth, compass orientation, etc. are in the domain of static measurements. On the other hand, dynamic measurement require sampling at a high rate (e.g., 100 Hz). Examples of dynamic responses are acceleration, strain, wind velocity, tilt etc. The sampling rate for dynamic responses must be at least twice the largest frequency of interest. To ensure signal integrity, high-quality anti-aliasing filters must be used for dynamic measurements. Moreover, the measurements must be tightly synchronized, which is a difficult task, as each wireless sensor has its own local clock. For example, a 1 ms synchronization error between two measured acceleration responses will result in 3.6 degree error in the phase angle at 10 Hz and 36 degree error at 100 Hz [6], which can be identified falsely as damage.

2. *Reliable Communication.* Many issues intrinsic to the wireless sensor must be addressed to ensure reliable communication. Wireless communication is not reliable unless lost packets are properly transmitted and tracked. The performance of wireless communication is not only affected by the distance between nodes, but also network environment. For example, when multiple nodes are trying to send packets at the same time, the packets collide and are lost during communication. Packet loss may degrade measurement signals because it interferes with acquiring accurate data acquisition.

3. *Power Management.* Power management is not an issue in a traditional wired sensor implementation; the sensors can remain active at all times and thus have the ability to be interrogated at any time to acquire data. Unlike such wired systems, one of the most critical features of a successful wireless sensor deployment is the implementation of careful power management. Energy saving can be implemented by imposing duty cycle (i.e., sleep and wake) allows the sensor network to sleep most of the time. In SHM for civil infrastructures, energy harvesting through a solar panel and wind power can be employed to extend the operational life of wireless sensor network. Energy saving and harvesting should be balanced to achieve long-term full-scale deployment.

4. *Data Management.* The management of data collected from a WSS network is critical, given that each sensor node acquires large amounts of data. For example, four channels of 16-bit data are collected at 100 Hz for an hour take 3MB of memory. If tens or hundreds of sensor nodes have to send the data to the base station, data inundation can occur. Note that the time for data acquisition and transmission is heavily dependent on the sampling rate, measurement time, size of network, number of bits on ADC and channels. Data aggregation that processes raw measurement into useful information (e.g., acceleration into displacement/cable tension) is necessary to manage such data challenges.

These lessons inform the development of the next-generation WSSN platform for civil infrastructure monitoring.

3. Design of the next-generation wireless smart sensor platform

This section describes the design and development of the Xnode Smart Sensor. The section first introduces overall design philosophy and then describes hardware and software framework enabling its implementation.

3.1 Design Philosophy

The primary motivation for developing a next generation wireless sensor system was to provide powerful hardware and a robust software framework for both campaign-style and long-term SHM. The hardware must have high-resolution (24 bit) and high sampling rate (>10 kHz) data acquisition, a power microprocessor suitable for high data throughput applications and data aggregation, and an RF transceiver that allows for long-range (up to 1 km) and reliable communication. In terms of the software framework, a middleware service-oriented framework that supports network and application scalability (e.g., data collection protocol, time synchronization, etc.), software packages that incorporate libraries for hardware and data processing (e.g., sensor driver, numerical tools, SHM algorithm, etc.), and a user-friendly interface are required. For the next-generation sensor to be deployed on full-scale structures,

autonomous network operation, a maintenance-friendly environment such as over-the-air programming, automatic report generation of faults, and power management should be considered.

Aligning with these requirements, the Xnode has been developed as a next-generation wireless platform for structural monitoring applications. Table 1 show the comparison of the Xnode with other wireless sensor platforms in terms of hardware.

Table 1. Comparison of selected wireless sensor platforms [7].

Platform	Maximum Processor Frequency	Expandable Data Storage	Radio Range	ADC Resolution (bits)	Number of Sensing Channels	Sampling Rate	Energy Harvesting
WaspMote [13]	14	2GB	7 km	-	7	-	X
Microstrain [14]	N/A	-	2 km	16	7	1kHz	X
iMote2 [12]	416	-	300 m	-	-	-	-
Martlet [10, 11]	80	32GB	>500 m	12	9	3kHz	X
Xnode	204	4GB	1 km	24	8	16kHz	X

3.1. Xnode Hardware

The Xnode consists of three boards which are the process board, radio/power (RP) board and the sensor board. The processor board, the mini4357 developed by Embest Technology, features an LPC4357 microcontroller from NXP that operates with ARM Cortex M0/M4 microcontroller at frequencies up to 204MHz, which can be used to execute on-board computation and data acquisition. The non-volatile memory available on the mini4357 is 32 MB of SDRAM, in which is used for temporary data storage and processing. The mini4357 has various general purpose input/output (GPIO) pins and interfaces such as serial peripheral interface (SPI) and inter-integrated circuit (I2C).

To extend the data storage size for high sampling application, the SD card can be plugged into the RP board that provides extensible storage space of several GB. The RP board includes a power management circuit that controls charging from wall power and solar panels. The radio transceiver in the RP board is a 2.4 GHz radio for low-power wireless communication (Atmel AT86RF233). The communication reaches up to 1km line-of-sight with maximum transfer rates of 250 kbps.

The sensor board shown in Fig. 4 employs a 24-bit ADC (Texas Instruments ADS131E8) which has 8 channels allowing maximum sampling rate up to 16 kHz. In terms of sensing, the 3-axis analog accelerometer (LIS344ALH) takes 3 channels, leaving up to 5 channels available for external analog sensors. Built-in strain circuitry is provided to accommodate up to 3 channels of strain sensing; the measured electrical signal is easily converted into strain through embedded shunt calibration.

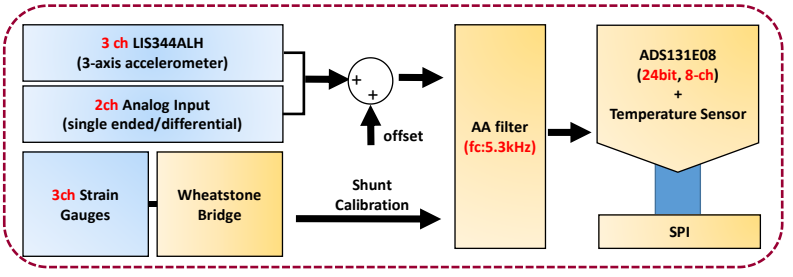

Fig. 4. Schematic for the Xnode sensor board.

The MEMS accelerometer has selectable range setup for ±2g and ±6g with noise density of 50 ug/$\sqrt{\text{Hz}}$. The analog input is added with signal offset such that the resulting signal stays within 0-3.3V range. Strain gauges are connected to the sensor board through external connector, and the resulting differential signal is directly fed through the ADC. All analog signals are AA filtered to reject undesirable high-frequency component. The ADC transfer 8-ch of data through SPI communication with LPC4357.

The developed hardware is stacked together to comprise an integrated sensor node. The sensor node is packaged in an IP67 environmentally hardened enclosure (see Fig. 5). Through the connectors on either side of the enclosure, solar panel, wall-power, and external sensors can be easily plugged.

Preliminary Initial testing shows that the 24-bit ADC can achieve a dynamic range of 140 dB (ENOB: 21.1).

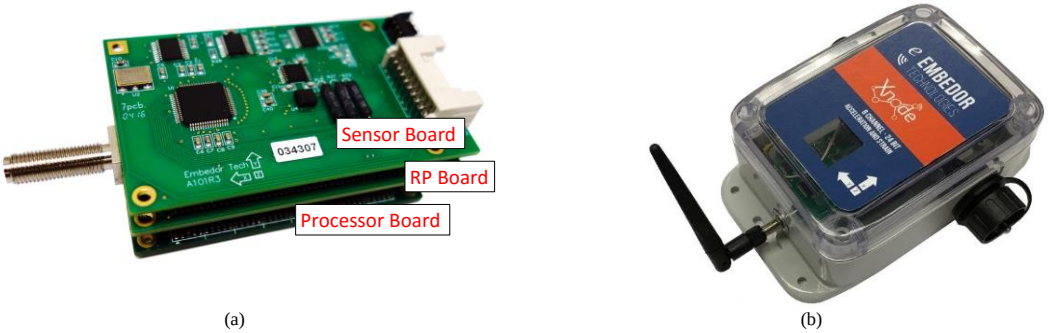

(a) (b)

Fig. 5. Xnode Smart Sensor: (a) stacked modular boards; (b) weather-proof enclosure.

3.2. Xnode Software

The emergence of wireless smart sensor platforms with powerful computational capabilities has enabled wireless SHM applications; however, as the demands of wireless SHM systems increase, certain properties of event-driven operating systems for these sensor nodes, such as the TinyOS operating system of the Imote2, have begun to impose limitations on the development of SHM systems. The problematic characteristics include static resource allocation, single-application focus, lack of real-time scheduling support, and dependence on a non-standard programming language. To address these limitations, the Xnode has been developed based on a real-time operating system (FreeRTOS), commonly used for industrial control systems and similar applications.

One key benefit of the Xnode software platform is the more flexible application framework. Moving to this new platform enables several benefits for users compared to the Imote2 (TinyOS-based system), mainly due to the availability of a real-time scheduler. FreeRTOS provides a priority-based preemptive scheduler, as well as inter-task communication and coordination tools (e.g., queues, mutexes, and semaphores). It can efficiently address the limitations of event-driven operating systems on low-power microprocessors. In particular, long-running, low-priority tasks can no longer block important function such as sensor sampling and radio communication (see Fig. 6).

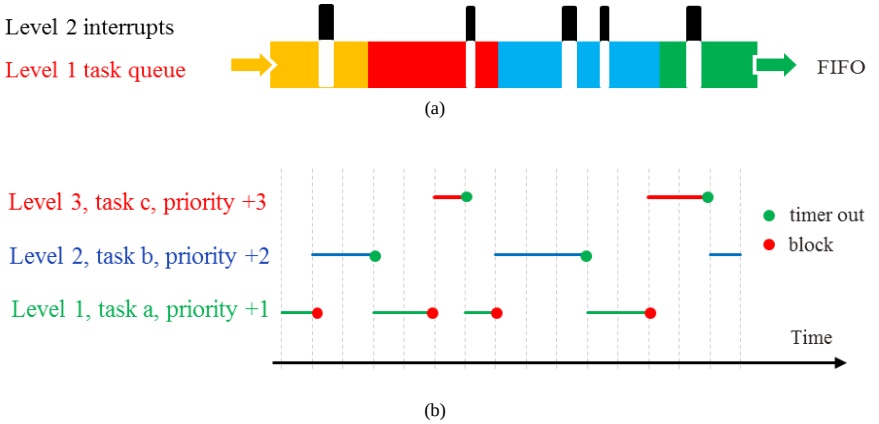

Fig. 6. Comparison of task scheduling behavior in (a) TinyOS and (b) FreeRTOS [8].

The Xnode retains the successful SOA-based middleware functionality of the Illinois SHM Toolsuite, allowing the rapid development of application functionality based on composing the available middleware modules for

fundamental WSSN functionalities (synchronized sensing, reliable communication, time synchronization, power management, etc.), as well as application-level services specific to SHM (cable tension estimation, system identification, modal analysis, etc.). Fig. 7 shows the outline of the implementation of the RemoteSensing application providing synchronized distributed data acquisition over the WSSN.

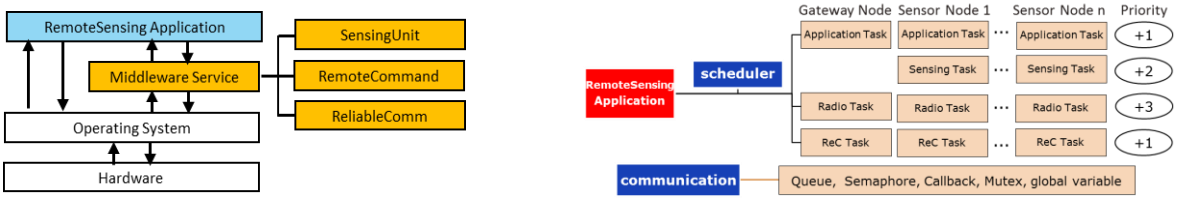

Fig. 7. Outline of the RemoteSensing application structure and its implementation in FreeRTOS [8].

Based on the experience of the Jindo Bridge deployment in the Imote2/TinyOS-based environment, the Xnode platform takes effort to be more open and standardized for easier development and interoperation with other software and hardware platforms. The standard C language is used for application development, in place of a custom nesC variant, which allows for much simpler portability of applications with the Xnode platform. Many libraries and numerical algorithms implemented in C can be used directly, without modification, in the Xnode code. Additionally, the radio communication is based on the IPv6 protocol stack, widely adopted by the Internet of Things (IoT) community, opening the door to potential integration of heterogeneous devices inside a single WSSN.

4. Discussion

As a wireless sensor platform, the Xnode Smart Sensor is clearly differentiated from other available platforms in its capabilities and intended uses. Similar to the Imote2, the Xnode supports high-fidelity, high-sampling rate applications requiring precise synchronization among hundreds of sensor channels. Combined with the Illinois SHM Toolsuite, the Xnode is a research enabler across a range of civil engineering applications and use cases that are currently difficult to implement due to insufficient resolution of available ADCs, lack of software support, and/or the complexity of implementing low-power distributed embedded systems.

With the emergence of IoT technologies, the availability of more standardized hardware, network protocols, and software interfaces promise that the near future will bring the possibility of heterogeneous WSSNs, combining different sensor platforms in a single deployment. Such deployments will be able to take advantage of the unique features of different WSS platforms, such as power efficiency, processing capability, ADC resolution, and sensor selection on an as-needed basis to fit the requirements of a particular monitoring deployment. The Xnode takes the first steps on this path by utilizing a standardized network protocol stack and providing open APIs to its middleware services.

The unique high-fidelity synchronized distributed sensing capabilities of the Xnode also provide a cost-effective alternative to wired data acquisition systems for structural health monitoring. Previous wireless platforms lacked either ADC resolution, communication range, or network scalability to serve as a viable replacement for wired systems. Considering that a large portion of the wired monitoring system cost results from the cabling between the sensors and the data acquisition system, wireless sensors are an attractive alternative, especially for large civil structures, offering the potential for low-cost, continuous, and reliable SHM.

5. Conclusion

This paper discussed the motivation and primary design philosophy for the development of a next-generation wireless smart sensor platform intended for high-fidelity dynamic structural health monitoring applications. Various hardware and software issues are taken into account based on the lessons learned from recent efforts to develop, stabilize, and operate full-scale wireless smart sensor networks for SHM of civil infrastructure. High-fidelity, multi-

scale responses can now be captured by the Xnode Smart Sensor platform with a synchronized, distributed data acquisition application that can also be extended to perform in-network data processing and analysis. The Xnode takes steps to increase the standardization of the WSSN environment for SHM applications, which up to now has been fragmented and reliant on systems focused solely on a single platform or even a single deployment. However, much work remains to be done to integrate and standardize the various WSSN-based solutions developed by the community.

References

[1] Celebi, M., Purvis, R., Hartnagel, B., Gupta, S., Clogston, P., Yen, P., O'Connor, J. and Franke, M. (2004). Seismic instrumentation of the Bill Emerson Memorial Mississippi River Bridge at Cape Girardeau (MO): A cooperative effort, Proceedings of the 4th International Seismic Highway Conference, Memphis, Tenn, USA.

[2] Spencer Jr., B.F., Ruiz-Sandoval, M & Kurata, N. (2004), Smart sensing technology: opportunities and challenges, Structural Control and Health Monitoring 11, 349-368.

[3] Pakzad, S.N., Fenves, G.L., Kim, S., Culler, D.E., (2008), Design and Implementation of Scalable Wireless Sensor Network for Structural Monitoring, ASCE Journal of Infrastructure Engineering, 14(1): 89-101.

[4] Rice, J.A., Mechitov, K., Sim, S.H., Nagayama T., Jang S., Kim R., Spencer B.F., Agha G., Fujino Y., (2010). Flexible smart sensor framework for autonomous structural health monitoring, Smart Structures and Systems 6(5–6): 423-438.

[5] Jang S, Jo H, Cho S, Mechitov K, Rice JA, Sim SH, Jung HJ, Yun CB, Spencer BF, Agha G. (2010). Structural health monitoring of a cable-stayed bridge using smart sensor technology: Deployment and evaluation. Smart Structures and Systems 6(5–6): 439–459.

[6] Nagayama, T. and Spencer Jr, B.F. (2007). Structural health monitoring using smart sensors. Newmark Structural Engineering Laboratory Report. University of Illinois at Urbana-Champaign.

[7] Rodenas-Herraiz, D., Soga, K., Fidler P., and de Battista, N. (2016). Wireless Sensor Networks for Civil Infrastructure Monitoring – A Best Practice Guide. ICE Publishing. ISBN: 978-0-7277-6151-4.

[8] Fu, Y.G., Mechitov, K.A., Hoskere, V., Spencer, Jr., B.F. (2016). Development of RTOS-based wireless SHM system: benefits in applications. International Conference on Smart Infrastructure and Construction. Cambridge, UK.

[9] Agha, G. (1986). Actors: A Model of Concurrent Computation in Distributed Systems, MIT Press.

[10] Dong, X., Zhu, D., Wang, Y., Lynch, J.P., and Swartz, R.A. (2014) Design and Validation of Acceleration Measurement Using the Martlet Wireless Sensing System, ASME 2014 Conference on Smart Materials, Adaptive Structures and Intelligent Systems, Newport, RI, USA.

[11] Kane, M., Zhu, D., Hirose, M., Dong, X., Winter, B., Häckell, M., Lynch, J.P., Wang, Y., Swartz, A. (2014). Development of an extensible dual-core wireless sensing node for cyber-physical systems. Proc. SPIE 9061, Sensors and Smart Structures Technologies for Civil, Mechanical, and Aerospace Systems.

[12] Nachman, L., Huang, J., Shahabdeen, J., Adler, R. and Kling, R. (2008). Imote2: Serious computation at the edge. International Wireless Communications and Mobile Computing Conference, 1118-1123.

[13] Libelium (2016). WaspMote. http://www.libelium.com/products/waspmote/

[14] MicroStrain (2015). V-Link-LXRS Datasheet. http://www.microstrain.com/wireless/v-link

Available online at www.sciencedirect.com

ScienceDirect

Procedia Engineering 00 (2017) 000–000

Procedia Engineering

www.elsevier.com/locate/procedia

Sustainable Civil Engineering Structures and Construction Materials, SCESCM 2016

Sustainable construction for Singapore's urban infrastructure – some research findings

Khim Chye Gary Ong[a,*]

[a]*Department of Civil and Environmental Engineering, National Univeristy of Singapore, Singapore*

Abstract

Many cities around the world can afford the old model of urban sprawl, where the city boundary grows outwards. However, in small city states like Singapore, evolving the city of the future will be very different. Singapore requires development of holistic sustainable technologies and solutions for sustainable infrastructure to meet future social and economic needs. This includes adopting building designs, construction methods and materials that are environmentally-friendly, as well as using materials and resources that have sustainable supplies. A brief update of some research findings to address Singapore's infrastructural sustainability needs is presented.

Peer-review under responsibility of the organizing committee of SCESCM 2016.

Keywords: Sustanable; construction; urban; infrastructure; microwave-assisted beneficiation, design for disassembly.

1. Introduction

More than half the world lives in cities and this is expected to grow. Many cities can afford the old model of urban sprawl, where the city boundary grows outwards. However, in city states like Singapore, evolving a city of the future will be very different. Singapore as a city state with virtually no natural resources has unique needs to be met in developing a holistic model and infrastructural solutions for future sustainable urban development. This includes adopting building designs, construction methods and materials that are environmentally-friendly, as well as using materials and resources that have sustainable supplies.

* Corresponding author. Tel.: +65-6516-2169; fax: +65-6779-1635.
E-mail address: ceeongkc@nus.edu.sg

Peer-review under responsibility of the organizing committee of SCESCM 2016.

Research on sustainable infrastructural development in Singapore is on-going. A number of interesting projects are targeted at developing sustainable solutions to meet challenges, unique to Singapore. One such project involves using microwaves to increase the yield and quality of recycled materials. This novel technique utilizes microwave heating to separate the components of recycled concrete aggregate (RCA) for reuse. Heating causes the cementitious mortar adhering to the surface of the RCA particles, to delaminate from the granitic aggregates. Another project briefly described in this paper involves partnering the Housing Development Board, to design high-rise buildings that, like building blocks, can be disassembled and re-used. Such work aims to provide a sustainable supply of construction materials available locally, which can reduce over-reliance on imported sand and aggregates.

2. Microwave-assisted beneficiation of recycled aggregate concrete

The use of recycled aggregates in structural applications is limited due to the presence of adhering cementitious mortar on the individual recycled aggregate particles. The adhering mortar has been reported to result in higher porosity, higher water absorption, lower modulus of elasticity and weaker interfacial zone (ITZ) between the newly cast cementitious mortar and the recycled aggregates [1, 2, 3]. The microwave-assisted beneficiation method takes advantage of the differences between the electromagnetic and thermal properties [4, 5, 6] of the coarse aggregate, granite, and adhering cementitious mortar to cause delamination at the ITZ, separating the granitic aggregate from the adhering cementitious mortar. The results of both experimental and analytical studies show that microwave heating is effective in increasing the yield and quality of the recycled concrete aggregates compared to more traditional methods of recycling [4, 5, 6].

2.1. Analytical results

Analytical modeling was used for the microwave-assisted beneficiation system shown in Fig. 1. The system utilizes three frequencies 2.45, 10.6 and 18 GHz representative of the characteristics of typical low, intermediate and high frequencies together with a constant incident microwave power of 1.1 MW /m^2. Typical results obtained are presented in Fig. 2 and 3. For clarity, Fig. 2 and 3 show only the temperature developed within the first 10 cm thick surface layer of the concrete block when subjected to microwave heating. The amount of energy dissipated in the concrete specimen varies significantly with its electromagnetic properties. The electromagnetic properties of concrete are a function of factors including concrete constituent materials and mix proportions, water content, microwave frequency, temperature, etc. The significant effects of concrete water content (Fig. 2 and 3) and microwave frequency on the heating process have been confirmed [4, 5, 6].

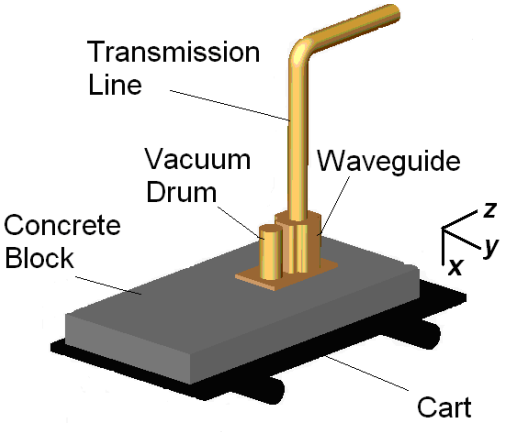

Fig. 1. Sketch of the microwave heating system

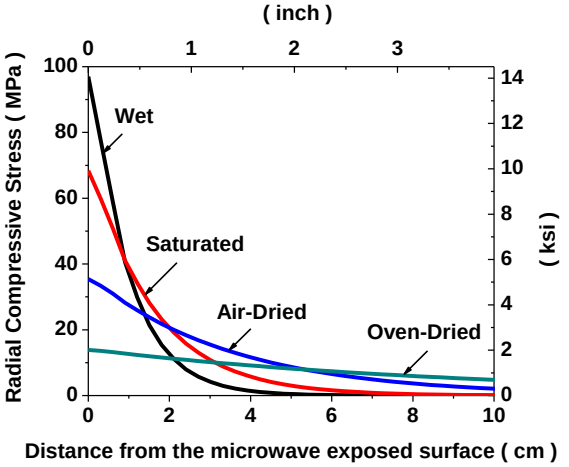

Fig. 2. Radial compressive stress in concrete after 2 seconds of microwave heating at 10.6GHz frequency

The results indicate that drenching of the concrete surface may be used to increase the efficiency of the microwave-assisted beneficiation process as considerably higher stresses confined in a thinner surface layer may be generated in a wet concrete when compared to a dry concrete [6]. However excessive amounts of water may not be desirable as energy would be unnecessarily consumed in generating steam from the surface water present. The temperature reached and the stress generated in the concrete seemed to vary proportionally with the microwave initial power and heating duration. Typical results plotted in Fig. 2 shows the thermal stress development developed within the concrete block. The results confirmed that the stresses developed were significant and sufficient to cause delamination at the concrete surface [7]. The model was expanded to study the concomitant contribution of pore pressure (Fig. 3) developed due to microwave heating until concrete surface delamination occurs.

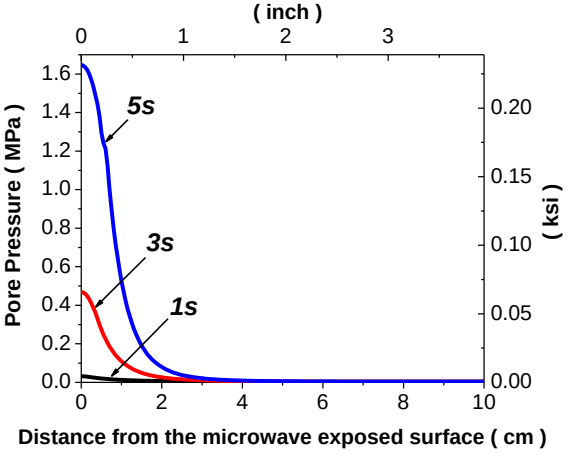

Figure 3: Pore pressure in saturated concrete after 5 seconds of microwave heating

The feasibility of the new pilot microwave assisted beneficiation system to improve the quality of RCA was investigated by modeling the temperature rise and plotting the temperature distribution in individual RCA particles when subjected to high frequency microwave heating. The particles were assumed to be spherical and typical results (Fig. 4) shows that a high temperature differential may be developed in the layer of adhering cementitious mortar, especially at the interface between the natural granite aggregate and the adhering cementitious mortar. These high temperature differentials result in high thermal stresses at the interfacial zone ITZ and thus are effectively harnessed in detaching the adhering cementitious mortar portion from the RCA. The spalling depth of the surface layer of the aggregate particle and the microwave exposure time for spalling to take place are inversely proportional to microwave frequency.

Once the adhering cementitious mortar is delaminated from the surface of RCA, the yield and quality of the resultant aggregates would improve significantly. Experimental results obtained confirmed the capability of the microwave assisted beneficiation system to remove the adhering mortar within a very short period of exposure. Fig. 5 shows samples of aggregate particles after being subjected to microwave heating. The adhering cementitious mortar detached cleanly from the granite aggregates. Light brushing is sufficient to dislodge the loosely attached mortar after microwave heating. The original surface of the granite aggregate was clearly visible (Fig. 5). The analytical results obtained yielded results which were of much use as background information for the design of a pilot microwave-assisted beneficiation facility to improve the yield and quality of RCA [7]. The processes involved can be further fine-tuned to address various decontamination, handling, production, storage and safety needs for a fully functional system to be incorporated in the actual production of RCA using this microwave-assisted beneficiation system.

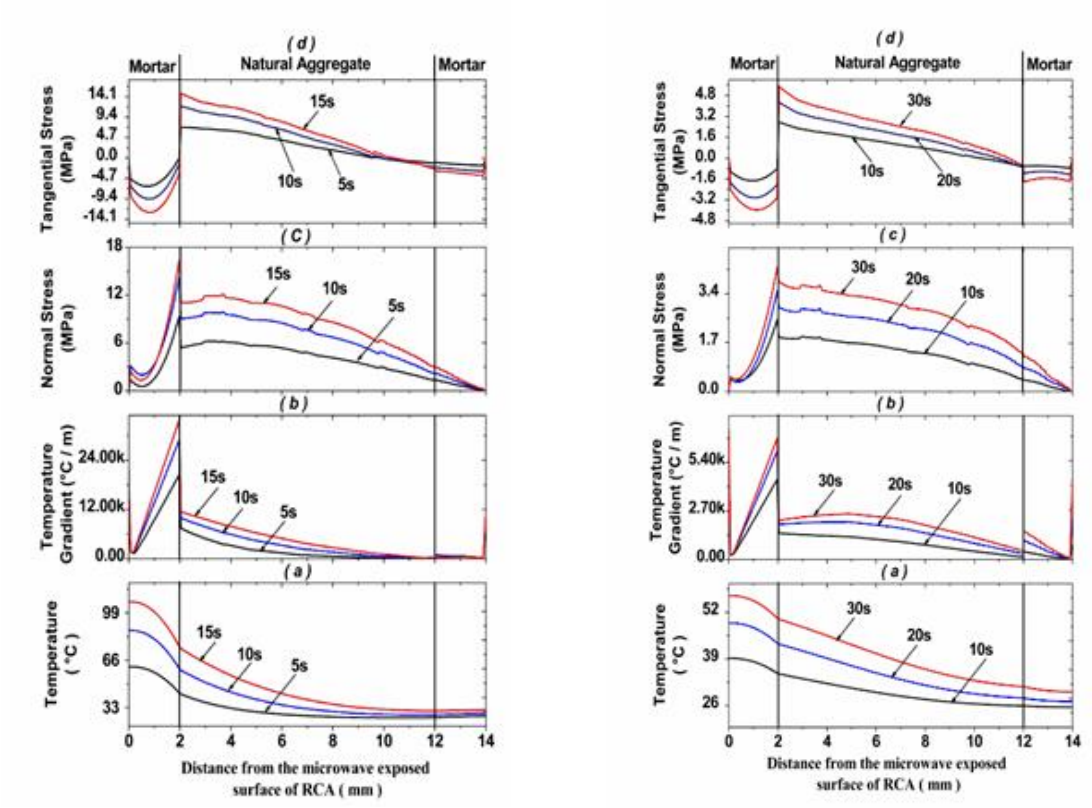

(a)Saturated RCA particle (b) Air dried RCA particle

Fig. 4 Temperature, Temperature gradient, Normal stress and tangential stress in a RCA particle subjected to microwaves of frequency 2.45 GHz and 10kW power.

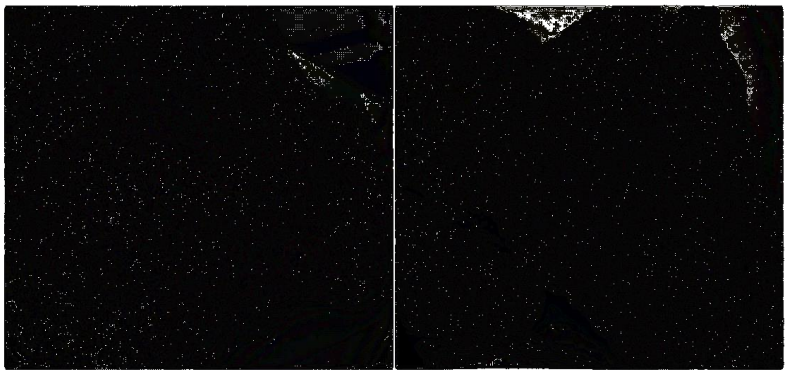

(a) Before beneficiation (b)Same particle after beneficiation

Fig. 5. Surface of RCA before and after microwave-assisted beneficiation

3. Design for Disassembly

In Singapore, older buildings are often demolished to make way for new ones, while having plenty of service life left in them. If these buildings had been designed for disassembly (DfD) their structural components could be reincarnated as component parts in the new buildings [8,9]. Currently, most of the recycled aggregates from demolition

debris are used in land reclamation, roads, and in non-structural applications, as they cannot replace fully fresh stocks of aggregates used in constructing new structures [2, 8, 9]. Additional resources are needed to produce such recycled aggregates. They have to be sorted, followed by a series of crushing, sieving and grading operations. Reuse of pre-cast concrete structural components in new buildings would take recycling a step further, by removing the need for recycling the bulk of demolition debris. Premature demolition, which generates demolition wastes for recycling and disposal, would become unnecessary. The volume of fresh stocks of construction materials imported into Singapore for building new buildings would also be reduced.

3.1 Development of DfD system (assemblies and components)

To facilitate ease of disassembly of precast structural components, several types of connection systems were designed [9, 10]. Full scale testing was conducted to study the ultimate, serviceability, and demountability performance of the proposed DfD connections. Fig. 6 illustrates schematically one example of the proposed DfD connections. Finite element simulation was also conducted to provide deeper insights on the connections' behavior and performance. Study on the deconstruction techniques to be used with the proposed precast connection was also performed with a novel pre-embedded anchor systems. The test results showed that the proposed connections registered adequate performance to be used in high rise residential buildings, typical of those found in Singapore [9, 10].

3.2 Information and management system to support DfD

One of the challenges for successfully implementing the proposed DfD system is the availability of an efficient information system. Unlike conventional precast concrete construction, keeping a permanent record of all the information with regards to DfD components and assemblies deployed in the various buildings as an asset register is critical [11]. This information must be acquired comprehensively, evaluated faithfully, and managed efficiently. It must also include information gathered when the building structure has been subjected to the legislated periodic structural assessment excercises [12]. Furthermore, it should be noted that this information system is not one that is used only before the construction of a structure, nor is it one that is just called into play right before deconstruction is carrie out. As shown in Fig. 8, it should capture information on the whole life history of each DfD structural component and sub-assembly. This means not only the capture of initial design and construction of each structural components' configurations information, but also all information pertaining to any upgrading or reconditioning works [12] carried out on each individuial component and sub-assembly during service. Sucvh information have be captured, store and made accessible for future reference for ease of management and reference [11].

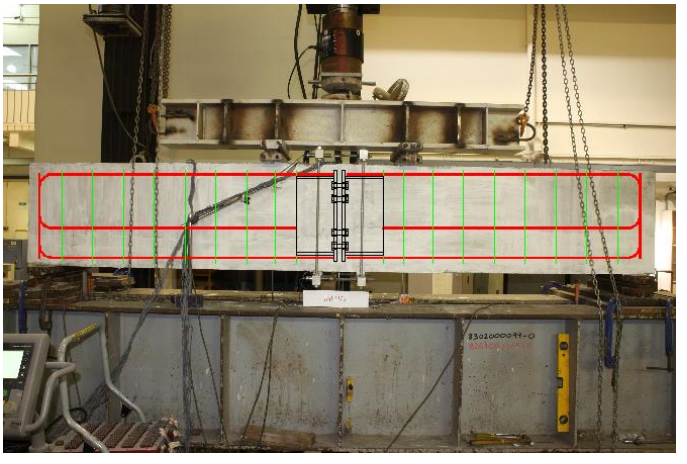

Fig. 6. Proposed DfD connection specimen under four-point-bending testing

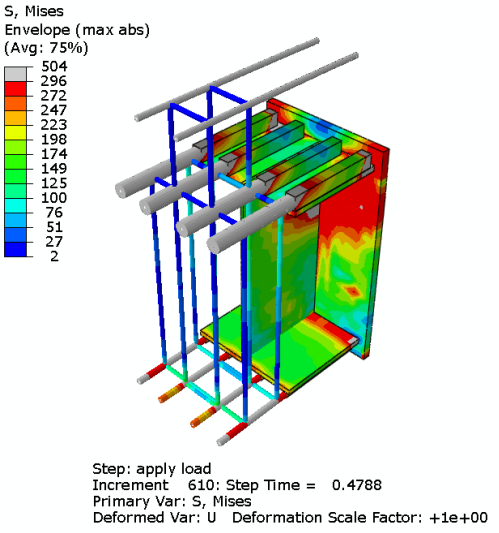

Fig. 7. Von-Mises stress contour of the main steel components present in a typical DfD connection subjected to bending moment

Extensive works have been done on the development of the proposed information management system through the use of Building Information Modelling (BIM) software. The information management system targets to contain all the relevant information of the DfD components such as geometry, materials, detailing, and annotated in a library of DfD connections. This can be used later for further optimization analyses such as carbon footprint, energy and cost analyses, as a part of the information evaluation system [11]. An sample analysis of DfD adoption is shown in Fig. 9, which compares a typical precast structure using the conventional construction method vis-à-vis using the proposed DfD system. It is realized that the incorporation of the DfD concept to a typical precast high rise residential structure at present to increase initial construction costs and embodied energy. Nevertheless, significant potential savings could be obtained when subsequent service life cycles are taken into consideration. For the example shown, cost savings of up to 42% and a reduction in the embodied energy of up to 38% could be obtained in the assumed scenario of two phases of cycles of service life.

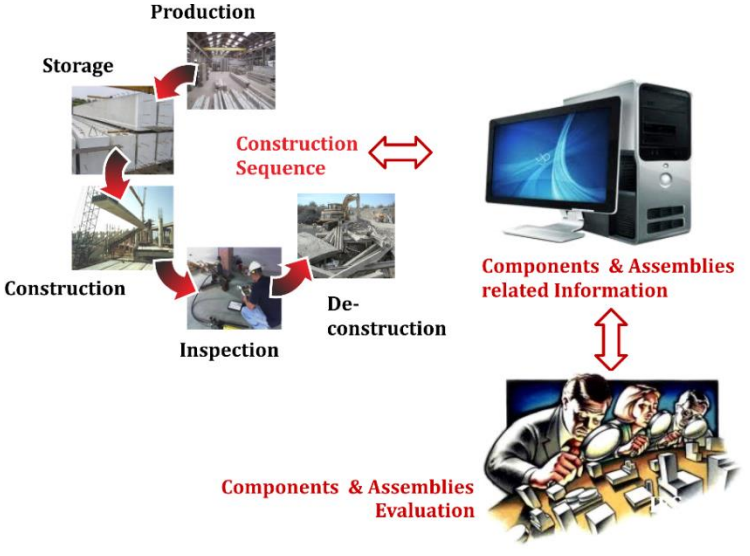

Fig. 8. DfD information and management system

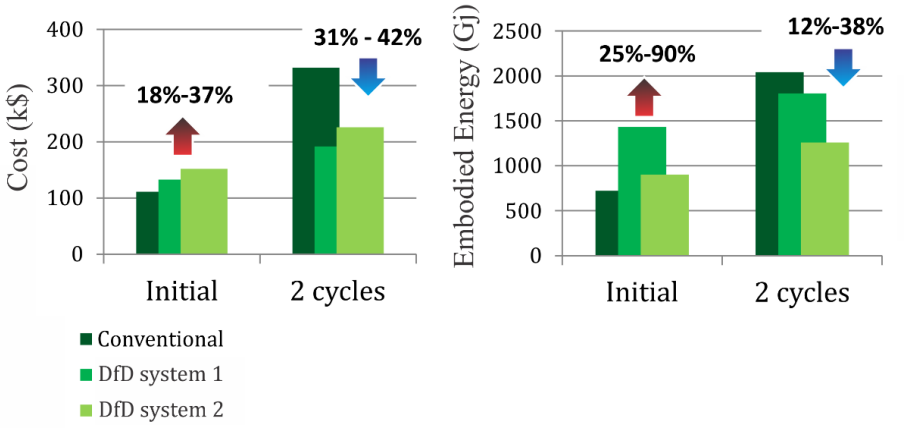

Fig. 9. Comparison of cost and energy analysis between conventional and DfD **system**

3.3 DFD Prototypes

In order to further explore and investigate the feasibility of the proposed DfD system, a half scale DfD prototype mock-up was constructed based on a typical 2-room residential unit layout. The main intention of the DfD prototype was to simulate the various phases of a typical DfD structure (i.e. initial construction, deconstruction, and reconstruction phases), and to provide field observations on possible difficulties that may arise during each of these phases. The results showed that DfD implementation for high rise residential buildings is possible and can be realized with ease in Singapore [11].

Fig. 10. Half-scale models of DfD prototypes

3. Conclusions and Summary

Spiraling construction costs are here to stay, due to increased global demand and rising costs of construction materials and manpower. With dwindling resources and an urgent need to preserve the environment, the concept of unlimited supplies of construction materials is no longer viable. Stakeholders in the construction industry and members of the public must work together to develop sustainable infrastructural solutions, so that future generations will also be able to live, work and play comfortably in Singapore.

Acknowledgements

The two projects are funded by the Ministry of National Development's Research Fund for the Built Environment. Contributions by colleagues in NUS and HDB and past and present students are gratefully acknowledged.

References

[1] R. Sri Ravindrarajah, C. T. Tam, Properties of concrete made with crushed concrete as coarse aggregate, Magazine of Concrete Research. 37, 130 (1985) 29-38.
[2] V. M. Tam, C. M. Tam, Re-use of Construction and Demolition Waste in Housing Developments, Nova Science Publishers, New York, 2008A.
[3] A. Akbarnezhad, K. C. G. Ong, M. H. Zhang, C. T. Tam, T. W. J. Foo, (2013), Effects of the parent concrete properties and crushing procedure on the properties of coarse recycled concrete aggregates, Journal of Materials in Civil Engineering. 25, 12 (2013) 1795-1802.
[4] A. Akbarnezhad, K. C. G. Ong, Microwave decontamination of concrete, Magazine of Concrete Research. 62, 12 (2010) 879-885.
[5] A. Akbarnezhad, K. C. G. Ong, M. H. Zhang, C. T. Tam, T. W. J. Foo, Microwave-assisted beneficiation of recycled concrete aggregates. Construction and Building Materials. 25, 8 (2011) 3469-3479.
[6] A. Akbarnezhad, K. C. G. Ong, Thermal stress and pore pressure development in microwave heated concrete, Computers & Concrete, 8, 4 (2011) 3469-3479.
[7] K. C. G. Ong, A. Akbarnezhad, Microwave-assisted Concrete Technology – Production, Demolition and Recycling, CRC Press, Taylor & Francis Group, 2015.
[8] K. C. G. Ong, Sustainability in Singapore's urban infrastructure, Proceedings 35th International Conference of Our World of Concrete and Structures, Singapore. (2010) 1-9.
[9] L. R. Chandra, K. C. G. Ong, A. Akbarnezhad, et al., Designed for disassembly system for sustainable precast construction, International Seminar of Concrete Technology, Semarang, Indonesia (2013) 51-61.
[10] K. C. G. Ong, Z. Lin, R. C. Lado, C. T. Tam, S. D. Pang, Experimental investigation of a DfD moment-resisting beam-column connection, Engineering Structures, 56 (2013) 1676-1683.
[11] A. Akbarnezhad, K. C. G. Ong, R. C. Lado, Economic and environmental assessment of deconstruction strategies using building information modeling, Automation in Construction, 37 (2014) 131-144.
[12] K. C. G. Ong, K. Kawaai, C. T. Tam and S. D, Pang, Size-effect of early age shrinkage at the interface between fresh cementitious mixtures and hardened concrete substrate in a tropical environment, Proceedings 37th International Conference of Our World of Concrete and Structures, Singapore (2012) 309-320.

Available online at www.sciencedirect.com

ScienceDirect

Procedia Engineering 00 (2017) 000–000

Procedia Engineering

www.elsevier.com/locate/procedia

Sustainable Civil Engineering Structures and Construction Materials, SCESCM 2016

Design, material properties and structural performance of sustainable concrete

Harald S. Mueller[a], Michael Haist[a], Jack S. Moffatt[a], Michael Vogel[a,*]

[a]*Institute for Concrete Structures and Building Materials, Karlsruhe Institute of Technology, 76131 Karlsruhe, Germany*

Abstract

Green concretes, also termed eco-concretes, with reduced cement content may provide an alternative for improving concrete sustainability independently of used supplementary cementitious materials. However, to evaluate the sustainability of these new types of concretes not only the ecological impact due to the composition may be regarded but in particular also their technical performance, i.e. their mechanical, physical and chemical properties, have to be taken into consideration. Consequently, this paper introduces first the index Building Material Sustainability Potential, which is applied in combination with the service life prediction for cement-reduced concretes using probabilistic methods. Moreover, the composition of green concretes is indicated, and related test results on the performance of green concretes are presented. The potential of green concrete for applications in practice is shown by the structural performance of graded concrete members being loaded in flexural tests.

Peer-review under responsibility of the organizing committee of SCESCM 2016.

Keywords: sustainability; graded concrete; green concrete; service life design; reliability

1. Introduction

The building industry is affected by the ongoing sustainability debate more than any other industry, due primarily to the pronounced environmental impact resulting from the production of building materials, the erection of buildings and structures and the subsequent use thereof [1]. This holds especially true for concrete structures, as the production of this material – and here especially the production of the raw material cement – is highly energy intensive and the source of substantial emissions of CO_2 resulting from the production process [2].

* Corresponding author. Tel.: +49 (0) 721 608-42277; fax: +49 (0) 721 608-47796.
E-mail address: michael.haist@kit.edu

1877-7058
Peer-review under responsibility of the organizing committee of SCESCM 2016.

There are different approaches to mitigating the emissions of CO_2 associated with the use of structural concrete in view of its composition. Besides the partial replacement of Portland cement clinker by supplementary cementitious materials or new types of binders, a very efficient and promising approach consists in a tremendous reduction of the cement (binder) content of the concrete. However, this only leads to a truly sustainable concrete if the resulting performance of this cement-reduced concrete, i.e. its mechanical, physical and chemical properties, may be kept almost identical compared to ordinary structural concrete. This means that for the evaluation of the sustainability of these new types of concretes not only the ecological impact due to the composition may be regarded but in particular also their technical performance.

Against this background the paper at hand introduces first the index Building Material Sustainability Potential, which takes into consideration the environmental impact of the concrete and its constituent materials, the performance of the concrete and its service life. Eco-concretes, also termed green concretes, have been produced and test results for the performance of these concretes are given. The development principles applied during the mix design procedures of the presented concretes are explained elsewhere, see [3]. The focus of the paper at hand rather is placed on outlining the calculations related to the Building Material Sustainability Potential (BMSP). Nevertheless, flexural tests on concrete beams are additionally shown, indicating very promising results if a grading with different concrete types including eco-concrete is applied.

2. Definition of the building material sustainability potential

To evaluate the sustainability of new types of concrete (green concrete) it is inadequate to consider just the prevention of CO_2 emissions being achieved e.g. by the partial replacement of Portland cement clinker by supplementary cementitious materials. It is necessary also to take into consideration at least the performance of the material and its service life.

Since the required service life of concrete structures normally ranges between 50 to 100 years, their environmental impact is spread over a long time period. From this it is evident that the sustainability of the concrete increases with increasing service life. Further, the sustainability of building structures requires a reduction of the environmental impact associated with the material, erection, maintenance and operation processes and a concurrent increase of the strength and durability of the materials and structures, respectively, at their maximum technical performance. These interactions may be expressed by means of Eq. 1 (see also [4]).

$$\text{Building Material Sustainability Potential (BMSP)} \sim \frac{\text{Service Life} \cdot \text{Performance}}{\text{Environmental Impact}} \tag{1}$$

Even though the definition given above differs from standard definitions of the term sustainability, it is well in line with the latter, addressing the three basic pillars of sustainability – i.e. environmental aspects (by introducing the environmental impact) as well as social and economic aspects (hidden in the service life and performance parameters). As social and economic aspects, however, are extremely difficult or even impossible to evaluate during the concrete development process (i.e. the mix design), the definition given in Eq. 1 provides engineers with a simple tool to quantify the advantages and disadvantages of a specific concrete type with regard to its potential as a sustainable material. The exploitation of this potential during the design and construction process depends on the designer and user of the building or structure.

It must be noted that all three parameters included in Eq. 1 are rather complex and may depend on the composition and interdependence of further parameters. For example, performance may be considered as the strength or the deformation characteristics as well as in terms of characteristics related to durability. The latter is a function of various physical and chemical attacks, which are certainly interrelated. Moreover, Eq. 1 connects the three parameters linearly, and no special weighting is applied to any of these parameters. However, for the time being it is neither possible nor reasonable to display Eq. 1 in a more complex way. This may be done when further research results justify extensions of this approach.

According to Eq. 1, three basic approaches to a sustainable use of concrete exist: 1st is the optimization of the composition of the concrete regarding its environmental impact while maintaining an equal or better performance and service life; 2nd is the improvement of the concrete's performance at equal environmental impact and service life; 3rd

is the optimization of the service life of the building material and the building structure at equal environmental impact and performance. Finally, a combination of the above named approaches seems reasonable.

3. Investigated raw materials

Following the approach of minimizing the environmental impact of concrete during the design phase, materials were selected with low environmental impact as judged by environmental impact indicators. Table 1 presents an overview of environmental impact indicator data representative of the materials used. The data in Table 1 demonstrate that the constituent material cement is critical for the environmental impact of concrete due to its high global warming potential (GWP). While the (GWP) of superplasticizers is similar to that of cement, it is of minor importance on account of the small dosages of this substance in concrete

Table 1. Typical life cycle inventory data for cements and inert granular concrete constituent materials.

Material	Primary energy consumption Non-renew. [MJ/kg]	Renew. [MJ/kg]	Global Warming Potential **GWP** [kg CO_2 /kg]	Ozone Depletion Potential **ODP** [kg R11 /kg]	Acidification Potential **AP** [kg SO_4 /kg]	Nutrification Potential **NP** [kg PO_4 /kg]	Photochem. Ozone Creation Potential **POCP** [kg C_2H_4 /kg]	Source
Cements								
CEM I 32.5	5.650	$8.74 \cdot 10^{-2}$	0.951	$1.64 \cdot 10^{-8}$	$5.31 \cdot 10^{-4}$	$3.30 \cdot 10^{-5}$	$2.20 \cdot 10^{-6}$	[5]
CEM I 52.5	5.800	$9.71 \cdot 10^{-2}$	0.476	$1.79 \cdot 10^{-8}$	$5.74 \cdot 10^{-4}$	$3.50 \cdot 10^{-5}$	$2.36 \cdot 10^{-5}$	
Cement industry (EPD)	2.451	$6.58 \cdot 10^{-2}$	0.691	$1.50 \cdot 10^{-8}$	$8.30 \cdot 10^{-4}$	$1.2 \cdot 10^{-4}$	$1.0 \cdot 10^{-4}$	[6]
Stone powders and aggregates								
Quartz powder 0-0.22 mm	0.820	$3.16 \cdot 10^{-2}$	$2.34 \cdot 10^{-2}$	$4.98 \cdot 10^{-9}$	$1.58 \cdot 10^{-4}$	$6.75 \cdot 10^{-6}$	$5.57 \cdot 10^{-6}$	[5]
Quartz sand	0.539	$1.29 \cdot 10^{-2}$	$1.02 \cdot 10^{-2}$	$2.10 \cdot 10^{-9}$	$7.54 \cdot 10^{-5}$	$3.00 \cdot 10^{-6}$	$2.58 \cdot 10^{-6}$	
Sand	0.022	$1.49 \cdot 10^{-3}$	$1.06 \cdot 10^{-3}$	$2.30 \cdot 10^{-10}$	$6.57 \cdot 10^{-6}$	$2.99 \cdot 10^{-7}$	$2.39 \cdot 10^{-7}$	
Gravel	0.022	$1.49 \cdot 10^{-3}$	$1.06 \cdot 10^{-3}$	$2.30 \cdot 10^{-10}$	$6.57 \cdot 10^{-6}$	$2.99 \cdot 10^{-7}$	$2.39 \cdot 10^{-7}$	
Admixtures								
Superplasticizer (PCE based)	27.95	1.20	0.944	$3.29 \cdot 10^{-8}$	$1.19 \cdot 10^{-2}$	$5.97 \cdot 10^{-3}$	$5.85 \cdot 10^{-4}$	[7]

As binders, two cements, the first being a CEM I 52.5 R according to [8] and the second being a micro-cement with strongly reduced particle size, were selected for the investigations. No product specific life cycle inventory data were available for the micro-cement, but as it is produced by separating the fine particles from a CEM I 52.5 R, it is expected that the data will be very similar with a slight increase in renewable primary energy consumption, assuming the separation process is powered by a renewable energy source. As the availability of supplementary cementitious binder materials may decline relative to future concrete demand, no supplementary cementitious materials were included in this research.

Coarse and fine aggregate fractions consisting of inert quartz gravel and sand fractions, inert quartz powders and a silica fume were selected to make up the majority of the solid material in the granular matrix of the concretes. Selected properties of the cements and inert materials used are presented in Table 2.

The particle size distribution of all granular constituents was optimized using the CIPM Model by Fennis [14] and adjusted to yield mixes with maximum packing density and minimum voids content. A detailed description of this procedure can be found in [3, 4]. The particle size distribution of the solid materials used is shown in Fig. 1. The silica fume is not included in herein, as agglomeration causes the measurement of an unrealistically coarse particle size distribution in densified product. Additionally, a superplasticizer was also included in the mixtures and dosed according to the recommendations made in [14].

Table 2. Properties of cements and inert aggregates investigated.

Reactive components				
Property	Dimension	CEM I 52.5 R	Micro-cement	Silica fume
Density [9]	[g/cm³]	3.117	3.110	2,225
Blaine value [10]	[cm²/g]	5800	6900	-
Time of initial set [11]	[min]	170[1)]	77	-
Compressive strength $f_{c,28d}$ [12]	[MPa]	68.0[1)]	106.3	-

Inert aggregates							
Property	Dimension	Quartz powder 1	Quartz powder 2	Sand 0.1/1 mm	Sand 1/2	Gravel 2/8 mm	Gravel 8/16 mm
Density[9, 13]	[kg/dm³]	2.648	2.650	2.650	2.61	2.51	2.54
Water absorbtion [13]	[m.-%]	-	-	0.2	0.3	1.8	1.5
Blaine value [10]	[cm²/g]	18.000[1)]	1448	-	-	-	-

1) Data supplied by producer

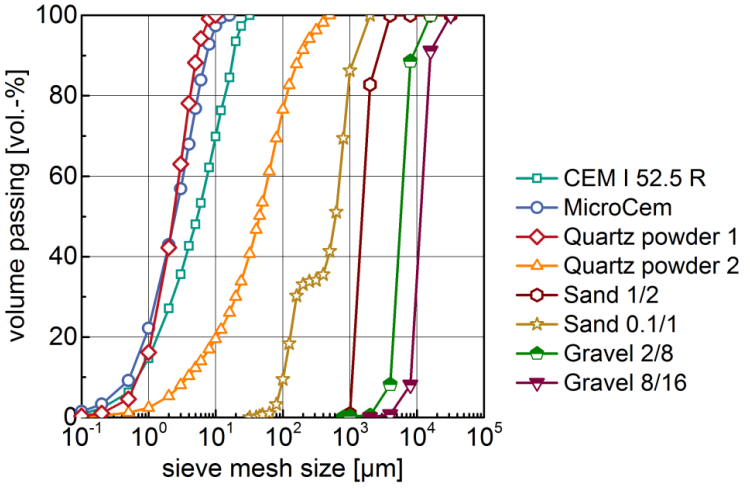

Fig. 1. Particle size distribution curves of the cements and inert granular constituent materials used

4. Composition and properties of investigated mixes

Based on the raw materials detailed in Sec. 3, a total of 6 different concrete mixes with cement contents ranging between 4 vol.-% and 10 vol.-% of all solid particles were developed. The composition and selected properties of the mixes are detailed in Table 3.

The mix design process consisted of the following steps: Firstly, the raw materials of the concrete were selected with the objective of minimizing the content of materials with pronounced environmental impact within the concrete mixture.

Secondly, the cement content within the concrete was defined to be decreasing from 10 vol.-% to 6, 5 and 4 vol.-% of the total solids volume contained in each mixture. Each mixture contained only one cement, either the CEM I 52.5 R or the micro-cement described in Sec. 3

Thirdly, the volume content of each inert granular material was adjusted to maximize the inert material content in the concrete while taking into consideration the influence of cement particles on the packing density. The particle packing model CIPM by Fennis [14] was used to judge the particle packing density while adjusting the granular mixture composition.

Finally, the fresh concrete properties of the mixtures were optimized by adjusting the water content in each mixture. Each mixture was provided with a PCE-based superplasticizer according to the recommendations made in [14].

The composition of the mixes detailed in Table 3 is characterized by cement contents between 113 kg/m³ to 268 kg/m³ in the fresh concrete of either the CEM I 52.5 R or the micro-cement. Additionally, in one mixture the cement

CEM I 52.5 R was combined with micro-silica fume by replacing 5 % by mass of the cement by the corresponding mass of micro-silica fume (referred to as SF-CEM I). Hereby the effect of an improved interfacial transition zone was studied. The reference concrete was adjusted to have a w/c-ratio of 0.43 with a cement content corresponding to the minimum requirements of EN 206-1 [15].

Table 3. Mixture composition and properties of the developed concretes.

Raw material / characteristic value	Dimension	Concrete mixture					
Mixture parameters							
Cement content in dry mix	[vol.-%]	4.0	4.0	4.0	5.0	6.0	10.0
Grain size distribution (fit parameter n)	[-]	0.34	0.34	0.34	0.34	0.34	0.34
Cement type	[-]	CEM I	µCEM	SF-CEM I	CEM I	CEM I	CEM I
Mixture composition							
Cement	[kg/m³]	113	111	109	138	162	268
Quartz powder 1		96	96	96	94	92	91
Quartz powder 2		120	121	120	118	69	23
Sand 0.1/1 (mm)		519	520	520	490	497	441
Sand 1/2 (mm)		434	435	434	424	415	436
River gravel 2/8 (mm)		482	483	482	471	461	459
River gravel 8/16 (mm)		506	507	506	495	484	482
Water		87	85	87	106	126	130
Superplasticizer (PCE based)		6.5	6.4	6.5	6.0	5.7	6.2
w/c-ratio	[-]	0.64	0.64	0.65	0.67	0.69	0.43
Mixture properties							
Compressive strength $f_{cm,28d}$ [18]	[MPa]	76.9	79.0	76.6	69.8	58.2	102.6
Degree of compactability c [16]	[-]	1.25	1.21	1.19	-	-	-
Flow value a [17]	[mm]	-	-	-	390	450	480
Inverse carbon. resistance R_{ACC}^{-1} Mean value / standard deviation	[(10^{-11} m²/s)/ (kg/m³)]	18.91 / 6.83	0.39 / 0.33	14.74 / 5.63	29.59 / 9.69	42.91 / 12.95	--
Global warming potential (GWP)	[kg CO_2/m³]	75	74	76	87	97	146

The fresh concrete was tested for its compactability c according to [16] or its flow value a according to [17] depending on the flow characteristics of the mixture. Specimens were casted, demolded at the age of 2 days, cured in water until the age of 7 days and stored at 20 °C and 65 % r. h. until the age of 28 days, then tested for their compressive strength according to [18]. The corresponding results are detailed in Table 3 and show that the investigated concretes provide high compressive strengths combined with significantly reduced environmental impact compared to standard concretes. The environmental impact of each concrete is represented here by its global warming potential (GWP) and has been calculated based on the environmental impact and content of each raw material as specified in Sec. 3.

Besides the properties in the fresh state and the mechanical properties, the concretes were also tested for their durability under common environmental exposures such as freeze-thaw attack with de-icing salt and carbonation. These experimental results served in the calculation of the service life expected for these concretes.

Fig. 2 shows the results of freeze-thaw tests conducted according to the CDF-method as described in [19] and [20].

As can be seen from the results detailed in Fig. 2, neither the tested reference concrete with a cement content of 10 vol.-% corresponding to 268 kg/m³, nor the concretes with reduced cement content fulfilled the requirements for a concrete corresponding to exposure class XF4 (high water content with chloride attack) according to [15] with a maximum allowable spalling of 1500 g/m². This result was expected. However, the experimental data also shows that the capillary suction and the freeze-thaw resistance of mixes with 4 vol.-% of cement show lower water absorption and a lower spalling than mixes with cement contents of 5 and 6 vol.-%, respectively. Despite its significantly higher w/c-ratio of approximately 0.63, the mix containing 4 vol.-% of micro-cement exhibited a similar, though slightly inferior freeze-thaw resistance than the reference concrete with a cement content of 10 vol.-% and a w/c-ratio of 0.43.

This result in combination with the declining performance of mixes with increasing cement content can be explained by the reduced surface area of hardened cement paste per unit area of concrete under attack, as the cement content is reduced. Since only the hardened cement paste is susceptible to a freeze-thaw attack, this effect obviously offsets in part the detrimental effect of an increased w/c-ratio. Unfortunately, the amount of data available is still too small to derive a general law which quantifies both effects.

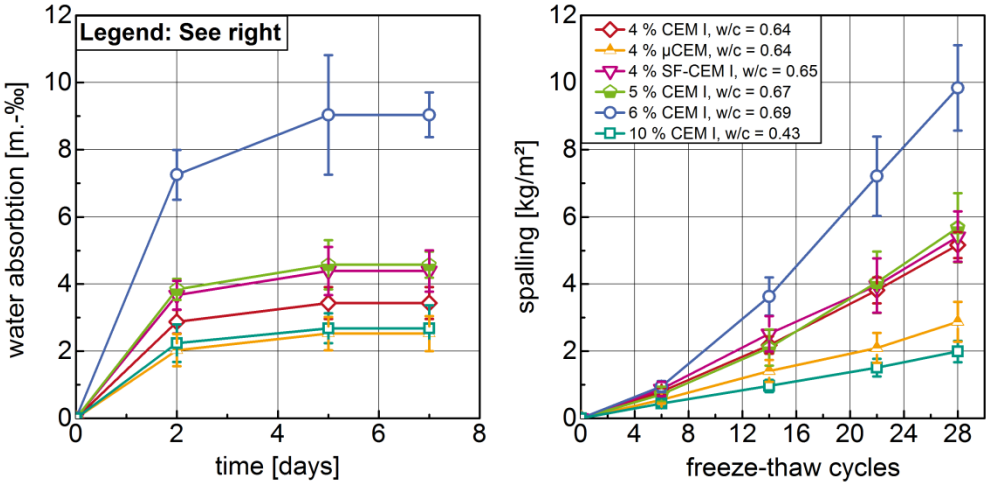

Fig. 2. Measured capillary suction (left) and concrete spalling (right) of investigated mixes in the CDF-test according to [19] and [20].

In order to investigate the influence of the interfacial transition zone (ITZ) on the durability of concretes with low cement content, in the mix designated “4 % SF-CEM I”, 5 % by mass of the Portland cement were replaced by a micro-silica fume. It was dosed to the coarse aggregates in order to enhance a localization of these particles on the coarse aggregate surfaces. The comparison of this mix with the corresponding reference mixture, i.e. the mix containing 4 vol.-% of Portland cement, does not show any difference in the free-thaw-behavior. Here it appears that the w/c-ratio of the cement matrix is generally too high for the ITZ to have any significant effect on the freeze-thaw resistance. Small differences, however, become apparent when comparing the results of the water absorption test. Here the mix containing micro-silica fume exhibits higher water absorption than the mix without silica.

A very important aspect in the evaluation of the durability of the investigated concretes is their resistance against a CO2-induced carbonation. Therefore, beam shaped samples with dimensions of 100 x 100 x 440 mm³ were casted, demoulded after 2 days and stored in water at 20 °C until the age of 7 days. Then the beams were removed from water storage and exposed to dry conditions at 20 °C and 65 % r. h. until the age of 28 days. At this age, half of the beams were removed from the climate chamber and exposed to an increased CO2 concentration of 2 vol.-% at 20 °C and approximately 70 % r. h. Both the samples carbonating under normal and under increased CO2 concentration were investigated for their carbonation depth by splitting the samples at four points along the length of the beam and applying phenolphthalein to the surfaces of the split cross sections. The carbonation depth of each concrete was determined using one beam, measuring inward at 3 points along each of the 4 edges of the split surfaces. The mean value of the carbonation depth was formed for each mixture out of the 48 measurements taken from the corresponding beam.

As can be seen from Fig. 3 (left), the reference concrete (w/c = 0.43) subjected to normal carbonation (i.e. approximately 0.04 vol.-% of CO2) does not show any carbonation at all, whereas the samples with reduced cement content exhibit a significantly increased carbonation. The worst performance in this comparison was also observed with the mix containing 6 vol.-% of cement, followed by the mixes with 5 and 4 vol.-% cement. While the differences between the 6 vol.-% mix compared to the 4 and 5 vol.-% mixes are of statistical significance, the differences between the latter two are not. The same is true regarding the differences between the composite cement containing micro-silica fume and the corresponding mix without silica. Similar results with regard to the ranking of the performance of the investigated concretes can be found for the samples exposed to an accelerated carbonation at 2 vol.-% of CO2 in

Fig. 3 (right). In this test setup the reference concrete also did not exhibit any carbonation. The best performance of all cement-reduced concretes was found for the mix with 4 vol.-% of micro cement. Independently of the test set-up, the carbonation depth was lower than 1 mm, showing a good carbonation resistance, albeit a diminished carbonation resistance when compared to the reference mixture.

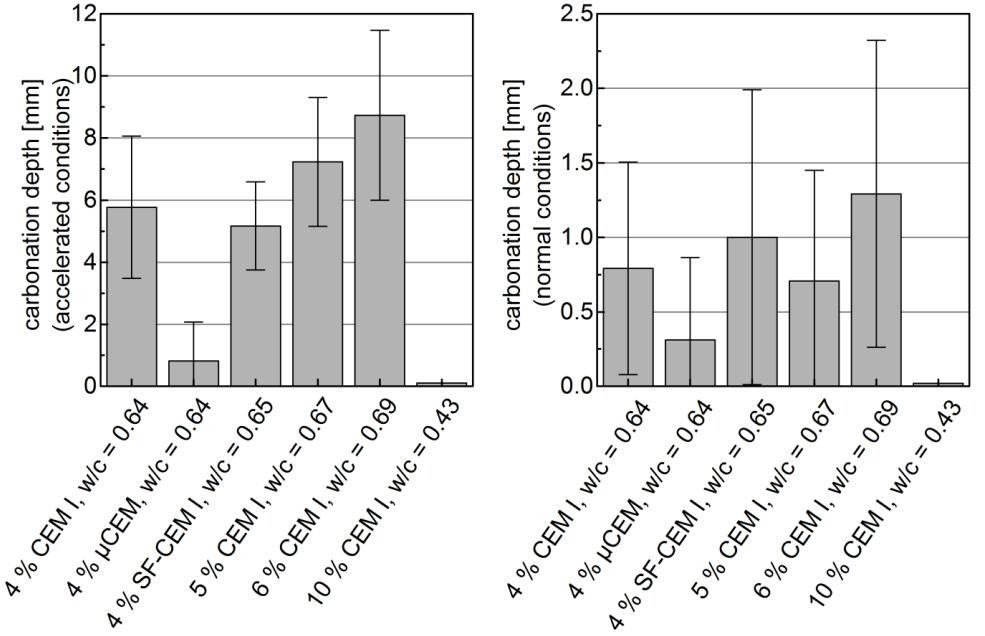

Fig. 3. Carbonation depth of concretes exposed to natural CO_2 environment at 20 °C and 65 % r. h. (left) and 2 vol.-% of CO_2 at 20 °C and approximately 70 % r. h. (right) at an age of 56 d (test procedure see text)

5. Service life design as a key to sustainable buildings and structures

As illustrated by Eq. 1, maximizing the lifetime of a building or a structure is a very efficient way to improve the sustainability of our built environment. Methods to predict the service life of a concrete structure and to design the structure accordingly are essential tools in the sustainability assessment process for sustainable buildings and structures. However, this aspect is often neglected in the current life-cycle assessment debate, leading to a single sided focus on a pure reduction of environmental impact while neglecting the durability and thus the sustainability of the designed structures.

The service life design process is dominated by assessing the alteration – i.e. ageing and often deterioration – of the material on one hand and the varying environmental exposures on the other. This requires in-depth knowledge of the deterioration mechanisms of concrete and on the variance of the influencing factors over time. The procedure of service life prediction will, in the following, be illustrated by means of the carbonation process applied to green concretes as presented in Sec. 4.

The time dependent carbonation of concrete can be described using Eq. 2, in which xc(t) describes the carbonation depth in (mm) at the time t. The dimensionless parameters ke, kc and kt take into account environmental conditions, curing and testing effects. RACC-1 is the inverse effective carbonation resistance of concrete and εt is the corresponding error term in ((mm2/years)/(kg/m3)). CS describes the surrounding CO2-concentration in (kg/m3) and W(t) is the dimensionless weather function, see [21]. With the experimental data depicted in Fig. 3, RACC-1 can be calculated for the green concretes (see Table 3).

$$x_c(t) = \sqrt{2 \cdot k_e \cdot k_c \cdot \left(k_t \cdot R_{ACC,0}^{-1} + \varepsilon_t\right) \cdot C_S \cdot \sqrt{t} \cdot W(t)} \qquad (2)$$

As a limit state criterion xc(t) = c, with c being the concrete cover, is introduced. The failure probability pf is defined as the probability for exceeding this limit state within a defined reference time period.

The loss of durability, i.e. the increase of the deterioration with time, reduces the reliability of a structure. In order to be able to evaluate this reliability at any age of the structure, a reference period for the service life has to be specified [22]. Based on Eq. 2, the time at which depassivation of the reinforcement occurs can be determined. By introduction of the reliability index β, a direct correlation between β and the failure probability pf is obtained. In case of a normally distributed limit state function Z = R – S (R: Resistance, S: Action), the failure probability pf can be directly determined using Eq. 3.

$$p_f = p\{Z<0\} = \Phi(-\beta) \tag{3}$$

The variable Φ(-β) denotes the distribution function of the standardized normal distribution (see [23]). The correlation between various values for the failure probability pf and the reliability index β is shown in Table 4. Note e.g. that the often used 5 % quantile in civil engineering is equal to a failure probability of 5·10-2, which corresponds to a reliability index β = 1.645.

Table 4. Values for the failure probability pf and the related reliability index β [23].

p_f	10^{-1}	10^{-2}	10^{-3}	10^{-4}	10^{-5}	10^{-6}	10^{-7}
β	1.28	2.32	3.09	3.72	4.27	4.75	5.20

The target values of the reliability index, βtarget, depend on the consequences of failure (loss of serviceability) and the relative cost of safety measures. Table 5 contains target values of the reliability index β for building components in the serviceability limit state (SLS), see [24, 25]. Considering the case of depassivation of the reinforcement due to carbonation or chloride ingress, the target reliability index is recommended as β = 1.3 according to [21].

Table 5. Target values of the reliability index β depending on the relative cost of safety measures.

Relative cost of safety measures	Reliability index β [24]	Reliability index β [25]
High	1.3 (pf ≈ 10 %)	1.0 (pf ≈ 16 %)
Moderate	1.7 (pf ≈ 5 %)	1.5 (pf ≈ 7 %)
Low	2.3 (pf ≈ 1 %)	2.0 (pf ≈ 2 %)

Fig. 4 shows a comparison of the resulting service life prediction for concrete structures subjected to carbonation with 40 mm mean concrete cover thickness (8 mm standard deviation) using a green concrete containing 113 kg/m³ (see Fig. 3, 4% CEM I, w/c-ratio = 0.64) and a reference concrete containing 320 kg/m³ of a CEM I 42.5 R with a w/c = 0.60 as described in [26, 27]. Further parameters in Eq. 2 were set according to the example in [27], representing environmental exposure conditions in the city of Munich, Germany. The reference concrete reaches the target reliability index of βtarget = 1.5 chosen in this case after 100 years, the selected green concrete after 72 years.

Combining the measured performance of the green concretes with the durability parameters determined by experiment and the probabilistic service life prediction, it is now possible to evaluate the sustainability potential as described in Eq. 1. Table 6 contains the results for the BMSP of a green concrete as compared to a normal concrete evaluated for a moderate reliability index of 1.5 (see Table 5) in the case of CO2-induced carbonation described above. Although the predicted service life of the green concrete is thirty years shorter than that predicted for the normal concrete, its high performance and reduced environmental impact compensate for this deficit within the sustainability potential index.

It has to be stated that the obtained result is just one among other examples, as only strength and carbonation are considered for the parameters of performance and service life in Eq. 1. Different results would be obtained if e.g. the freeze-thaw characteristics or the chloride ingress is taken into consideration. Moreover, combinations of these effecting parameters might be considered. However, further research is necessary to develop a suitable extended approach. Nevertheless, the simplification included so far does not put into question the particular value of Eq. 1 in view sustainability considerations.

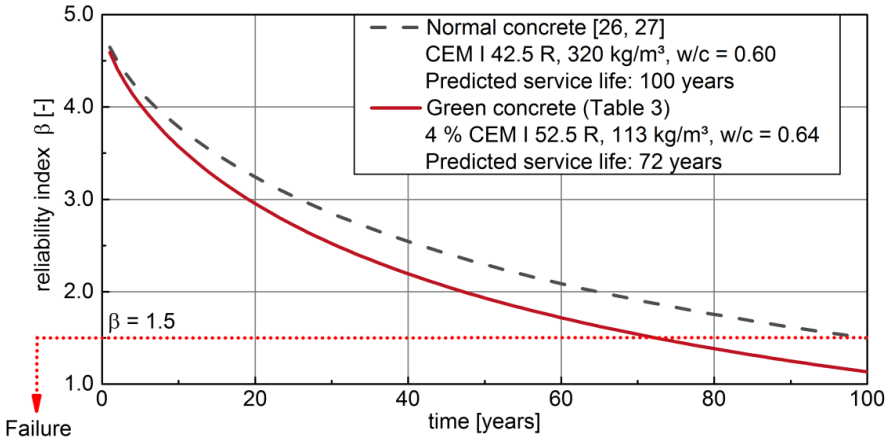

Fig. 4. Comparison of exemplary service life predictions between a developed green concrete and a normal concrete taken from literature data [26, 27].

Table 6. Evaluation of the sustainability potential of a green concrete in comparison to a standard concrete.

Concrete type	Dimension	Normal concrete	Green concrete 4 % CEM I 52.5 R
Cement type	-	CEM I 42.5 R	CEM I 52.5 R
Cement content	kg/m³	320	113
Water to binder ratio	-	0.60	0.64
Inverse carbonation resistance R_{acc}^{-1} (mean value / standard deviation)	$(10^{-11}$ m²/s)/(kg/m³)	13.4 / 5.2	18.9 / 5.6
Calculated service life	years	100	72
Compressive strength	MPa	38.4	76.8
Environmental impact	kg CO_2/m³	214	76
BMSP (See Eq. 1)	MPa·years/(kg CO2/m³)	17.9	72.8

6. Structural performance of graded concrete members

In order to investigate the load bearing characteristics of different types of concrete, deflection controlled three-point-bending tests, based on the DAfStb-Guidelines for fiber reinforced concrete [28], were carried out. In the experiments, steel reinforced and unreinforced beams with homogenous as well as with vertically graded concrete distributions over the cross section were tested. The graded beams typically contained a layer of UHPC in the tension zone and cement-reduced concrete in the compression zone, the transition zone being graded with layers of blends of these two root mixtures.

The beams with a cross section of 150x150 mm², 525 mm in length and, in the case of reinforcement, three equally spaced 8 mm steel reinforcing bars with 15 mm of concrete cover, were rested upon abutments separated by 450 mm and loaded centrally. The loading occurred in three stages with an increasing deflection rate. In the first stage, the deflection was increased at a rate of 0.1 mm/min until 0.5625 mm deflection was reached, corresponding to 0.125 % of the distance between the abutments. The stage was followed by a short pause, during which the beams were investigated for cracks and the crack widths were measured. In the second stage, the deflection was increased by 0.3 mm/min until the deflection of 2.625 mm was reached, corresponding to 0.50 % of the beam length. Again, cracks were marked and crack widths measured in the ensuing pause. In the third stage, the deflection rate was increased to 1.0 mm/min. The resulting load was continually recorded and the experiments were terminated when the load had decreased to 10 % of its maximum in the case of unreinforced beams, or the total deflection of 5 mm was reached in reinforced beams. Approximately 45 minutes were required for the testing of a single beam from mounting to demounting. Fig. 5 shows resulting loading versus deflection curves for reinforced beams together with an estimate of the binder material contained therein.

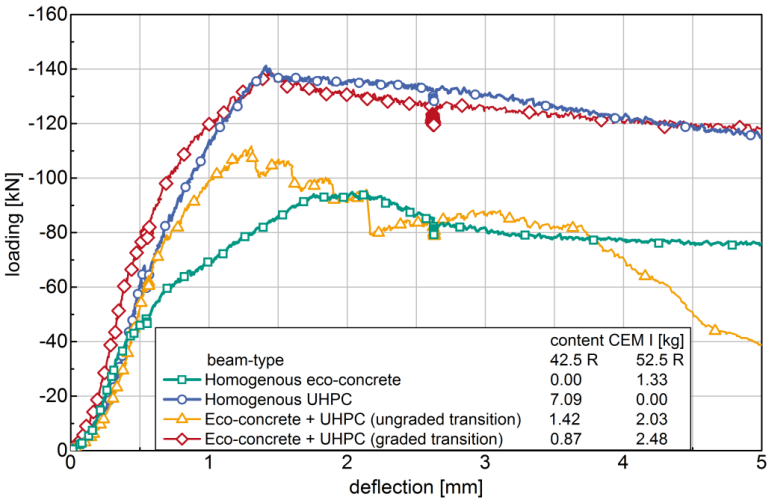

Fig. 5. Loading versus deflection curves of steel reinforced homogenous and graded beams. The cement content of each beam corresponds to unreinforced cross-sections.

It can be seen in Fig. 5 that at small deflection, the beams show quite similar behavior with the exception of the combination between eco-concrete and UHPC with a graded transition zone, which exhibits the highest load at all corresponding deflections. As the deflection increases beyond 0.5 mm, the homogenous eco-concrete beam shows the weakest load bearing capacity. The combination of eco-concrete and UHPC without a graded transition zone improves the performance of the beam somewhat, especially below 2 mm total deflection, but it is surpassed by the homogenous UHPC-beam and the beam with a graded transition zone. The UHPC-beam and the beam with a graded transition zone perform best and behave nearly identically above 1.5 mm deflection. These results are particularly interesting, when considering the amount of binder contained in each beam, which is a good indicator for their corresponding global warming potential. The results suggest that by strategically grading the concrete distribution over the cross section in bending members, load bearing characteristics of homogenous UHPC-beams can be achieved and even surpassed while using only a fraction of the binder material. In this case, the reduction of binder material between the homogenous UHPC-beam and the beam with a graded transition zone is approximately 50 %. The results shown here, however, are preliminary in nature. Further investigations are required and are currently ongoing.

7. Summary and conclusions

It is insufficient to consider only the environmental impact of the constituent concrete materials when evaluating the sustainability of concrete. Two further relevant parameters, the mechanical performance and the durability (service life) of the concrete, have to be taken into account as well. By means of the introduction of the Building Material Sustainability Potential (BMSP) index, these three interdependent parameters may be considered concurrently in order to optimize the sustainability.

It has been demonstrated that cement-reduced concrete can be produced while maintaining or even improving performance in compressive strength, raising potential for discussion of minimum cement contents within concrete standards. To evaluate the sustainability potential of the resulting concretes, however, their durability characteristics must also be considered.

Probabilistic service life design methods, relying on experiments and improved deterioration mechanism models, can be used to predict effectively the service life of concrete structures under defined environmental exposures. While experimental results indicate a deficit in the durability characteristics of cement-reduced concretes, this deficit may be insignificant depending on the intended exposure conditions. Due to significant increases in performance and strongly reduced environmental impact, the evaluation of the BMSP for one such concrete compared to a standard concrete indicates potential for a significant sustainability benefit when choosing the green concrete. Whether this

benefit outweighs any potential drawbacks will also depend on the proper management of necessary maintenance measures when the service life of the structures indeed expires.

Bending tests on reinforced graded concrete beams, where eco-concrete was placed in the compression zone and UHPC in the tension zone revealed a very positive load-deflection behaviour, while the environmental impact could be keep rather low compared to other concretes beams. However, further investigations are necessary to take full profit of the positive structural performance of graded concrete members when eco-concrete is applied.

The cement-reduced concrete mixtures presented are a first step toward producing sustainable concrete and abstaining from supplementary cementitious materials. While the BMSP of the examined green concrete greatly exceeds that of the reference concrete presented, more research regarding the durability of these mixtures must be performed.

Acknowledgements

The authors would like to thank the Helmholtz Association for funding this research.

References

[1] O'Brien, M. et al.: Eco-Innovation Observatory Thematic Report, April 2011, available: http://wupperinst.org/uploads/tx_wupperinst/EIO_WP4_ResEff_Constr_Report.pdf; last access: Oct. 2013
[2] International Federation for Structural Concrete (2012): Guidelines for green concrete structures. fib bulletin 67, Lausanne, Switzerland
[3] Moffatt, J. S.; Haist, M.; Mueller, H. S.: A study of the sustainability potential of cement reduced concrete. In: Proceedings of the II International Conference on Concrete Sustainability (ICCS16), Madrid, Spain, (2016)
[4] Haist, M. et al. (2014): Development principles and technical boundaries of concrete production with low cement content. In: Beton- und Stahlbetonbau 109, No. 3, pp. 202-215
[5] Bundesverband der Deutschen Ziegelindustrie e. V.: Green Building Challenge Handbuch. http://www.ziegel.at/gbcziegelhandbuch/default.htm
[6] Institut für Bauen und Umwelt (Hrsg.): Umweltproduktdeklaration nach ISO 14025 für Zement; Deklarationsnummer: EPD-VDZ-2012111-D, Inhaber: Verein Deutscher Zementwerke e.V., Düsseldorf, Ausstellungsdatum: 16.03.2012
[7] Schiessl, P.; Stengel, Th.: Nachhaltige Kreislaufführung mineralischer Baustoffe. Forschungsbericht der Technischen Universität München, Abteilung Baustoffe, München, 2006
[8] DIN EN 197-1:2011-11: Cement – Composition, specifications and conformity criteria for common cements. Beuth Publishers, Berlin
[9] DIN EN 1097-7:2008-08: Tests for mechanical and physical properties of aggregates – Determination of the particle density of filler – Pyknometer method. Beuth Publishers, Berlin
[10] DIN EN 66126:2015-08: Determination of specific surface area of disperse solids by the gas permeability technique – Blaine method. Beuth Publishers, Berlin
[11] DIN EN 196-3:2009-02: Methods of testing cement – Determination of setting times and soundness. Beuth Publishers, Berlin
[12] DIN EN 196-1:2005-05: Methods of testing cement – Determination of strength. Beuth Publishers, Berlin
[13] DIN EN 1097-6:2013-09: Tests for mechanical and physical properties of aggregates – Determination of particle density and water absorption. Beuth Publishers, Berlin
[14] Fennis, S. A. A. M.: Design of ecological concrete by particle packing optimization. PhD Thesis, Technical University of Delft, The Netherlands, 2010
[15] DIN EN 206:2014-07: Concrete – Specification, performance, production and conformity. Beuth Publishers, Berlin
[16] DIN EN 12350-4:2009-08: Testing fresh concrete – Degree of compactability. Beuth Publishers, Berlin
[17] DIN EN 12350-5:2009-08: Testing fresh concrete – Flow table test. Beuth Publishers, Berlin
[18] DIN EN 12390-3:2009-07: Testing hardened concrete – Compressive strength of test specimens. Beuth Publishers, Berlin
[19] Bundesanstalt für Wasserbau: „BAW-Merkblatt: Frostprüfung von Beton" Karlsruhe, 2012
[20] M.J. Setzer, G. Fagerlund, D.J. Janssen: RILEM recommendation for Test Method for the Freeze Thaw Resistance of Concrete – Test with Sodium Chloride Solution (CDF). In: Concrete Precasting Plant and Technology 4 (1997), pp. 100-106
[21] International Federation for Structural Concrete (2006): Model Code for Service Life Design. fib bulletin 34, Lausanne, Switzerland
[22] European Standard EN 1990:2010-12 (2010): Eurocode – Basis of structural design; German version EN 1990:2002 + A1:2005 + A1:2005/AC:2010. Beuth Publishers, Berlin, Germany
[23] Melchers, R. E.: Structural Reliability Analysis and Prediction. John Wiley & Sons, 2002
[24] Joint Committee on Structural Safety (JCSS) (2001): Probabilistic Model Code – Part I: Basis of Design
[25] Rackwitz, R. (1999): Zuverlässigkeitsbetrachtungen bei Verlust der Dauerhaftigkeit von Bauteilen und Bauwerken. Bericht zum Forschungsvorhaben T 2847. Fraunhofer IRB Verlag, Germany, 1999
[26] Gehlen, Ch. (2000): Probabilistische Lebensdauerbemessung von Stahlbetonbauwerken. Journal of the Deutscher Ausschuss für Stahlbeton, Vol. 510, Beuth Verlag, Berlin, Germany
[27] Gehlen, Ch. et al. (2011): Kapitel XIV Lebensdauerbemessung, In: Bergmeister, K., Fingerloos, F., Wörner J.-D. (Eds.), Beton-Kalender 2011, Teil 2, Kraftwerke, Faserbeton, Ernst & Sohn, Berlin, Germany, pp. 231–278
[28] German Committee for Reinforced Concrete: DAfStb-Guideline for Fibre Reinforced Concrete. Beuth Publishers, Berlin, 2012

Available online at www.sciencedirect.com

ScienceDirect

Procedia Engineering 00 (2017) 000–000

Procedia Engineering

www.elsevier.com/locate/procedia

Sustainable Civil Engineering Structures and Construction Materials, SCESCM 2016

Sustainable seismic design

Stephen Pessiki[a,*]

[a]*Lehigh University, 13 E. Packer Avenue, Bethlehem PA, 18015, USA*

Abstract

Traditional design of a seismic resistant system for a building structure has often relied on structural damage as the intended response of the structure to limit the increase in lateral force and to dissipate energy. The goal of this traditional design approach was life-safety, i.e. to prevent building collapse. Following this approach, a major seismic event can cause significant damage to the structure. This in turn requires extensive repair, or if the damage is severe enough, for the structure to be demolished. More recently, an alternative design approach has emerged that is intended to provide structures that remain damage free and self-center (i.e. exhibit no residual drift) after the earthquake. This paper describes this alternative approach, and discusses opportunities for improved sustainability through damage-resistant seismic design and renewable materials.

Peer-review under responsibility of the organizing committee of SCESCM 2016.

Keywords: Earthquake; seismic design; post-tensioning; sustainability

1. Introduction

Traditional design of a seismic resistant system for a building structure has often relied on structural damage (e.g. yielding of steel, non-linear compression response of concrete, etc.) as the intended response of the structure to limit the increase in lateral force and to dissipate energy. The goal of this traditional design approach was life-safety, i.e. to prevent building collapse. Following this approach, a major seismic event can cause significant damage to the structure. Two inherent limitations of this approach are: (1) the required nonlinearity or softening of the lateral force resisting system is caused by damage; and (2) residual lateral drift after a major seismic event. This in turn requires extensive repair, or if the damage is severe enough, for the structure to be demolished. The need for extensive repair or demolition is inconsistent with sustainable design and construction practices.

* Corresponding author. Tel.: +1-610-758-3494.
E-mail address: pessiki@lehigh.edu

Peer-review under responsibility of the organizing committee of SCESCM 2016.

To address the limitations of traditional approaches to seismic design, over the past twenty years a considerable amount of research has been devoted to developing self-centering, seismic-resistant building systems that offer recoverable energy-dissipation mechanisms and damage-free softening of lateral load response. As an example of the previous work in this field, Table 1 presents a collection of relevant studies performed by researchers at Lehigh University. Included in the table is the type of lateral force resisting system studied, as well as a list of publications that provide the details of each study. The common element in each of these systems is the use of post-tensioning to allow gap opening at specified locations in the lateral force resisting system under the action of seismic loading in a manner that leads to softening of the structural system. Thus softening is obtained by overcoming the prestressing force, and not through damage.

These post-tensioned seismic-resistant building systems are a distinct departure from the conventional ductile design approach, in which the structural system survives seismic excitation through controlled damage. By utilizing damage-free mechanisms to achieve the desired building response characteristics (e.g. geometric softening of lateral load response through gap opening at beam-column and/or wall-foundation joints; and energy dissipation through relative movement along frictional interfaces or viscoelastic deformations), these systems are not only resistant to structural collapse (enforcing the life safety performance objective), but they also have the potential to significantly improve sustainability and to lessen the economic impact of a seismic event by reducing infrastructure damage.

Table 1. Lehigh University research on post-tensioned seismic-resistant building systems.

Lateral Force Resisting System	Publications
Post-tensioned concrete rocking walls	Kurama et al. 1999a, 1999b, 2002; Perez et al. 2004a, 2004b, 2007, 2013; ACI, 2009; Keller and Sause, 2010; Rivera et al. 2013
Post-tensioned concrete moment-frames	El-Sheikh et al. 1999, 2000; Keller et al. 2010
Post-tensioned steel moment-frames	Garlock et al. 2005, 2007, 2008; Ricles et al. 2000, 2001, 2002; Peng et al. 2000; Rojas et al. 2005a, 2005b; Seo et al. 2005, 2009; Iyama et al. 2008; Lin et al. 2009a, 2009b
Post-tensioned steel rocking frames	Roke et al. 2006, 2009a, 2009b; Sause et al. 2006a, 2006b, 2006c, 2009a; 2009b, 2010

2. Illustration of a post-tensioned lateral force resisting systems – concrete walls

Fig. 1 illustrates in general how damage-resistant post-tensioned seismic systems work. The example shown in the figure is for a concrete wall, but similar responses are obtained from the other structural systems as well. Fig. 1 shows a schematic of a conventional cast-in-place reinforced concrete wall, an unbonded post-tensioned concrete wall, and an unbonded post-tensioned hybrid concrete wall. Also shown is the expected base shear-lateral drift of each wall. The conventional reinforced concrete structural wall (Fig. 1(a)) is a cast-in-place concrete wall, without post-tensioning, and with detailing to provide stable hysteretic behavior. Mild bonded steel reinforcement in the wall extends across the wall-foundation interface and is anchored in the foundation. Under the action of lateral load, the wall softens due to yielding of steel reinforcement and nonlinear stress-strain response of concrete (i.e. damage). Upon reversal of lateral load F, the wall will not necessarily return to zero drift position. Instead, upon removal of the lateral force, the wall can exhibit a residual drift.

Fig. 1(b) shows an unbonded post-tensioned wall (similar to the precast walls with post-tensioning for self-centering studied by Kurama et al. and Perez et al.). These walls exhibit self-centering behavior but they do not have any mild steel reinforcement crossing the horizontal joint between the wall and the foundation. Therefore, these walls undergo large drift without dissipating any excitation energy as illustrated in Fig. 1(b).

An unbonded post-tensioned hybrid concrete wall, illustrated in Fig. 1(c), includes unbonded post-tensioning, and also bonded longitudinal web reinforcement for energy dissipation. The lateral load-deflection response of the hybrid wall is a combination of the energy dissipation as in traditional structural walls, and self-centering as in unbonded post-tensioned precast concrete walls. In an event of seismic excitation, use of unbonded post-tensioning provides the wall with self-centering capacity and the mild steel reinforcement is designed to dissipate energy.

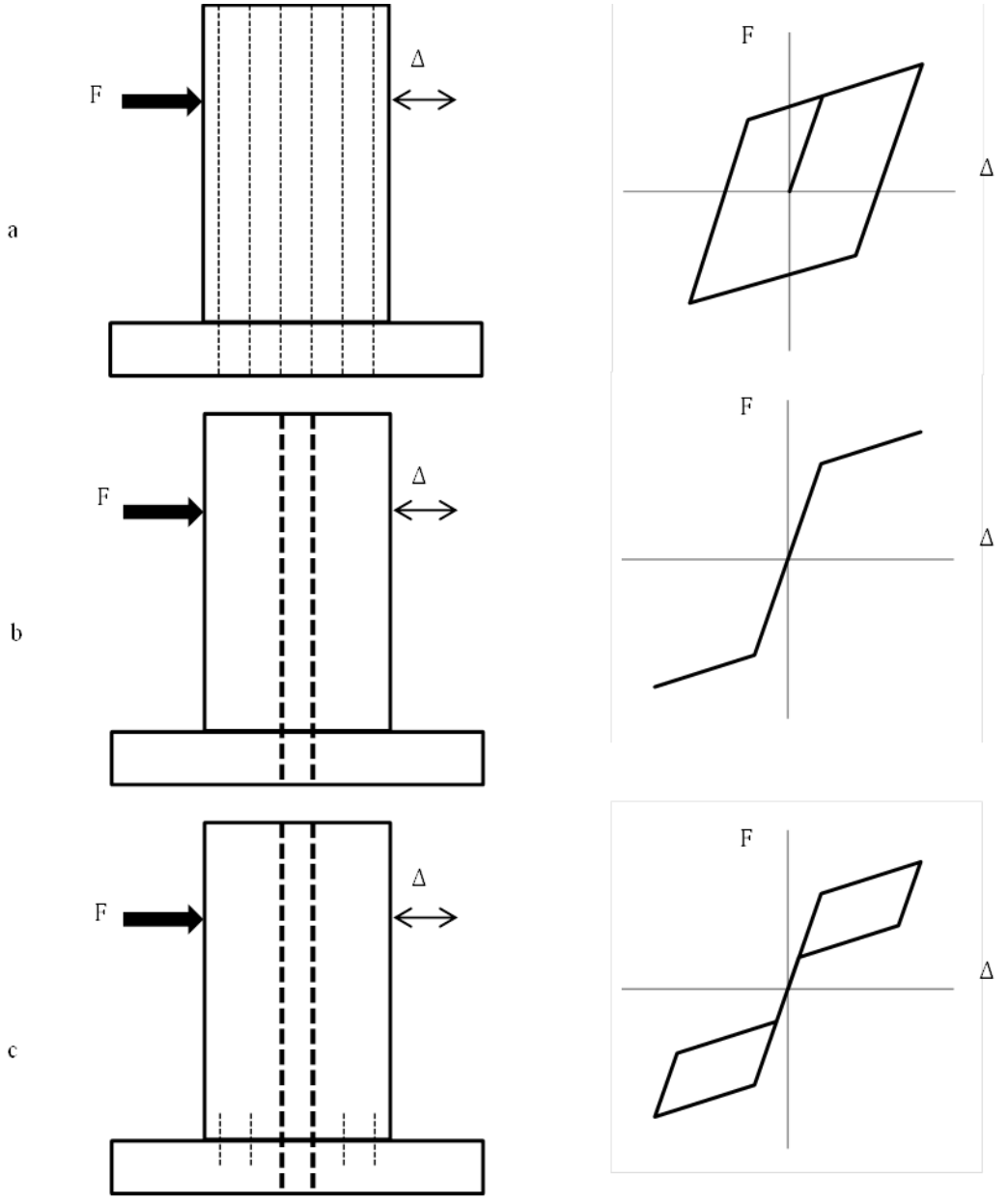

Fig. 1. (a) conventional cast-in-place wall; (b) unbonded post-tensioned wall; (c) unbonded post-tensioned hybrid wall.

Research has shown that the lateral load response of properly designed and detailed post-tensioned rocking walls can be characterized by four distinct limit states, which are illustrated in Fig. 2. If tensile strain demands at the base of the wall under lateral loading are below the pre-compression strain due to post-tensioning and gravity loading, and are within the linear elastic region for the component materials, the lateral load response is similar to that of a conventional wall. As tensile strain demands exceed the pre-compression strain, the wall begins to lift off of the foundation because the wall panel-to-foundation joint is ineffective in tension, i.e. only the unbonded post-tensioning steel is effective in resisting tensile force across the wall-foundation interface. This is referred to as the decompression limit. As the gap along the wall-foundation interface propagates under increased lateral load demand, the lateral load response begins to appreciably soften due to second-order geometric effects (referred to as the

effective linear limit). This softening elongates the periods of vibration for the structure, which tends to lower inertial force demands in the system for typical ground motions due to a reduction in transmissibility. From this point, the rocking wall continues to support additional loading until tensile strain demands in the post-tensioning steel reach yield. Following yielding, strain-hardening in the post-tensioning steel supports lateral loading at a greatly diminished stiffness. Failure of a well-designed wall, which resists buckling modes of failure, is marked by excessive damage in the compression toe of the wall or global instability.

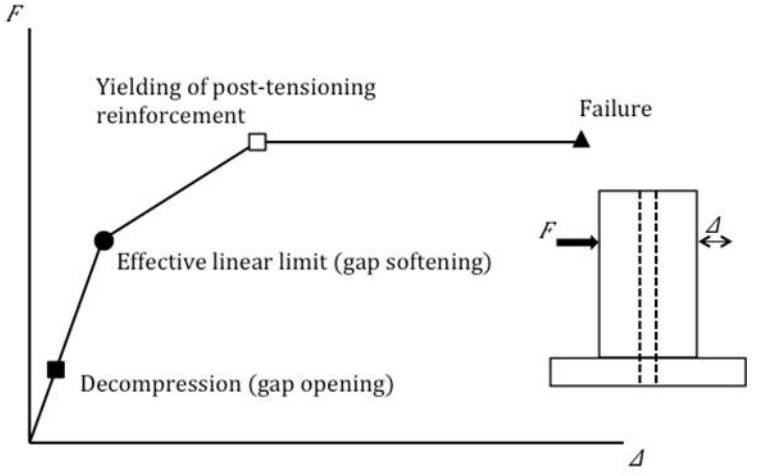

Fig. 2. Idealized monotonic lateral load response for post-tensioned walls.

3. Sustainable construction through damage-resistant seismic design and renewable materials

Until recently, much of the research on self-centering, seismic-resistant building systems (particularly in the U.S.) has been devoted to steel and concrete construction, whose industries have historically dominated the commercial and multi-family residential sectors. However, greater emphasis on sustainable construction practices, which has been motived by diminishing natural resources, rising construction costs, and concerns over the environmental impact of material harvesting and processing practices, has rejuvenated interest in renewable and readily available materials for building construction.

Seismic-resistant post-tensioned lateral force resisting systems that were developed for steel and concrete buildings are now being investigated for timber structures, as illustrated in Table 2, which presents a collection of recent studies on post-tensioned timber construction. In New Zealand, this technology has already made its way into practice with the construction of at least two post-tensioned timber buildings in 2011-2012 (Dekker et al. 2012; Holden et al. 2012).

Additional opportunities exist in other renewable materials as well. In Indonesia, for example, researchers are investigating laminated timber composites for structural applications that utilize abundant and fast growing native plant species, e.g. *Paraserianthes falcataria* and *Hevea brasiliensis Muell* (Awaludin et al. 2011, 2012a, 2012b, 2013a, 2013b). These species have been rarely used for structural applications due to their relatively low strength and stiffness, as compared to structural grade timber. However, their use in laminated veneer lumber (LVL), in which a built-up section is assembled by binding thin plies of the material with adhesive, is seen as a potential solution to diminishing timber resources. Made in a factory under controlled conditions, LVL has superior material uniformity compared to the base product and has been shown to provide a stronger, straighter section that is less susceptible to warping, twisting, bowing, or shrinking.

An important limitation to the widespread implementation of seismic-resistant post-tensioned construction is that the use of hydraulic rams for post-tensioning are not readily / economically available in all regions of the world, necessitating practical solutions that employ indigenous materials and adaptable construction practices. For example, design concepts such as hand-tensioned, spring-loaded rocking frames (currently being studied at Lehigh

University) may offer a cost-effective and practical alternative in developing regions where the full spectrum of construction technologies is not readily available, although more data is needed to validate these systems.

Table 2. Recent developments in seismic-resistant post-tensioned timber construction.

Research Area	Reference(s)
Experimental tests of laminated veneer lumber hybrid moment-frame beam-column, wall-foundation, and column-foundation assemblies	Palermo et al. 2005, 2006a, 2006b, 2006c
Design/modeling of seismic-resistant post-tensioned timber buildings	Newcombe et al. 2008; Smith et al. 2008a, 2008b
Experimental tests of post-tensioned timber moment-frame beam-column assemblies with supplemental passive damping	Smith et al. 2011a
Experimental study regarding the demountability, relocation, and re-use of post-tensioned timber buildings	Smith et al. 2011b
Construction of the Carterton Events Centre Auditorium in Carterton, New Zealand using post-tensioned laminated veneer lumber rocking walls	Dekker et al. 2012
Construction of the NMIT Arts and Media Building in Nelson, New Zealand using post-tensioned laminated veneer lumber rocking walls	Holden et al. 2012
Experimental tests of post-tensioned laminated veneer lumber rocking walls coupled with plywood sheets	Iqbal et al. 2012
Experimental tests of post-tensioned timber frames for multi-story seismic-resistant buildings	van Beerschoten et al. 2012

4. Summary

Traditional approaches to seismic design of seismic resistant systems for building structures, while satisfying the objective of life-safety, often result in buildings that require extensive repair or that must be demolished after a significant seismic event. More recently, an alternative design approach has emerged that is intended to provide structures that remain damage free and self-center after an earthquake, requiring less (if any) repair after the seismic event. This alternative design approach is well-developed for steel and concrete building systems, and has more recently been studied for timber systems as well. Opportunities remain for continued evolution of improved sustainability through more widespread implementation of self-centering damage-resistant seismic design, implemented with an awareness of continued development of renewable materials, and also with a recognition of local construction methods.

Acknowledgements

The author gratefully acknowledges the important original work performed by the graduate students, post-doctoral associates, visiting faculty, and faculty colleagues at Lehigh University. The work at Lehigh has resulted in important contributions to the growing body of knowledge on damage-resistant seismic systems. The references in this paper are an attempt to associate specific individuals with their contributions. Sponsors of the various research works are noted in the cited papers.

References

[1] American Concrete Institute (ACI) (2009) “Requirements for design of a special unbonded post-tensioned precast shear wall satisfying ACI ITG-5.1 (ACI ITG-5.2-09) and Commentary,” American Concrete Institute, Farmington Hills, MI.

[2] Awaludin, A., Sasaki, Y, Pradana, E, Danastri, D.A. (2011) “Mechanical properties of LVL Paraserianthes falcataria, *Technical Report*, Civil and Environmental Engineering Department,Universitas Gadjah Mada, Yogyakarta, August.

[3] Awaludin, A. (2012a) “Development of structural wall made from LVL Sengon (Paraserianthes falcataria): basic mechanical properties,” *Proceedings from the 1st International Conference on Sustainable Engineering Structures and Construction Materials*, Yogyakarta, September 11-13, 2012.

[4] Awaludin, A. and Suriani, E. (2012b) “Shear resistance of timber member to concrete foundation using lag screw fasteners,” *Proceedings from the 5th ASEAN Civil Engineering Conference*, Ho Chi Minh, Vietnam, October 25-26.

[5] Awaludin, A., Palaeowati, N., and Hariadi, S. (2013a) “Prediction of lateral resistance of timber joints with wood and bamboo dowel-type fasteners,” *Proceedings from the 3rd Engineering Annual Seminar*, Universitas Gadjah Mada, Yogyakarta, February 13.

[6] Awaludin, A., Pribadi, A., and Satyarno, I. (2013b) “Racking resistance of Paraserianthes falcataria wooden panels under monotonic load,” *accepted to the 6th Civil Engineering Conference in Asia-Pacific Region*, Jakarta, August 2013.
[7] Dekker, D., Chung, S., and Palermo, A. (2012) “Carterton Events Centre Auditorium pres-lam wall design and construction,” *Proceedings from the 2012 NZSEE Conference*, New Zealand, Paper No. 53.
[8] El-Sheikh, M.T., Sause, R., Pessiki, S., and Lu, L.W. (1999) "Seismic behavior and design of unbonded post-tensioned precast concrete frames," *PCI Journal*, Precast/Prestressed Concrete Institute, Vol. 44, No. 3, May/June, pp. 54-71.
[9] El-Sheikh, M.T., Pessiki, S., Sause, R., and Lu, L.W. (2000) "Moment-rotation behavior of unbonded post-tensioned precast concrete beam-column connections," *ACI Structural Journal*, American Concrete Institute, Vol. 97, No. 1, pp.122-131.
[10] Garlock, M., Sause, R., and Ricles, J.M. (2004) "Design and behavior of post-tensioned steel moment frames," *Proceedings from the 13th World Conference on Earthquake Engineering*, Vancouver, B.C., Canada, August, (Paper No. 2560, CD-ROM).
[11] Garlock, M.M., Ricles, J.M., and Sause, R. (2005) "Experimental studies of full-scale post-tensioned steel connections," *Journal of Structural Engineering*, Vol. 131, No. 3, pp. 438-448.
[12] Garlock, M.M., Sause, R., and Ricles, J.M. (2007) "Behavior and design of post-tensioned steel frame systems," *Journal of Structural Engineering*, Vol. 133, No. 3, pp. 389-399.
[13] Garlock, M.M., Ricles, J.M., and Sause, R. (2008) "Influence of design parameters on seismic response of post-tensioned steel MRF systems," *Engineering Structures*, Vol. 30, No. 4, pp. 1037-1047.
[14] Holden, T., Devereux, C., Haydon, S., Buchanan A., and Pampanin, S. (2012) “Innovative structural design of a three storey post-tensioned timber building,” *Proceedings from the World Conference on Timber Engineering*, Auckland, New Zealand, July 15-19.
[15] Iqbal, A., Pampanin, S., Fragiacomo, M., Palermo, A., and Buchanan, A. (2012) “Seismic response of post-tensioned LVL walls coupled with plywood sheets,” *Proceedings from the World Conference on Timber Engineering*, Auckland, New Zealand, July 15-19.
[16] Iyama, J., Seo, C.-Y., Ricles, J., and Sause, R. (2008) "Self-centering moment resisting frames with bottom flange friction devices under earthquake loading," *Journal of Constructional Steel Research*, Vol. 65, No. 2, pp. 314-325.
[17] Keller, W.J. and Sause, R. (2010) “Analysis and design of unbonded post-tensioned concrete rocking walls for the 2010 E-Defense four-story seismic-resistant post-tensioned concrete test structure,” *ATLSS Report 10-04*, Center for Advanced Technology for Large Structural Systems, Lehigh University, Bethlehem, PA, 326 pages.
[18] Keller, W.J., Sause, R., and Seo, C.Y. (2010), “Preliminary design and pre-test numerical shake table simulations for an archetype self-centering building system utilizing post-tensioned concrete walls and frames, *NEES/E-Defense Collaborative Earthquake Research Program – 5th Planning Meeting*, Tokyo, Japan, Mar. 2, 83 pages.
[19] Kurama, Y. C., Pessiki, S., Sause, R., and Lu, L.W. (1999a) “Seismic behavior and design of unbonded post-tensioned precast concrete walls,” *PCI Journal*, Precast/Prestressed Concrete Institute, Vol. 44, No. 3, May-June.
[20] Kurama, Y. C., Sause, R., Pessiki, S., and Lu, L.W. (1999b) “Lateral load behavior and seismic design of unbonded post-tensioned precast concrete walls,” *ACI Structural Journal*, American Concrete Institute, Vol. 96, No. 4, July-August.
[21] Kurama, Y., Sause, R., Pessiki, S., and Lu, L.W. (2002) "Seismic response evaluation of unbonded post-tensioned precast walls," *ACI Structural Journal*, American Concrete Institute Vol. 99, No. 5, pp. 641-651.
[22] Lin, Y.-C., R., Ricles, J.M., Sause, R., and Seo, C.Y. (2009a) "Earthquake simulations on a self-centering steel moment resisting frame with web friction devices," *Proceedings from the 6th International Conference on Behavior of Steel Structures in Seismic Areas – STESSA 2009*, Philadelphia, PA, August 16-20, pp. 61-66.
[23] Lin, Y.-C., Ricles, J.M., and Sause, R. (2009b) "Earthquake simulations on a self-centering steel moment resisting frame with web friction devices," *Proceedings of the 2009 Structures Congress*, Austin, TX, April 30-May 2.
[24] Newcombe, M.P., Pampanin, S., Buchanan, A., and Palermo, A. (2008) “Seismic design and numerical validation of post-tensioned timber frames,” *Proceedings from the 14th World Conference on Earthquake Engineering*, October 12-17, Beijing, China.
[25] Palermo A., Pampanin S., Buchanan A., Newcombe M. (2005) “Seismic design of multi-storey buildings
using laminated veneer lumber (LVL),” *Proceedings from the* 2005 *NZEES Conference*, New Zealand, March 11- 13.
[26] Palermo A., Pampanin S., Fragiacomo M., Buchanan A., Deam B. (2006a) “Innovative seismic solutions for multi-storey LVL timber framed buildings, *Proceedings from the World Conference on Timber Engineering*, Portland, August.
[27] Palermo A., Pampanin S., Buchanan A. (2006b) “Experimental investigations on LVL seismic-resistant wall and frame subassemblies,” ECEES, *Proceedings from the 1st European Conference on Earthquake Engineering and Seismology*, Geneva, Switzerland, September 3- 8.
[28] Palermo A., Pampanin S., Buchanan A., Fragiacomo, M., and Deam, B. (2006c) “Code provisions for seismic design of multi-storey post-tensioned timber buildings,” ECEES, *Proceedings from the International Council for Research and Innovation in Building and Construction – Working Commission W18: Timber Structures*, Florence, Italy, August.
[29] Peng, S.-W., Ricles, J.M., Sause, R., and Lu, L.W. (2000) "Experimental evaluation of a post-tensioned moment connection for steel and composite frames in seismic zones," *Proceedings from the 6th ASCCS Conference on Steel and Concrete Composite Structures*, Los Angeles, pp. 721-728.
[30] Perez, F. J., Pessiki, S., and Sause, R. (2004a), “Seismic design of unbonded post-tensioned precast concrete walls with vertical joint connectors,” *PCI Journal*, Precast/Prestressed Concrete Institute, Vol. 49, No. 1, January-February.
[31] Perez, F. J., Pessiki, S., and Sause, R. (2004b), “Lateral load behavior of unbonded post-tensioned precast concrete walls with vertical joints,” *PCI Journal*, Precast/Prestressed Concrete Institute, Vol. 49, No. 2, March-April.
[32] Perez, F. J., Pessiki, S., and Sause, R. (2007) “Analytical and experimental lateral load behavior of unbonded post-tensioned precast concrete walls”, *Journal of Structural Engineering*, American Society of Civil Engineers, Vol. 133, No. 11, November.
[33] Perez, F.J., Pessiki, S., Sause, R., “Experimental Lateral Load Response of Unbonded Post-tensioned Precast Concrete Walls,” *ACI Structural Journal*, Vol. 110, No. 6, November-December 2013, pp. 1045-1055.

[34] Ricles, J.M., Sause, R., Garlock, M., Peng, S.W., and Lu, L.W. (2000) "Experimental studies on post-tensioned seismic-resistant connections for steel frames," *Proceedings from the 3rd International Specialty Conference on Behavior of Steel Structures in Seismic Areas – STESSA 2000*, Montreal, pp. 231-238.

[35] Ricles, J.M., Sause, R., Garlock, M.M., and Zhao, C. (2001) "Post-tensioned seismic-resistant connections for steel frames," *Journal of Structural Engineering*, Vol. 127, No. 2, pp.113-12.

[36] Ricles, J.M., Sause, R., Peng, S.-W., and Lu, L.W. (2002) "Experimental evaluation of post-tensioned steel connections," *Journal of Structural Engineering*, Vol. 128, No. 7, pp. 850-859.

[37] Rivera, M., Pessiki, S., and Sause, R. (2013) "Experimental and analytical evaluation of multi-story unbonded post-tensioned hybrid concrete walls," *ATLSS Report*, Center for Advanced Technology for Large Structural Systems, Lehigh University, Bethlehem, PA.

[38] Rojas, P., Garlock, M., Ricles, J., and Sause, R. (2005a) "Use of post-tensioned friction damped connections for seismic retrofit of steel moment resisting frames," *International Journal of Steel Structures*, Vol. 5, No. 3, pp. 265-276.

[39] Rojas, P., Ricles, J.M., and Sause, R. (2005b) "Seismic performance of post-tensioned steel moment resisting frames with friction devices," *Journal of Structural Engineering*, Vol. 131, No. 4, pp.529-540.

[40] Roke, D., Sause, R., Ricles, J., Seo, C.-Y., and Lee, K.-S. (2006a), "Self-centering seismic-resistant steel concentrically-braced frames," *8th U.S. National Conference on Earthquake Engineering*, Earthquake Engineering Research Institute, San Francisco, April.

[41] Roke, D., Sause, R., Ricles, J.M., and Gonner, N. (2009a), "Damage-free seismic-resistant self-centering steel concentrically-braced frames," *STESSA 2009, Proceedings from the 6th International Conference on Behavior of Steel Structures in Seismic Areas*, Philadelphia, PA, August 16-20, pp.3-10.

[42] Roke, D., Sause, R., Ricles, J.M., and Gonner, N. (2009b), "Design concepts for damage-free seismic-resistant self-centering steel concentrically-braced frames," *Proceedings from the 2009 Structures Congress*, Austin, TX, April 30-May 2.

[43] Sause, R., Ricles, J., Roke, D., Seo, C.-Y., and Lee, K.-S. (2006a), "Self-centering seismic-resistant steel concentrically-braced frames," *Proceedings from the 5th International Conference on Behavior of Steel Structures in Seismic Areas – STESSA 2006*, Yokohama, Japan, August pp. 85-90.

[44] Sause, R., Ricles, J., Roke, D., Seo, C.-Y., and Wolski, M. (2006b), "Self-centering steel frame systems," extended abstract, *4th NEES Annual Meeting*, Washington D.C., June.

[45] Sause, R., Ricles, J., Roke, D., Seo, C.-Y., and Lee, K.-S. (2006c), "Design of Self-Centering Steel Concentrically-Braced Frames," *4ICEE, 4th International Conference on Earthquake Engineering*, Taipei, Taiwan, October.

[46] Sause, R., Ricles, J.M., Lin, Y.-C., Seo, C.-Y., and Roke, D. (2009a), "Performance-based design of self-centering steel frame systems," *Proceedings from the ACES Workshop: Advances in Performance-Based Earthquake Engineering*, Corfu, Greece, July 4-7.

[47] Sause, R., Ricles, J.M., Lin, Y.-C., Seo, C.-Y., Roke, D.A., Chancellor, N.B., and Gonner, N. (2009b), "Validating performance of self-centering steel frame systems using hybrid simulation," *Proceedings of the 3rd International Conference on Advances in Experimental Structural Engineering*, San Francisco, CA, October 15-16.

[48] Sause, R., Ricles, J.M., Lin, Y.-C., Seo, C.-Y., Roke, D.A., and Chancellor, N.B. (2010), "Self-centering damage-free seismic-resistant steel frame systems," *Proceedings of the 7th International Conference on Urban Earthquake Engineering (7CUEE) & 5th International Conference on Earthquake Engineering (5ICEE)*, March 3-5, Tokyo, Japan.

[49] Seo, C.Y. and Sause, R. (2005) "Ductility demands on self-centering systems under earthquake loading," *ACI Structural Journal*, American Concrete Institute, Vol. 102, No. 2, March-April.

[50] Seo, C.-Y., Lin, Y.-C., Sause, R., and Ricles, J.M. (2009), "Development of analytical models for 0.6 scale self-centering MRF with web friction devices," *Proceedings from the 6th International Conference on Behavior of Steel Structures in Seismic Areas – STESSA 2009*, Philadelphia, PA, August 16-20, pp. 849-854.

[51] Smith, T., Pampanin, S., Fragiacomo, M., and Buchanan, A. (2008) "Design and construction of prestressed timber buildings for seismic areas," *New Zealand Timber Design Journal*, Vol. 16, No. 3, pp. 3-10.

[52]Smith, T., Pampanin, S., Buchanan, A., and Fragiacomo, M. (2008) "Feasibility and detailing of post-tensioned timber buildings for seismic areas," *Proceedings from the 2008 NZSEE Conference*, New Zealand, Paper No. 53.

[53] Smith, T., Wong, R., Newcombe, M., Carradine, D., Pampanin, S., and Buchanan, A. (2011a) "The demountability, relocation and re-use of a high-performance timber building," *Proceedings from the 9th Pacific Conference on Earthquake Engineering*, Auckland, New Zealand, April 14-16, Paper No. 187.

[54] Smith, T., Pampanin, S., Carradine, D., Buchanan, A., Ponzo, F., Di Cesare, A., and Nigro, D. (2011b) "Experimental investigations into post-tensioned timber frames with advanced damping systems," *Proceedings from the 2011 ANIDIS Conference*, Bari, Italy, September.

[55] van Beerschoten, W., Palermo, Carradine, D., and Law, P. (2012) "Unbonded post-tensioned timber gravity frames for multi-story buildings," *Proceedings from the 2012 ASEC Conference*, Perth, Australia, Nov. 28-Dec. 2.

Available online at www.sciencedirect.com

ScienceDirect

Procedia Engineering 00 (2017) 000–000

Procedia Engineering

www.elsevier.com/locate/procedia

Sustainable Civil Engineering Structures and Construction Materials, SCESCM 2016

Importance of soft processing (low-energy production) of advanced materials for sustainable society

Masahiro Yoshimura[a,b,*]

[a]*Department of Materials Science and Engineering, National Cheng Kung University, Tainan, Taiwan*
[b]*Prof. Emeritus. Tokyo Institute of Technology, Japan*

Abstract

In recent years, advanced materials (such as, engineering plastics, polymers, metals, alloys, semiconductors and ceramics) have been required to be produced used and then wastedin our modern lives. Those materials have been hardly produced in nature (bio-system), thus they have had been produced by artificially in industries. The industry systems are generally uses sophisticated artificial machines, parts and materials. Moreover, these industrials production have used fossil fuels and fine resources with high chemical potentials. Therefore, one must challenges to eliminate to use of fossil fuel(s) and fine resource to establish sustainable society. Here, I propose one of such challenges to produce advanced materials, particularly advanced ceramic materials by Soft-processing (Green method) using low-energywith low wastes, heats and exhausts.

Peer-review under responsibility of the organizing committee of SCESCM 2016.

Keywords: low energy production; soft processing; advanced material; sustainable society.

1. Water cycle on the earth and the production of Biological Materials [1-4]

As we know, the earth is unique "water planet" where water can be kept and cycled on the earth including, Hydrosphere, Atmosphere, and even Geosphere. These water-cycle could create organic materials then lives: viruses microbes, planktons, plants and animals. We, any life including humanscan survive eating those organic polymers as foods, and using them for clothing, housing and fuels for heat and light developing fromgathering natural foods products, human could artificially grown favorite food by “agriculture” and “pastoralism” in addition to

* Corresponding author. Tel.: +886-6-2757575; fax: +886-6-2346290.
E-mail address: yoshimur@mail.ncku.edu.tw

Peer-review under responsibility of the organizing committee of SCESCM 2016.

hunting/fishing/catching wild plants and animals. He/she could make such biologically producible organic polymers in larger scale but never successful to produce Advanced EngineeringMaterials: organic plastics, engineering polymers, metals & alloys, semiconductors, and ceramics expect several exceptional bio-minerals, as seen in Table 1 and 2. Therefore, those engineering materials being used in modern our societies must be produced and /or fabricated by artificial "Industry" using particular machines, chemical resources and energy resources. It is the principle and essential that environmental problems cannot be solved by sole biological systems because the advanced materials have seldom been produced by biological systems, but produced by artificial industrial systems on the earth. The latter have seldom been based upon water-cycle, as like in biological systems. Therefore, the industrial systems for advanced materials hardly possible to accommodate with the biological system based upon water cycle. However, one can apply water-cycle systems (=solution processing) to industrial ones by learning from biological systems. That is the key to consider a sustainable society on the earth. Some people have proposed (a) recyle of materials is also important as well as (b) reduced and (c) re-use, that is for sustainable society [5].

Table 1. Bio-producible Materials

Material	Examples
Organic Materials	1. Bio-molecules: Lipids, fatty acid, amino acid, Vitamins, Hormones, etc.
	2. Bio-polymers: Polypeptides, nucleic acids, sugars, cellulose, etc.
	3. Bio-plastics:
Inorganic Materials	Bio-minerals: Amorphous SiO_2, Fe oxides, Fe hydroxides, $CaCO_3$, Ca-phosphates, $SrSO_4$, etc.

**No other materials are able to be biologically produced!*

***Most of engineering materials and advanced materials as follows have never been biologically produced!!*

Table 2. Biologically non-producible Materials

Material	Examples
Organic Materials	1. Synthetic molecules: Many organic compounds
	2. Synthetic polymers: PE, PP, PET, ABS, etc.
	3. Synthetic plastics: Ployethylene, Ploypropylene, Nylon, Vinylon, etc.
Inorganic Materials	1. Semiconductors: Si, Ge, GaAs, InP, Carbons, etc.
	2. Metals & Alloys: Fe, Al, Cu, Steel, Bronze, etc.
	3. Ceramics: Al_2O_3, MgO, TiO_2, $BaTiO_3$, $NiFe_2O_4$, etc.

However, our modern materials cycle have rather over weighted to the environment of the Earth. As you see in the Figure. 1a, we can recycle the materials, waste and exhaust heats but they cost environmentally because more energies based upon like fossil fuels must be consumed to these recycle systems. That is (b), reduce and (c) re-use have less environmetanlly impacts but (a) re-cycles would not contribute to reduce the waste heats and materials. Because, one cannot reduce the Entropy in any thermodynamics process. Thereofre, low-energy production of materials Figure. 1b. In this proposal review's title, is the more important than re-cycle.

2. Thermodynamic Principles of Advanced Materials proceeding

Processing of advanced materials generally consists of two steps: (I) the synthesis of substances (ceramic, metallic, organic) that can be characterized by (1) a particular chemical composition, (2) a physical state including crystal structure, and (3) specific properties; and (II) materials fabrication (i.e., shape-forming and shape-fixing by firing/sintering, pyrolysis, melting, or casting) as shown schematically in Figure. 2 (right side). In this regard, it is very difficult to give desired shape, form, and size to inorganic ceramic materials, owing to their intrinsic brittleness. Organic materials, such as polymers and plastics, or metallic materials can be generally deformed when local stresses are applied over their yield stresses, but ceramics are susceptible to brittle fracture rather than plastic deformation.

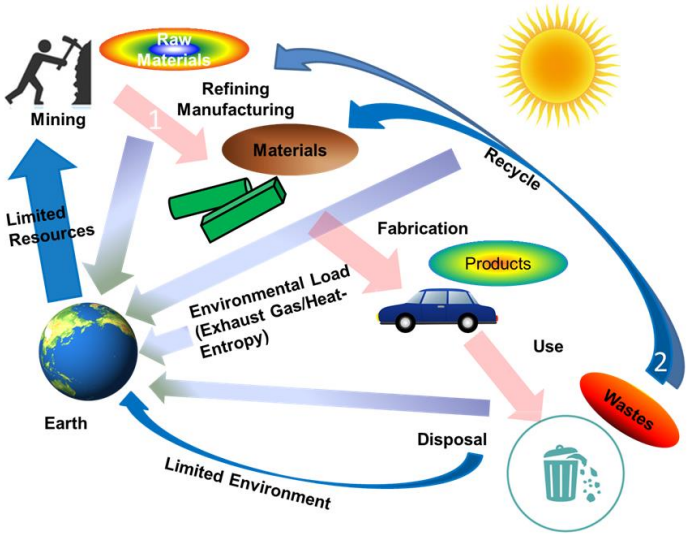

Figure 1a.Life cycle of artificial materials with environment/resources on the Earth.

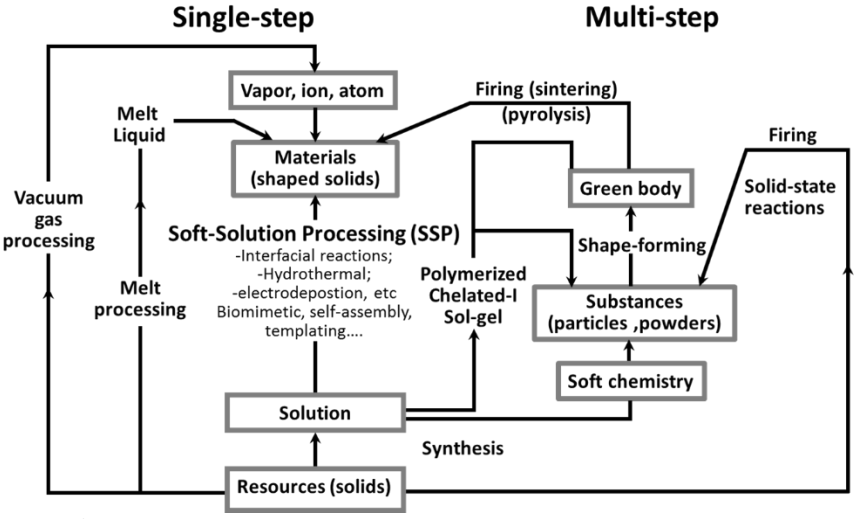

Figure 1b. Schematic diagram of the advanced materials processings and their energy consumptions. The right passes which have been widely used, consist of two steps: synthesis of powders of substances (having a particular chemical composition, a particular physical state including structure, and particular properties based upon composition and structure) and subsequent fabrication of the materials (via shape forming and shape fixing b firing/sintering, pyrolysis, melting, or casting). These passes are environmentally stressing, energy consuming, and expensive. An alternative processing using gas and/or vacuum can produce shaped materials by a single step but it require more energies than conventional multi-step one. Soft Solution Processing (SSP) aims to fabricate shaped materials preferably in a single step using solutions.

Melt/Cast Processes have hardly been applied to ceramic materials except for glasses. Thus most of ceramics have been fabricated via the two-step processes. The “classical” two-step processing method usually requires high temperatures and consumes a lot of energy, particularly in the case of ceramics. More recent processing routes using a gaseous phase (e.g., chemical vapor deposition (CVD), metalorganic chemical vapor deposition (MOCVD), etc. and physical vapor deposition (PVD) methods in a vacuum system [e.g., sputtering, molecular-beam epitaxy (MBE), etc.] can produce shaped material in a single step, but require even higher energy than standard high-temperature processes. Generally speaking, all of these techniques have resulted in environmental problems because their consumed energy results in exhaust gas(es) or exhaust heat (entropy). Vacuum systems especially seem to put more stresses on the

environment because they require continuous pumping to maintain a vacuum, and their exhaust gas(es) cannot be recycled due to their diluted large volumes.

However, one can fabricate specifically shaped, sized, reacted, and/or oriented materials, in situ, by Soft Solution Processing (SSP), in only one step (see left side of Figure. 2). The SSP can be defined as environmentally friendly processing usingsolutions, preferably aqueous solutions. It may provide similar results to every other processes using fluids (such as vapor, gas, and plasma) or beam/vacuum processing, while it is consuming less total energy than other processing routes.

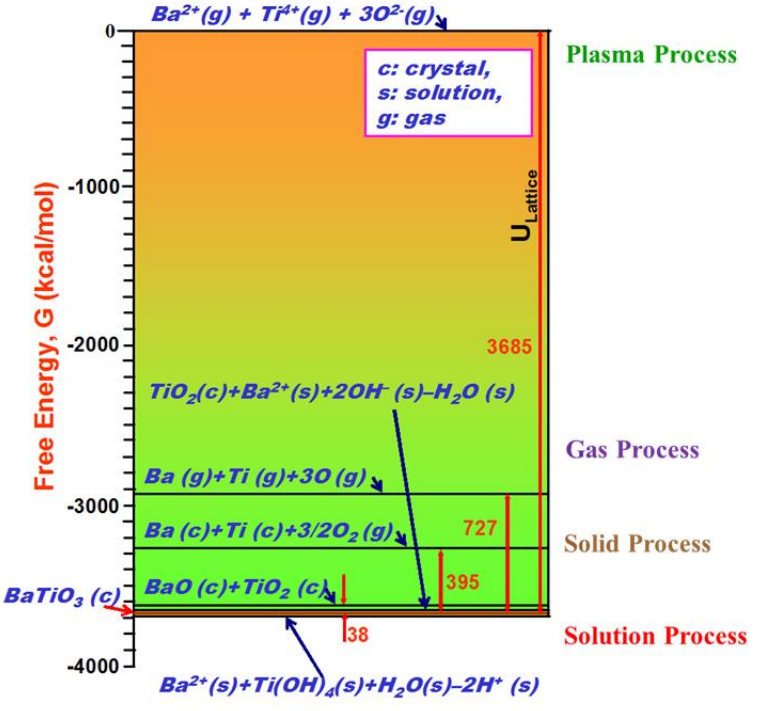

Figure 2. Energy diagram for the formation of BaTiO3 at 25° C. Huge excess of energy is necessary to create, vapor, gas or ion (plasma) from the solid as compared to creation of aqueous solution at the same temperature. This gives the thermodynamic explanation why processing of the advanced materials using aqueous solution consumes low energy in contrast to vapor/plasma processing.

More energy is needed to create melts, vapor, gas, or plasma than to form aqueous solutions at the same temperature. This can be demonstrated using the example of BaTiO3 (Figure. 3), which is one of the most important materials forthe electronics industry.

The driving force (△G) for the representative syntheses: Reactions (1)-(5) of $BaTiO_3$ are 38 kcal/mol, 727 kcal/mol, 3685 kcal/mol, 17 kcal/mol, and －14 kcal/mol, respectively, at a room temperature of 298K:

$$BaO_{(crystal)} + TiO_{2(crystal)} = BaTiO_{3(crystal)} \quad (1)$$

$$Ba_{(vapor)} + Ti_{(vapor)} + 3/2\,O_{2(gas)} = BaTiO_{3(crystal)} \quad (2)$$

$$Ba^{2+}_{(gas)} + Ti^{4+}_{(gas)} + 3O^{2-}{}_{(gas)} = BaTiO_{3(crystal)} \quad (3)$$

$$TiO_{2(crystal)} + Ba^{2+}_{(aq)} + 2OH^{-}{}_{(aq)} - H_2O_{(aq)} = BaTiO_{3(crystal)} \quad (4)$$

$$Ba^{2+}_{(aq)} + Ti(OH)_{4(aq)} - H_2O_{(aq)} - 2H^{+}_{(aq)} = BaTiO_{3(crystal)} \quad (5)$$

Any processing technique involving the gas/vapor phase requires a huge amount of energy (727-3685 kcal/mol) to make these gas/vapor precursors from solid raw materials, which are oxide or carbonate ores, and this energy must

then be released into the environment when solid BaTiO3 is formed from these precursors. On the other hand, since the lattice energy of BaO and TiO_2 can be compensated by the hydration (solvation) energies of Ba^{2+} and Ti^{4+} ions, solution processing consumes very little energy, if activation energy ($\triangle G*$) for the synthesis can be overcome. Generally speaking, $\triangle G*$ is inversely proportional to ($\triangle G-n$), where n=2 for the homogeneous nucleation process. The gaseous species are always in high-energy states, thus there is sufficient energy ($\triangle G$, $\triangle G*$) for the reaction to yield crystalline compounds with a desired shape/size by means of several steps such as diffusion, adsorption, reaction, nucleation, and growth.

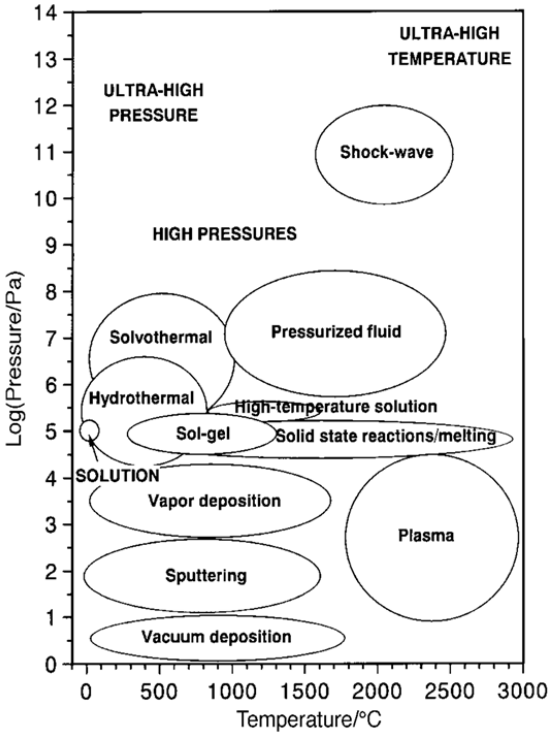

Figure 3. Schematic p–T diagram for preparative techniques for advanced ceramic materials.

On the other hand, species in aqueous solutions are hydrated (or chelated by some complexing agents), thus they are stabilized by the hydration (or chelation) energies and have only a small $\triangle G$ for the reaction. In those cases, relatively high activation energies are necessary for the reaction to occur by defeating those hydration (chelation) energies of ions. Electro- or electroless-plating for metals is achieved by reducing metal ion(s) electrochemically or chemically. However, in the case of ceramics, anions must be oxidized at the same time when cations are reduced. Therefore, some particular activation processes, such as electro-, photo-, sono-, complexo-, organo- or mechano-activation are required to accelerate the kinetics for synthesizing crystallized single- or multi-component ceramic materials from the solution.

3. Soft processing for Fabrication of Nanostructure Materials

Figure 3 is a schematic pressure-temperature (P–T) map for various kinds of materials processes. It shows a broad range of processing conditions, while only a small range corresponds to solution processing. Solution processing is located in the P–T range characteristic for living conditions on earth, which implies that it is environmentally friendly. On the other hand, all other processing routes are associated with increasing (or decreasing) temperature and/or increasing (or decreasing) pressure in a very wide range; therefore, they consume much more energy and can be considered environmentally stressing. Although the environmental problems created by materials processing have

been argued from various points of view—ecologically, biologically, technologically, economically, and even politically—the most scientific arguments are the thermodynamic ones.

In recent years, researchers have focused on nanostructures, which have in fact been known and produced even on the industrial scale for many decades. This particular interest in nanostructures and nanostructured materials is due to (1) the unique properties exhibited by substances and materials when their crystallite size decreases below 100 nm (i.e., into the nanoscale);[6](2) the necessity for miniaturization in electronic integrated circuits;and (3) new applications for nanostructured devices, especially in electronics [7]. Nanostructures have been fabricated in the form of powders, films, and bulk materials [8]. Nanostructured powders exhibit improved sinterability [9].

Coatings derived from nanostructured powders exhibit improved wear resistance (for example, WC/Co cutting tools [10]). Magnetic multi-layered nanostructures have found wide application as information-storage media [11]. Nanostructured thin films can find application as electronic quantum devices such as tunnel junctions [12] and quantum wells, wires, and boxes [7,8]. High-Tc supercon-ductors tailored on the nanometerscale can be used as superconducting interconnects and Josephson junctions [13]. Future dynamic random-access memory (DRAM) capacitors with information capacities of 1 Gbyte or more will have to enter the 10–100-nm range [7]. Ceramic membranes with a pore size as small as 2.5 nm have beenused for gas or liquid separation and as catalysts [14]. Nanostructured bulk mate-rials exhibit improved strength and toughness [15]. A very good example of a natural organic–ceramic nanostructure (containing mostly hydroxyapatite crystals and collagen fibers) withmultiple levels of organization and excellent mechanical properties is bone [16]. Preparation of an analogous artificial material is presently extremely difficult, in spite of several attempts [16,17].

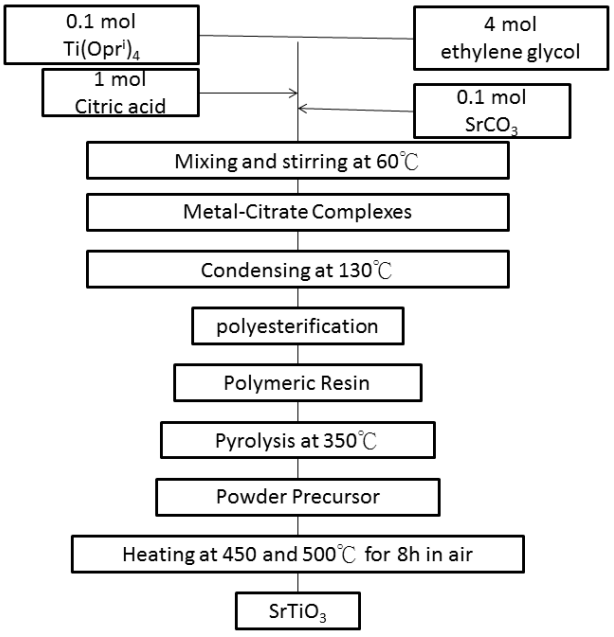

Figure 4. The flow chart for preparing $SrTiO_3$ by the IPCMethod. The molar ratio of Ti(Opr^i)$_4$/CA and ED was 0.1/0.1/1 and 4, respectively.

These are just some important examples. Comprehensive reviews of the synthesis, properties, and applications of nanostructured materials have been published elsewhere [18]. The market for nanostructured powders and coatings in the United States is increasing at an average annual rate of nearly 30% [6] CVD, PVD, and MBE have been widely used to produce nanostructures [19]. Although these techniques have multiply.

4. Composition and shape controlled particles by Solution Processing

Recently, nano-particles have been studied in various methods. Particularly, solution processings have been employed to fabricate those of double (multiple) component oxides because multiple components would be dissolved

as solutes homogeneously in a solution. This is the main reason why such solution processings have been regarded as advanced processings for oxide powders. As seen in Table 3, which has been revised from previous one [20,21], traditional solid state syntheses would give products with poor quality [20, 22-23]. Chemical processings like precipitation, coprecipitation, hydrolysis, pyloysis and/or physical processings like evaporation, burning and spraying, might give larger supersaturation to bring about formation of a huge numbers of nuclei. Therefore precipitation of nanoparticles from solutions have been rather common and easy task. However, there exist difficulties in controlling of the composition, shape and the crystallizing of particles in those methods. Because homogeneously reacted and crystallized particles require simultaneous supersaturations, precipitation and crystallization/reaction for different components, which are very difficultor almost impossible for multiple components of cations. Therefore these wet chemical methods, which have been called as Soft Chemistry (ChimieDouce) or Soft Chemical routes, need calcination after precipitation [3,4]. The calcination mightassure complete reaction and crystallization for multi-components particles but it would bring about sintering of particles (powders), thus milling(s) and/or grinding(s) after the calcination appear to be essential (see Table 3) in most wet-chemical pro- cessings.

Table 3. Comparison in advanced oxide powder processes, revised from previous Table [*M. Yoshimura and H. Suda, Hydroxyapatite and Related Materials," edited by P. Brown, (CRC Press, 1994) 45. **K. Byrappa and M. Yoshimura, "Handbook of Hydrothermal Technology,"(Noyes Publications, Park Ridge, NJ, USA 2001) Solution (Chemical) processes give powders with higher purity, better reactivity, more homogeneous, and more controlled shape than solid state reaction. Among them, Polymerized Complex Method can give the most compositionally homogeneous one, and Hydrothermal Process can give morphology controlled one. The latter has also the merits of no requirement of calcinations and milling steps.

	Solid state reaction	**Coprecipitation**	**Polymerized complex**	**Sol-gel**	**Hydrothermal**
Cost	Low-moderate	Moderate	High	High	Moderate
State of development	Commercial	Commercial/ demonstration	R&D	R&D	Demonstration
Compositional control	Poor	Good	Excellent	Good-excellent	Good-excellent
Morphology control	Poor	Moderate	Moderate	Moderate	Good
Powder reactivity	Poor	Good	Good	Good	Good
Purity (%)	<99.5	>99.5	>99.9	>99.9	>99.5
Calcination step	Yes	Yes	Yes	Yes	No
Milling step	Yes	Yes	Yes	Yes	No

To improve homogeneity of the composition, three dimensional network forming of components (gel forming) before calcinations seems to be important which prevent the separation/segregation of various components during pylorizing. In this regard, "Polymerized Complex Methods," which have been generalized from the Pechini method, have originally been proposed in our group in 1991/1992 [22,24]. Various cations can form their complex by complexing agent like citric acid, and then those complex can be polymerized by poly- merizingagents like ethylene glycol to polyester net-work (=polymer gel). The gel containing homogeneously distributed chelated cations can be pyrolized to amorphous solids then crystallized into homogeneous compounds and/or homogeneous solid solutions. These processes do not include any sol formation step, where compositional separation/segregationmay often happen, nor include sol gel transformation. Therefore, we have given the name, "Polymerized (or Polymelizable) Complex Methods," as one of gel methods or polymer precursor routes but distinguished from sol-gel methods [22,24].

Now many of crystallized particles (powders) with homogeneous compositions could be fabricated for per-ovskites, photocatalysts, and superconductors [22-25]. As an example, the procedure and the result of $SrTiO_3$ by "Polymerized Complex Method" are shown in Figures. 5 and 6 for the XRD pattern and TEM images, respectively. Another direction has been investigated to improve crystallization and reaction of particles with multi- components without calcinations and/or firing. It is hydrothermal processing where those precipitates are activated to react and crystallize in crystalline particles through dissolution/precipitation and/or adsorption/desorption in a high temperature solution [21,26]. Well crystallized shaped particles, from nano-meter size to centi-meter size, with desired morphologies;polyhe- drons, needles, whiskers [21, 27], etc. Recently, numbers of people are interested in the hydrothermal processing of multi-components oxide particles due to their merits described above (Table. 3). We have published those works on ZrO_2 [28-30], CeO_2 [31], $LaCrO_3$ [32], HfO_2 [33], CeO_2/ZrO_2 [34], Hydroxyapatite [35,36], $BaTiO_3$ [37], $LiCoO_2$ [38], $LiFe_5O_8$ [39], $ZnFe_2O_4$ [40], NiS [41], CdS [42], ZnS [43], etc.

Figure. 6 shows the nano crystals of ZrO_2/CeO_2 prepared hydrothermally [44,45]. Electrochemical reactions; anodic dissolution, anodic oxidation, or even discharging, etc., might help to form those crystalline particles. We have, therefore, proposed Hydrothermal-Electrochemical Methods for the fabrication of multi-components oxides particles and/or films. We have developed mono-dispersed nano-particles via hydrothermal method combining with polymer complex method. When we have started from complexed Cerium species like Oleic acid, they will change to monomer→dimer→clusters, then became nanocrystals after the growth of nuclei. The nano-crystals surface would be covered those oleic acids as the surfactant, thus never touched together to give strong agglomeration, can be seen in Figure 6 [45].

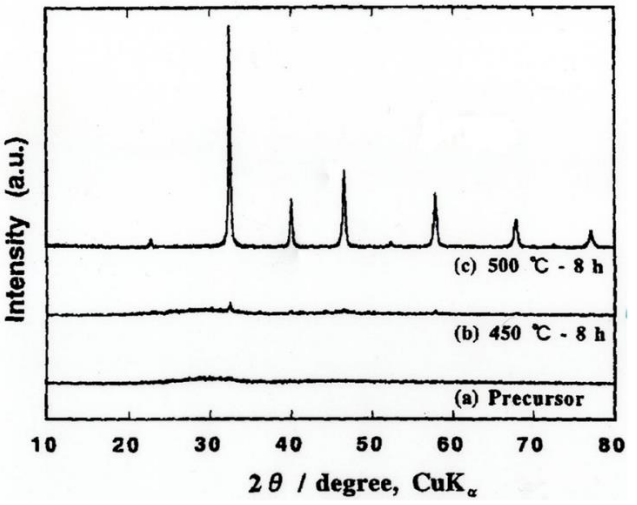

Figure 5.XRD diffraction pattern of (a) the IPC-derived powder precursor for $SrTiO_3$ and of samples heat-treated in static air (b) at 450°C for 8h and (c) 500°C for 8 h.

5. Ceramics by Soft Solution Processing

Fabrication of double oxide films from solutions is rather easy when the solutions and/or derived gels on a substrate can be fired (calcined, pyrolized, sintered) after dried and/or solvent removal, thus most of studies have used these procedures like dip, spin or spray coatings, sol-gel methods and/or electrophoretic depositions as seen in Figure. 1.

Those processes have significantly been developed in recent works, but they still have similar problems for particles; inhomogeneous reactions and crystallization as described previously. In addition, other problems must be consideredfor films, that is; (1) adhesion of the film to the substrate and (2) cracking of the film on the substrate, both of which are caused from shrinkage of materials during crystallization upon firing. Thus thicker and denser film have more serious problems in those processings. Moreover, we must consider (1) why “firing” is required to fabricate double oxide films?, (2) how much does it cost both economically and environmentally? One hasburned fuels which have high chemical potentials to get a high temperature for “firing”ceramic or its precursor materials (and its substrate, too), and then wasted exhaust gases and heats into the environment. Those exhaust gases and heats must be counted as an environmental cost [1-3]. Use of gaseous precursors instead of solution precursors is much more costed as described in the Section II.

If we can directly fabricate ceramic (i.e. double oxides) films in a solution without post-firing, we can avoid most of above mentioned problems. Of course it is difficult, more difficult than fabrication of ceramic particles because nucleation and growth rates of ceramic compounds must be matched with the precipitation rates of the multiple components. Particularly it is difficult that reactions must proceed among multiple components to form ceramic compounds without “firing.” However, it is not impossible that crystalline double oxide films can be fabricated directly in a solution when a chemical driving force existed to form and to crystallize the double oxide [1-3]. For example, interfacial reactions between the substrate [A] and the solute [B] could be activated chemically and/or electrochemically to form the compound ABOx in film shapes. In 1989 [46], we succeeded at the first time to fabricate $BaTiO_3$ thin film on a Ti substrate in a $Ba(OH)_2$ solution at $\geq$ 100°C with electrochemical activation; anodic

oxidation/dissolution by 1-10 mA/cm^2. Figure. 7. Since then similar techniques, called by Hydrothermal electrochemical Methods, have been applied to fabricate a lot of double oxides successfully at low temperatures of RT-200°C: $SrTiO_3$[47,48], (Sr, Ba)TiO_3 [48], $CaWO_4$ [50], (Ba, Sr, Ca)WO_4 [51,52], $BaMoO_4$ [53], YVO_4[54], $LiNiO_2$[55], $LiCoO_2$[56-58], $PbTiO_3$[59], $LiNbO_3$, $BaFeO_3$, MFe_2O_4(M=Zn, Mg) [60], etc., in our group. The mechanism of formation andnano-/micro-structure control have been investigated in detail for $SrTiO_3$ [48,49], $BaTiO_3$ [49,61], and $LiCoO_2$ [55-58]. Figure 8 shows the nanostructure of $SrTiO_3$ film prepared by hydrothermal electrochemical method [48]. $BaTiO_3$ film can be formed by microwave heating of Ti substrate in $Ba(OH)_2$ solution upto 100°C[62].

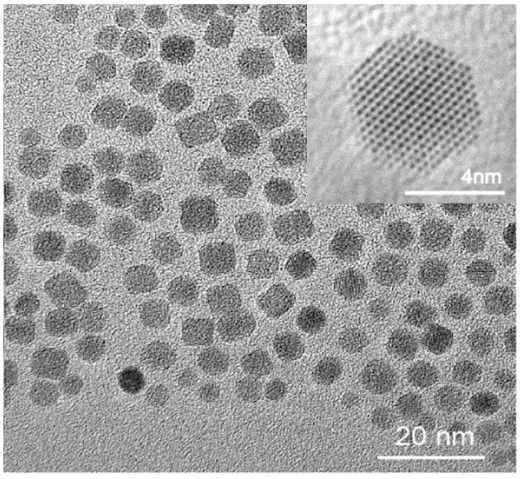

Figure 6. TEM images and the corresponding particle-size distributions of the CeO_2 nanoparticles hydrothermally prepared at 200 °C for 6 h. An inset HR-TEM image of a CeO_2 quasi-nanocube.

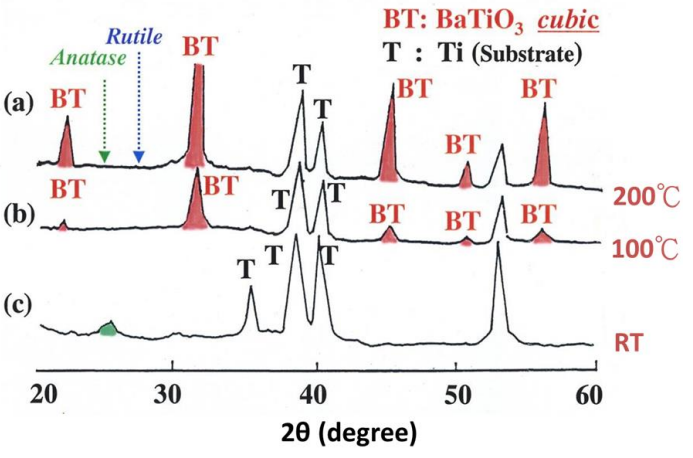

Figure 7. XRD pattern of the surface of $BaTiO_3$ films fabricated by thehydrothermal-electrochemical method.

6. Direct pattering of ceramics by Soft-Solution Processing

When we have activated/stimulated those reaction locally and/or moved the reaction points dynamically, we can get patterned ceramic films directly in solution with out any post heading, masking or etching [63, 64]. Those directpatterning methods differ from previous patterning methods which consist ofmulti-step processes, for example: (1) synthesis of particles of compounds orprecursors; (2) dispersion of the particles into a liquid (“ink”) (Figure.9); (3) patterning of the particles on a substrate by printing of the “ink”; (4) consolidation and/or fixing of the particles’ pattern by heating. For example, some results for zirconia ceramics and PZT films fabricated by ink-jet printing have

already been reported. However, in almost all the reports, jet printing has been used only as a method to give a pattern of solid particles on the substrate. The substrate with the pattern of solid particles must be fired at a high temperature to fix, sinter of solidify them. Otherwise, the substrate using a specialbinder to fix the solid particles must be fired to remove that binder. In any case, these techniques are not fabricating a patterned film by reaction, but fabricating a pattern of particle that requires post-firing.

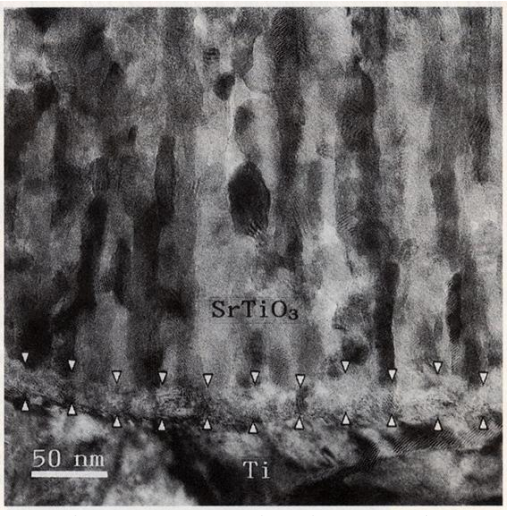

Figure 8. Magnified TEM Image of the $SrTiO_3$ film/Ti substrate interface of the SrTiO3 film with potentiostatic electrolysis at + 8.0 V vs. Ag/AgCl in 0.5M $Sr(OH)_2$ Solution of pH 14.2 at 150°C. Arrows indicate boundaries of a polycrystalline layer of Ti oxides whose microstructure is different from the columnar one of the overlying, inner $SrTiO_3$ layer.

The notable feature of "Direct Patterning" is that each reactant reacts directly on site, at the interface with the substrate. Therefore, the chemical driving force of the reaction, A+B=AB, can be utilized not only for synthesis but also for crystallization and/or consolidation of the compound AB. We have reported $CaWO_4$ patterning on paper at RT, as shown in Figure. 10 [65]. It is rather contrasting to general (Figure. 1) patterning methods where thermal driving force of past-firing is mostly used for theconsolidation of the particles.

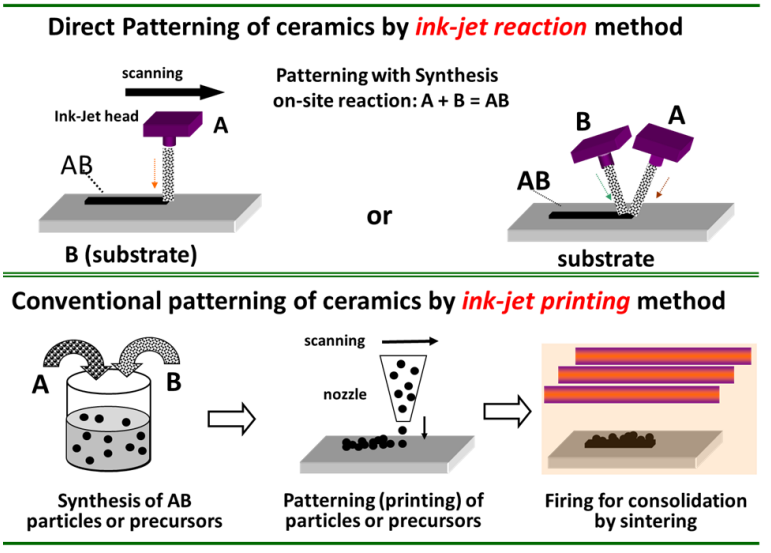

Figure 9. The conventional patterning require post-firing for the consolidation and fixing of particles or their precursors like sols, gels, etc. after their printing.

The present technique has many merits as follows: (1) it needs simple equipment that is easy to control, (2) the process is therefore very safe and harmless, (3) it allows "Direct Patterning" without masking, etching or complicated surface treatments, (4) it needs fewer reactants and lower energy and cost and (5) it is easy to recover the reactants. Therefore, our "Direct Patterning" methods should be economically and environmentally friendly, avoiding excess consumption of energy and resources, and minimizing emission of waste, for example excess heat and gaseous by-products like CO_2 and H_2O. Furthermore, our direct-patterning of ceramics to allow to fabricate TiO_2 patterns on glass substrate on a hot plate (275°C) by Ink-jetted of a Ti precesor solution [Figure. 11]. They are dense and reached 400nm thick by 20 times overlayed in 20 mins. CeO_2 dense films have also been succeeded similarly , $BaTiO_3$ films need above 600°C in air then cracked easily. A critical review on TiO_2 and ZnO films can be seen in 2013, then (Graphene and their hybrid) have been fabricated in aqueous and non-aqueous solvent by local activation of liquid/solid interfaces have been developed recently [66-68].

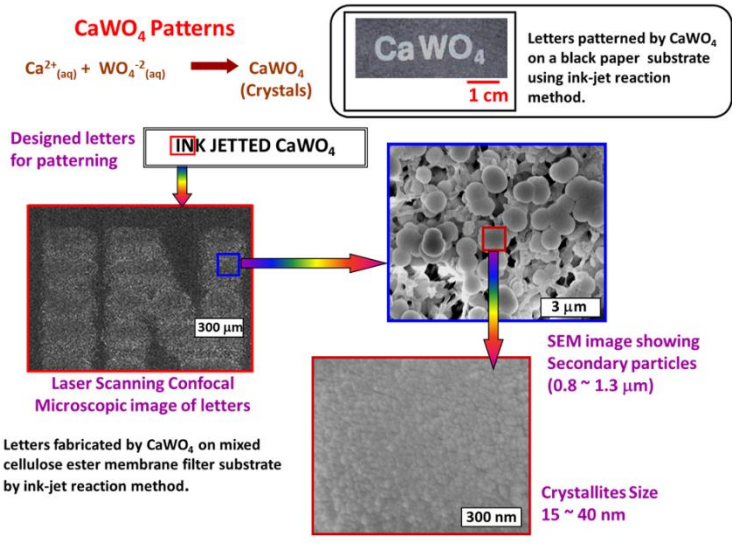

Figure 10. $CaWO_4$ patterning on paper at RT by ink-jet Method.

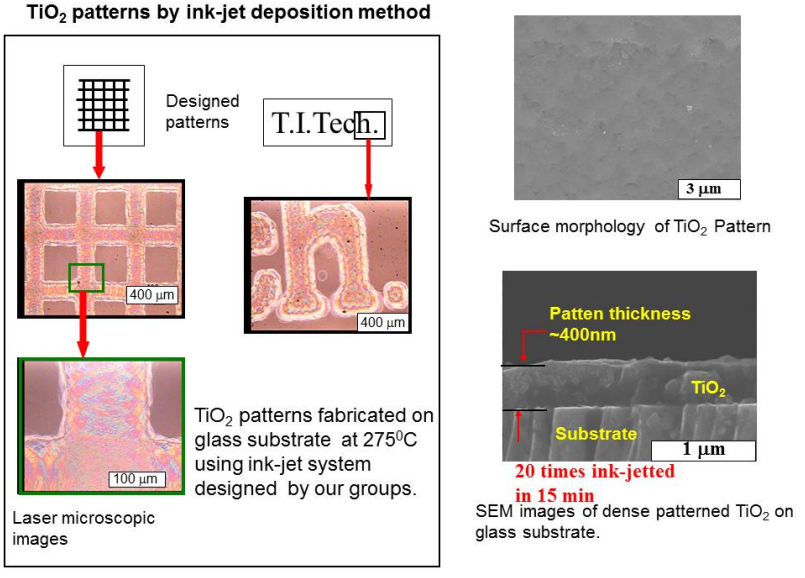

Figure 11. TiO_2 patterns by Ink-Jet Deposition Method.

7. Conclusions

Considering themodynamical factors in the materials and theirprocessings, we have been proposed Soft Solution Processing(SSP) for advanced materials particularly ceramics, because ceramics have generally been fabricated by highly energy consuming processes like multi-step processes including powder synthesis, shape forming and shape fixing, or more energetic processes usinggaseous molecules, atoms and/or ions under vacuum. The SSP has been developedfrom Soft Chemistry (ChimieDouce), which aims low energetic synthesis ofinorganic substances using aqueous solutions as precursors or reaction media. SSP targets to fabricate directly shaped/sized/located and/or oriented materialsrather than synthesis of substances in solutions with minimum steps because shape forming and shape fixing seem to consume more energies for ceramic materials rather than their syntheses.

We have developed (1) Polymelized (or Polymeliz-able) Complex Methods to prepare ceramic powders with homogeneous compositions, (2) Hydrothermal Methods to prepare well crystallized shaped ceramic particles. Furthermore, we have succeeded to prepare (3) various ceramic films and patterns on substrates directly in/from solution(s) without post-firing as the developments of SSP. We believe the SSP, which have learned from nature but not limited in natural products like biominerals, should become more important for near future to establish “sustainable societies” if possible.

References

[1] M. Yoshimura, et al., J. Mater. Res. 13 (1998) 796.
[2] idem. J. Mater. Chem. 8 (1998) 2043; and 9 (1999) 77.
[3] idem. MRS bulletin, Special Issue of Soft-Solution Processing 25 (2000) 12.
[4] M. Yoshimura, J. Mater. Sci., 41 (2006) 1299.
[5] D. Kai, et. al.,Green Chem., 18 (2016) 1175.
[6] Y. S. Lee, Nanostructured materials, in Self-Assembly and Nanotechnology: A Force Balance Approach, John Wiley & Sons, Inc., Hoboken, NJ, (2008) pp. 183–219.
[7] Harry K. Charles Jr., Johns hopkinsApl Technical Digest, 26, (2005) 402.
[8] J. Y. Fan, X. L. Wu, P. K. Chu, Pro. Mater. Sci. 51 (2006) 983.
[9] B. K. Kim, G. G. Lee, G. H. Ha, D. W. Lee, Metals and Mater.5, (1999) 109.
[10] T. Kagnayaa, et.al, Wear, 267 (2009) 890.
[11] W. Kuch, Nat. Mater.2 (2003) 505.
[12] C. R. Nash, J. C. Fenton, N. G. N. Constantino, P. A. Warburton, J. Appl. Phys.116 (2014) 224501.
[13] F Schmidl, Superconductor Sci. and Technol, 8 (1995) 9.
[14] R. J. R. Uhlhorn, K. Keizer and A. J. Burggraaf, J. Memb. Sci., 66 (1992) 259.
[15] M. A. Meyers, A. Mishra, D. J. Benson, Prog. Mater. Sci. 51 (2006) 427.
[16] T. Gong, J. Xie, J. Liao, T. Zhang, S. Lin, Y. Lin, Bone Research 3 (2015) 15029.
[17] L. Feng, Adv. Mater.14 (2002) 1857.
[18] T. Guo, Cryst. Eng. Comm. 17 (2015) 3551.
[19] N. M. Ghazali, Nanoscale Res Lett.9 (2014) 120.
[20] W. J . Dawson, Am. Ceram. Soc., Bull.67 (1988) 1673.
[21] M. Yoshimura and H. suda, “Hydroxyapatite and Related Materials,” edited by P. Brown, (CRC Press, 1994) 45.
[22] M. Kakihana and M. Yoshimura, Bull. Chem. Soc. Japan 72 (1999) 1427.
[23] M. Kakihana: J. Sol-Gel Sci. and Tech. 6 (1996) 7.
[24] M. Kakihana, and M. Yoshimura et al., J. Appl. Phys. 71 (1992) 3904.
[25] M. Kakihana and K. Domen, MRS Bull 25 (2000) 27.
[26] K. Byrappa and M. Yoshimura, “Handbook of Hydrothermal Technology,” (Noyes Publications, Park Ridge, NJ, USA 2001).
[27] M. Yoshimura, H. Suda, K. Okamoto and K. Ioku, J. Mater. Sci. 29 (1994) 3399.
[28] E. Tani, M. Yoshimura and S. Somiya, J. Am. Ceram. Soc. 66 (1983) 11.
[29] idem. ibid 64 (1981) c-181.
[30] M. Yoshimura and S . Somiya, Mater. Chem. and Phys. 61 (1999) 1.
[31] E. Tani, M. Yoshimura and S . Somiya, J. Mater. Sci. Lett.1 (1982) 461.
[32] M. Yoshimura, S -T. song and S . Somiya, YogyoKyokaishi 90 (1982) 91.
[33] S . Somiya, M. Yoshimura, H. Toraya and Y. Fushii, Z. Anorg. Allgem. Chem. 540/541 (1986) 251.
[34] A. Ahniyaz, T. Fujiwara and M. Yoshimura, J. Nanoscience and Nanotechnology 4 (2004) 233.
[35] K. Ioku, M. Yoshimura and S . Somiya, Nippon Kagaku Kaishi (J. Chem. Soc., Japan), 1988 (no. 9) 1565.
[36] M. Yoshimura, F. Koh, P. Sujaridworakun, T. Fujiwara, D. Pongkao and A. Ahniyaz, Mater. Sci. and Engineering C 24 (2006) 521.
[37] S -E. Yoo, M. Yoshimura and S . Somiya, J. Mater. Sci. Letter 8(5) (1989) 530.

[38] K- S . Han, S -W. Song, T. Watanabe and M. Yoshimura, Electrochem. andSolid State Lett. 2 (1999) 63.
[39] A. Ahniyaz, T. Fujiwara, S -W. Song and M. Yoshimura, Solid State Ionics 151 (2002) 419.
[40] S -H. Yu, T. Fujino and M. Yoshimura, J. Mag. and Mag. Mater. 256 (2003) 420.
[41] S -H. Yu and M. Yoshimura, Adv. Funct. Mater.12 (2002) 277.
[42] S -H. Yu, J . M. calderonmoreno, T. Fujiwara, T. Fujino, R. Teranishiand M. Yoshimura, Langmuir 17 (2001) 1700.
[43] S -H. Yu and M. Yoshimura, Adv. Mater.14 (2002) 276.
[44] T. Taniguchi, N. Sakamoto, T. Watanabe, N. Motsushito, M. Yoshimura, J. Phy. Chem. C 112 (2008) 4884.
[45] T. Taniguchi, T. Watanabe, N. Sakamoto, N. Motsushito, M. Yoshimura,Cryst. Growth & Design 8 (2008) 3725.
[46] M. Yoshimura, S -E. Yoo, M. Hayashi and N. Ishizawa, Japan J. Appl. Phys. 28 (1989) l2007.
[47] S -E Yoo, M. Hayashi, N. Ishizawa and M. Yoshimura, J. Am. Ceram. Soc. 73 (1990) 2561.
[48] K. Kajiyoshi, M. Yoshimura, et al., ibid.79 (1996) 613.
[49] K. Kajiyoshi, M. Yoshimura, et al. J. Mater. Res. 11 (1996) 169.
[50] W- S. Cho, M. Yoshimura, et al., Appl. Phys. Lett.66 (1995) 1027.
[51] W- S. Cho, M. Yoshimura, et al., Appl. Phys. Lett.68 (1996) 137.
[52] W- S . Cho and M. Yoshimura, Euro. J. Solid State and Inorg.Chem. 34 (1997) 103.
[53] W- S .Cho and M. Yoshimura, Solid State Ionics 100 (1997) 143.
[54] T. Watanabe, W- S .Cho, W. L. Suchanek, M. Endo, Y. Ikuma and M. Yoshimura, Solid State Science 3 (2001) 183.
[55] K-S Han, S -W. Song and M. Yoshimura, Chem. of Mater. 10 (1998) 2183.
[56] S -W. Song, K- S . Han and M. Yoshimura, J. Am. Ceram. Soc. 83 (2000) 2839.
[57] K- S . Han, S -W. Song, H. Fujita and M. Yoshimura, ibid.85 (2002) 2444.
[58] T. Watanabe, H. Uono, S -W. Song, K- S . Han and M. Yoshimura,J. Solid State Chem. 162 (2001) 364.
[59] W- S . Cho and M. Yoshimura, J. Mater. Res. 12 (1997) 833.
[60] S -H. Yu and M. Yoshimura, Chem. of Mater.12 (2000) 3805.
[61] Z. Wu and M. Yoshimura, Solid State Ionics 122 (1999)161.
[62] J -H. Lee, N. Kumagai, T. Watanabe and M.Yoshimura, Solid State Ionics 151 (2002) 11.
[63] S -W. Song, H. Fujita and M. Yoshimura, Adv. Mater.14(4) (2002) 268.
[64] T. Fujiwara, Y. Nakagawa, T. Nakaue, S -W. Song, R. Teranishi, T. Watanabe and M. Yoshimura, Chem. Phys. Letters 365 (2002) 369.
[65] R. Gallage, A. Matsuo, T. Fujiwara, T. Watanabe, N. Motsushito, M. Yoshimura, J. Electtroceram. 22, (2008) 33.
[66] M. Yoshimura, J. Solid State Electrochem. 12 (2008) 775.
[67] J.-J. Wu, W-. P. Liao, M. Yoshimura, Nano Energy, 2 (2013) 1354.
[68] J. Senthilnathan, K. Sanjeev Rao, M. Yoshimura, J. Mater. Chem. A, 2 (2014) 3332.

Available online at www.sciencedirect.com

ScienceDirect

Procedia Engineering 00 (2017) 000–000

Procedia Engineering

www.elsevier.com/locate/procedia

Sustainable Civil Engineering Structures and Construction Materials, SCESCM 2016

Societal burden and engineering challenges of ageing infrastructure

Klaas van Breugel[a,*]

[a]*Technical Univerisity Delft, Faculty of Civil Engineering & Geosciences, Stevinweg 1, 2628 CN Delft, The Netherlands*

Abstract

Ageing is an inherent feature of nature and, hence, of materials, structures and systems. Yet, it seems a rather new topic in both science and engineering. The main reason for increasing attention for ageing as a topic is the growing awareness that, particularly in industrialized countries, ageing of our assets is a financial burden for the society. It touches our environment and a country's economy. It affects the overall sustainability of our planet and deserves, therefore, our utmost attention. In this contribution the urgency and challenges of ageing of concrete structures are addressed. Recent estimates of the extent of the issue and how ageing problems are dealt with in different disciplines, reactive or pro-active, are mentioned. The complexity of ageing problems will be evaluated by looking in more detail to the evolution in concrete mix design and the consequences thereof for the long-term performance of concrete structures. In this evaluation different kinds of driving forces contributing to ageing will be identified. Emphasis will be on ageing of concrete infrastructure and the need of research on ageing phenomena will be addressed.

Peer-review under responsibility of the organizing committee of SCESCM 2016.

Keywords: ageing; infrastructure; risks; societal impact; concrete; research investment.

1. Infrastructure – Backbone of a country's prosperity

Architecture has been defined as the *art* and *science* of *designing* and *constructing* buildings and other physical structures for human shelter or use. In this definition the word shelter is meant in the broadest sense of the term. Going back to ancient times people needed shelter for protection against storms, rain and snow, direct sun shine and cold weather. For protection against hostile tribes cities were built surrounded by massive city walls. Dykes were built to protect against floods. Besides the need for shelter an increasing need for mobility emerged. For mobility of people roads and waterways were built. Aqueducts were built to transport water over long distances. With the

* Corresponding author. Tel.: +31 (0)15 27 84954;
E-mail address: k.vanbreugel@tudelft.nl

Peer-review under responsibility of the organizing committee of SCESCM 2016.

industrial revolution there was also an increasing need of energy and energy transport, requiring the design and construction of energy supply systems. To save densely populated cities from catastrophic water pollution, sewage systems were designed and installed. Large railway systems were built to enable long-distance transport of people and goods by train. Via bridges, viaducts and tunnels otherwise isolated transport networks became connected. All this illustrates that a modern society is inconceivable without a well-developed physical infrastructure. An infrastructure which, according to Long [1], accounts for about 50% of the country's national wealth.

When putting this in a global perspective, the infrastructure's value has been rated at € 37 trillion [2,12]. This is the value of the *existing* infrastructure, which is considered crucial for the prosperity and well-being of our society. In this respect Gann [3] argues that "The construction's significance to wealth creation and quality of life extends *beyond* its direct economic contribution. The products create an infrastructure that supports existing and newly emerging social and economic activities". And he continues saying; "If inadequate or inappropriate buildings and structures are produced, or they are poorly maintained and adapted, then social and economic life is compromised".

In a recent study of the McKinsey Global Institute [2] estimates were published of future investments in infrastructure worldwide needed to ensure economic stability and growth. In order to catch up with the prognosticated economic growth an investment of more than € 41 trillion was considered necessary in the period 2013-2030. This figure included the infrastructure for transport (roads, ports, rail, airports), water, telecommunications and power plants. This amount was based on an evaluation of money spent on infrastructure in 84 countries, accounting for more than 90% of the global gross domestic product (GDP). Table 1 gives the breakdown of investments over different categories.

Table 1. Estimated needs for global infrastructure in different categories in the period 2013-2030 [2].

Category	Reference	Required investment [4]
		× € 1,000,000,000,000
Roads	OECD[1]	12.2
Rail	OECD	3.3
Ports	OECD	0.5
Airports	OECD	1.4
Power	IEA[2]	8.8
Water	GWI[3]	8.4
Telecommunication	OECD	6.8
Total		41.4

1) Organization for Economic Co-operation and Development
2) International Energy Agency
3) Global Water Intelligence
4) Conversion rate 2013: 1 US$ = € 0.73

There is no doubt: economic stability and growth are unconceivable without an appropriate infrastructure. Without this infrastructure the economy would come to a complete stop. The infrastructure, however, is subject to *ageing*. Our assets – roads, railways, energy infrastructure, etc. - are still in use, but many of them beyond their initially presumed lifetime. The ageing process to which our assets are subjected is not a matter of bad luck or poor workmanship. In essence it is a natural law. If ageing and its potential impact on the quality of a country's infrastructure is not well diagnosed, this may lead to a situation of uncertainty or even societal instability. It is for this reason that stakeholders want to increase their knowledge and perception of ageing phenomena. Owners want to know how long it will take before on-going ageing processes require intervention or result in damage or even fatal failure. For this purpose reliable predictive tools are needed to forecast the rate and impact of ageing processes.

2. Ageing as a general phenomenon

2.1. The omnipresence of ageing

Ageing is everywhere around us [4]. Huge mountains seem to keep their shape, but from a closer look at the surface of rocks we learn that this surface gradually changes. Snow, rain, frost, light, wear, wind and sunshine are powerful enough to crumble the strongest rock. Mountains age! Like mountains, also man-made infrastructure works are exposed to climate conditions and change their performance, beit in a very slow process of ageing. As indicated in the foregoing, the infrastructure and industrial facilities can be considered as the 'physical hardware' of a modern society. All this hardware is ageing. Sometimes for better, but generally for worse. Ageing is everywhere! The ubiquitousness of ageing is an inherent feature of materials, structures and systems, either natural or man-made.

2.2. Driving forces

In general terms ageing is defined as a change of performance with elapse of time. It is not immediately clear, however, how time *per se* can result in a change of performance. How can a material 'at rest' change its performance? For an answer to this question it is important to realize that time is not a 'loading' to which a material is exposed, but the *domain* in which we describe changes in performance. Time *as such* is not the *cause* of these changes. But if time *as such* is not the cause of changes, what is, then, the cause of changes of a material, structure or system that is, at the macro scale, in a status of 'rest'?

A closer look at any piece of matter tells us that the status of rest only applies to a certain level of observation. Going down to the atomic scale there is motion all the time. Any change of position of atoms, or *basic building blocks*, takes place in the time domain and is considered the origin of ageing of materials. Hence, ageing is an *inherent feature* of materials.

On top of this inherent feature of matter we see, at a little larger scale, a variety of *gradients*, which promote basic building blocks of matter to start moving. These gradients concern, for example, temperature, humidity and radiation, and they may cause changes at the surface of the material. In heterogeneous materials – and below a certain scale all materials are heterogeneous! – numerous interfaces exist. All these interfaces are preferred locations for the occurrence of a variety of gradients. Interfaces also offer sites for chemical and electrochemical activity, resulting in changes of the microstructure with elapse of time.

Porous materials continuously communicate with their environment and never reach a moment of 'rest'. This ongoing communication of these materials, or better, systems, induces alternating stress and strain fields in the system, gradually affecting the micro- and nanostructure of a material and hence its performance.

The foregoing survey illustrates that a status of 'rest' is hardly conceivable. At smaller scale there is motion all the time. Gradients in temperature and stress promote basic building blocks to change their position, resulting in infinitesimally small changes, i.e. ageing. In fact basic entropy laws 'explain' why the basic building blocks of materials want the change position and hence cause ageing. This perception of ageing may enable us to understand ageing phenomena and to develop strategies for mitigating the impact of ageing.

3. **Ageing assets**

3.1. Ageing infrastructure

In the Introduction it has been mentioned that the value of the worlds infrastructure has been estimated at € 37 trillion. When with elapse of time ageing causes a loss of performance of infrastructure buildings, enormous amount of money are involved! Reports from the United States indicate that the effect of ageing on the infrastructure performance has been dramatically underestimated. Hoff [5] refers to a 1990 report of the National Research Council of the USA in which it was indicated that $2 to $3 trillion are needed over the next 20 years to repair all the concrete structures in the USA that were suffering from corrosion or poorly built and maintained. For repair and upgrading of bridges in the USA a budget has been estimated of US$ 140,000,000,000 [6]. In his thorough survey of the state of

US infrastructure Lange [7] quoted the ASCE Infrastructure Report Card [8], which estimates a required investment by 2020 of $ 3.6 trillion for repair and maintenance of infrastructure. This investment was considered a must for ensuring the vitality of the infrastructure as basis for the US economy, but also for accomplishing new sustainability goals. Ageing was mentioned as a prominent issue this respect. Lange [7]: “Ageing is relevant to sustainability because long service life is the best way to make concrete construction more sustainable. Ageing has many attributes, bus materials durability is among the most threatening”.

A substantial part of the infrastructure stock has been built between the fifties and eighties of the past century. The presumed average service life of infrastructure buildings is 50 to 80 years. This means that in the coming decades these structures reach the end of their lifetime and a period of renewal is eminent. Schematically this is shown in Fig. 1. Note that in this figure only the prognosticated cost for replacement of obsolete infrastructure is considered. Costs for maintenance and repair of the structures is not involved, but are huge. According to the Office for National Statistics of the UK 55% of all the money spent in the building industry is spent on new-built and 45% is spent on repair and maintenance [10].

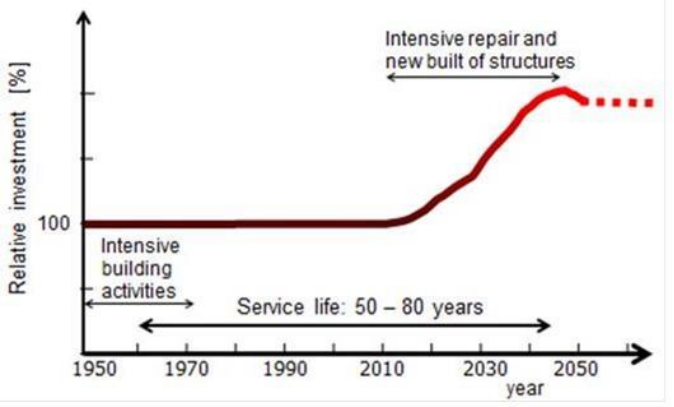

Figure 1 Stages in the lifetime of buildings: End of the lifetime of many structures is eminent [9].

It has to be mentioned that an assumed service life of 50 to 80 years applies to structures built according to, at that time, modern standards and presupposes good workmanship and, hence, good quality structures. In upcoming economies the quality of the infrastructure and the estimated service life of structures can substantially differ from the above mentioned figures. The average service life of civil buildings in China has been reported to be 20-30 years and of marine ports 10-20 years [11]. This is much shorter than the above mentioned 50 to 80 year service life required for many large infrastructure projects in Europe and further emphasizes the need of serious consideration of ageing phenomena.

3.2. Ageing plants

Another category of infrastructure where ageing is a major issue is that of large (petro)chemical and power plants. A brief summary of data, facts and concepts is given below.

3.2.1. Chemical plants

Chemical plants and refineries are vital for production of a variety of products. The size and complexity of chemical plants make them vulnerable for accidents. Chemical plants have got their present size through a process of gradual expansion. Subsequent extensions of plants were designed according to different codes and built with different materials while using different building technologies. Whereas the typical life cycle of a plant has been estimated at 25 years, the ‘effective’ age of large plants is highly heterogeneous with respect to both its real age and its functional age. Because of this heterogeneity it is not easy to judge the actual state of ageing of these plants.
Research Report RR 8238 “Plant ageing study” of the Health and Safety Executive [13] gives an overview of ageing issues in chemical plants. The report gives definitions of ageing and discusses the impact of ageing on plant safety.

Based on three principal databases of three incidents reports, i.e. RIDDOR [14], MARS [15] and MHIDAS [16], the relevance of ageing was illustrated. The MARS study showed that approximately 60% of incidents could be related to technical integrity and, of those, 50% have ageing as a contributory factor. Hence, ageing is a contributory factor in 30% of the incidents. The percentage of incidents with ageing as a contributory factor is considered likely to increase with time as assets age. Ageing may affect the installations, piping and containments as well as the Electrical, Control and Instrumentation (EC&I) equipment. Figure 2 shows the results of the MARS incidents with ageing as the cause of failure.

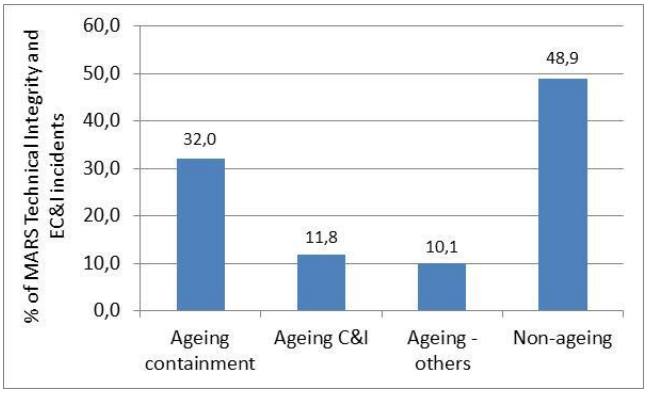

Figure 2 Proportion of incidents on chemical plants with ageing as the cause (After [15]; MARS study).
(EC&I: Electrical, Control & Instrumentation equipment)

3.2.2. Nuclear Power Plants

Maybe more than in any other industrial sector ageing is a key-issue in the nuclear industry. In the 1990s the International Atomic Energy Agency (IAEA) [17] started publishing a comprehensive set of reports on ageing management. The urgency for doing this was the fact that the majority of existing nuclear power plants had reached an age of 20-30 years. These plants were then old enough to discover new ageing phenomena that had slowly developed over the preceding decades. Moreover, new ageing phenomena were emerging as a result of more severe service conditions associated with increased plant performance, e.g. through implementation of the long-term operating experience obtained and/or the application of new technologies.

Even though predictions of the consequences of failure of components of a nuclear power plants vary and can be contradictory, there is no doubt that major accidents should be prevented at ‘all’ costs. For that reason emphasis in this sector is on *proactive* management of ageing. This in contrast with a ‘run to failure’ strategy, whereby components are replaced once they fail. The primary aim of proactive ageing management programs is to ensure the availability of safety functions throughout the service life of the plant. Moreover, effective management of ageing is also essential for achieving the desired plant performance and profitability of the plant, which is, in the end, of importance for the society as a whole.

The aim of materials ageing management of structures, systems and components is to maintain the design safety margins above the specified requirements. Based on experience it is known that many failures are the result of ageing mechanisms, such as general and local corrosion, erosion-corrosion phenomena, radiation, thermal embrittlement, fatigue, creep, vibration and wear [17]. To ensure a high level of plant safety it is recommended to manage ageing effectively and proactively. Effective proactive ageing management presupposes that we know how far we actually stay away from the moment a material, structural component or system will fail. This, on its turn, presupposes that we have predictive models for the relevant ageing mechanisms and that we are able to monitor the progress of degradation with time accurately and reliably [12]. In this respect the effect of radiation on the long-term properties of materials is a serious point of concern. Gamma radiation does affect the microstructure of cement paste. In the late fifties it has been reported already that the compressive strength of the primary reactor shield in the Oak Ridge National Laboratory-Graphite Reactor was decreased within the first layers, i.e. within one foot of

ordinary concrete, due to radiation [18]. Since then a negative effect of radiation on the compressive strength of concrete has been confirmed several times (see for example Basyigit et al [19].

Not only the cement paste, but also the aggregate may suffer from radiation. According to William et al. [20] the reactivity of silica-rich quartz to alkali can increase significantly by exposure to nuclear radiation, thus increasing the risk of alkali-silica reaction in concrete containing aggregates that are otherwise known as typically nonreactive.

According to the IAEA report Nr. 62 [17], radiation embrittlement that leads to changes in bulk material properties has been successfully modelled already. The predictability, however, of corrosion, wear and high cycle fatigue, however, which produce changes at material surfaces and interfaces, was considered relatively low. The resulting uncertainty about the performance of vital plant components has caused significant nuclear power plant unavailability and increased costs for operation and maintenance.

Important to mention is that operating experience in the nuclear industry has revealed degradation and failures caused by previously unrecognized ageing mechanisms. Hence, the IAEA stated that, in addition to improving the understanding and predictability of known ageing mechanisms, there is a need to develop technology and techniques for early detection of new ageing mechanisms. Sensitive and reliable monitoring and control devices are needed and thorough understanding of running processes in a plant. Particularly performance of materials under coupled loads requires more research [20]. In-depth mono-scale and multiscale models are among the promising strategies to address these complex problems [21].

4. Strategies to mitigate the impact of ageing

If ageing is an all-present and practically unavoidable phenomenon from which materials, structures and systems always suffer, the question rises how the rate of ageing can be controlled and reduced. For an answer to that question we have to go back to the driving forces of ageing again. Internal interfaces, stress concentrations and different types of gradients were mentioned in this respect. Having this in mind a few basic approaches can be distinguished for decreasing the proneness to ageing, viz: 1) Materials design; 2) Adaptive approach and 3) Symbiosis [12].

4.1. Materials design

Since ageing is an inherent feature of materials, solutions for ageing require interventions at fundamental materials level. Knowing this, solutions for ageing problems can be sought in different directions. At the materials level basically two approaches are conceivable, i.e. the preventive approach and the reactive approach.

a. Materials design - preventive approach

Heterogeneous materials, characterized by many internal interfaces and stress and strain concentrations, are prone to minor damage, i.e. microcracking. Knowing this, designing materials with less internal heterogeneity and hence less internal interfaces and less concentrations of stress and strain, will yield materials that are less prone to ageing. A more homogenous material, however, may also exhibit a higher brittleness. How a material performs in a structure, therefore, depends on the type of loading and load combinations to which the structure is exposed. The price of advanced materials with a reduced proneness to ageing will generally exceed that of traditional materials. Maintenance and repair costs, however, will be lower. Schematically this is shown in Fig. 3a, where the performance with elapse of time of two systems is presented [23,24]. System A is made of a traditional material and system B of a low-ageing material. Fig. 3c shows the evolution of the costs of those systems with time. Taking both the initial costs and the costs for repair and maintenance of the two systems into account, the total life cycle costs of system B will be lower than of the initially chapter system A. In other words: Spending more money initially to ensure a higher quality pays off [25].

b. Materials design - reactive approach

Since materials always exhibit some sort of heterogeneity, and hence of internal concentrations of stress and strains, the occurrence of internal damage can be considered as an unavoidable fact. In that case designing for *self-healing* might be a solutions for ageing problems. Damage is then seen as the *trigger* for starting a self-healing

process that heals the damaged zone. In this way the lifetime of the material can be extended. Figure 3b schematically shows the performance of a structure made with self-repairing material [23,24]. On the occurrence of a small crack or the start of any physical or chemical degradation process, the material gradually starts to repair itself and the structure will regain its original level of performance or a level close to that. The initial costs might be substantially higher (Fig. 3d). The absence of maintenance and repair costs, however, can finally result in a financially positive situation for the owner. It has to be born in mind that also a healed material is still a material that ages!

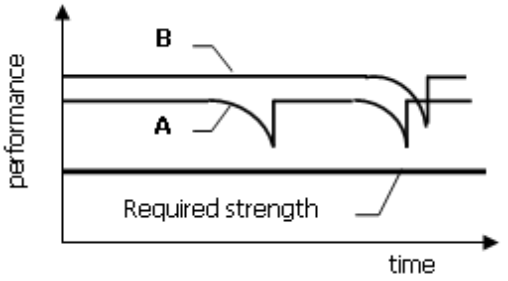

3a Traditional system A and low-ageing system B

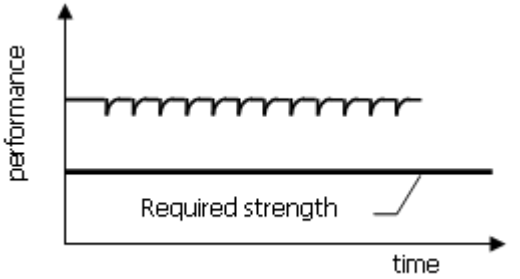

3b System made with self-healing material

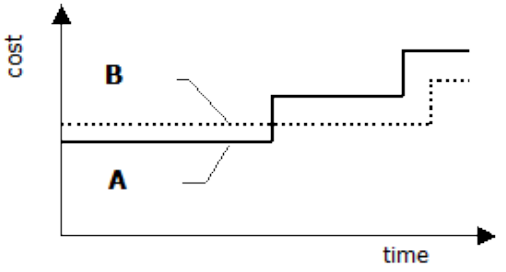

3c Evolution of costs of traditional and low-ageing systems

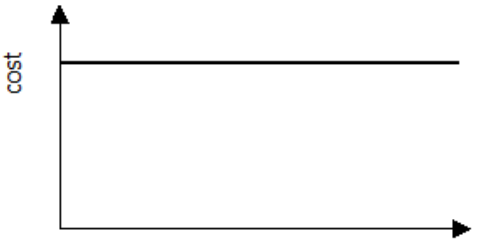

3d Evolution of costs of a self-healing system

Figure 3 Performance of a traditional (A) and low-ageing (B) system. b: Performance of a self-healing system. c: Costs of traditional and low-ageing systems A and B. d: Costs of self-healing system. Note: Interest and inflation not considered [23,24]

4.2. Adaptive approach

Often the materials used for designing and realizing structures are ‘just there’, not leaving room for any modification of the material in order to reduce their proneness to ageing. In those cases it is crucial to know the dominant ageing mechanisms of these materials and the dominant influencing factors. Aware of the relevant ageing mechanisms and influencing factors, structures can be designed in such a way that ageing phenomena will proceed in a controlled way. May be also the exposure conditions can be controlled in order to control or slow down ageing processes, thus extending the lifetime of the structure or system.

4.3. Symbiosis

Particularly in architecture situations are conceivable where ageing can be considered an acceptable, or even wanted phenomenon. Facades which deteriorate in a controlled manner, mirroring the ‘seasons’ of a particular building, may add something to the architectural design. Also structures for which only a short lifetime is required may benefit from inherent ageing phenomena. In this symbiosis approach ageing is not an enemy that has to be beaten, but a collaborator to reach an ageing-stamped goal. It should be emphasized that the symbiosis approach is not a matter of ‘let it happen’. It still requires in-depth understanding of the prevailing ageing process in order not to be surprised by any unexpected discrepancy between desired and actual performance of the structure.

5. Ageing of concrete structures - example

5.1. Observations regarding the performance of concrete bridge deck

If we want to learn about ageing studies of the performance of old structures may be helpful. Such a study has been undertaken by Mehta in 2001 [26]. A brief discussion of this study was published recently [27] and will be presented below.

Mehta analyzed the performance of concrete bridge decks of bridges built in four subsequent periods in the twentieth century. The first period was the period before 1930, the second between 1930 and 1950, the third from 1950 to 1980 and the fourth from 1980 to present. The concrete mixtures used for the bridge decks were characterized by the chemical composition and the fineness of the cement. The cements used in the first period, before 1930, had a C_3S content less than 30% and a Blaine surface of 180 m^2/kg. Consequently the rate of hydration was low. The performance of many bridge decks made with these cements was quite good.

The cements used in the second period were ground finer, to a Blaine fineness between 180 and 300 m^2/kg. The construction and building technology used for the bridge decks were similar to those used in the first period. The authors reported that the bridge decks built in the second period were less durable than those built before 1930.

The structures that were built between 1950 and 1980 appeared to have more durability problems than those built before 1950. The cements used in this period had a fineness up to 400 m^2/kg and a C_3S content beyond 60%. With the aim to get a denser and more durable concrete the w/c ratio was lower than in the first two periods. The higher C_3S content and the higher fineness of the cement had increased the early strength of these mixtures. This made it possible to build faster. This, however, had resulted in a higher probability of early-age thermal cracking and, on top of that, higher autogenous shrinkage of the low water-cement ratio mixtures. The higher proneness to early-age (micro)cracking was the most plausible reason for durability problems at later ages.

In the fourth period the tendency to go for higher strengths continued. Generally this was realized by using mixtures with a low water-binder ratio. The use of low water-binder mixtures further increased the risk of cracking. For bridge decks moderate strengths between 30 and 45 MPa were found. Among 29 bridge decks the cracking in 44 MPa bridge decks was twice that in 31 MPa bridge decks.

5.2. Ageing of more advanced concrete mixtures – possible causes

Mehta's inventory of the performance of bridge decks illustrates how the pressure from the market to build faster has created a demand for mixtures with a high early strength. This was made possible by using finer cements with a higher C_3S content. The price of this, however, was a higher probability of early-age cracking of the bridge decks.

Generally speaking it holds that for realizing thinner and more slender structures concretes with a higher final strength are required. A high final strength is attainable by reducing the water-binder ratio. The use of (super)plasticizers has made it possible to reduce the water-binder ratio of concrete mixtures to values even below 0.2. With these low water-binder ratio mixtures dense concretes are obtained with a very low permeability. This is good for the concrete's resistance against ingress of aggressive substances. At the same time, however, the concrete's proneness to (micro)cracking increases, mainly because of increased autogenous shrinkage.

Another reason for a higher cracking risk of high strength and ultra-high strength concretes are the high temperatures that occur as a result of high cement contents. By optimizing the particle packing of the aggregate fractions the amount of cement, and hence the peak temperatures, can be reduced. A low cement content is also considered positive from the sustainability point of view (lower carbon footprint). A low cement content, however, also has a drawback: it reduces the inherent self-healing capacity of the concrete. From the self-healing point of view a not too low cement content and the use of 'old', coarsely ground cement is favorable. This partly explains the outcome of Mehta's inventory that old bridge decks performed better than newer ones. In the terminology of this paper we would say that the old concrete mixtures with coarse cement and with a low C_3S content were less prone to ageing than modern mixtures with finely ground cements with a high C_3S content. Moreover, it lends support to the plea of Aitcin et al [28] for using 'good old' Type I/II clinker if good performance of concrete structures is our goal.

6. Investments for the research agenda in view of mitigating the impact of ageing

In the forgoing sections it has been explained that ageing of infrastructure buildings is a huge financial burden for the society. A possible way to reduce this burden is by reducing the maintenance costs and extending the lifetime of infrastructure. The possibilities for realizing savings on the long-term were briefly addressed in section 4 (see also Fig. 3). In that section it was indicated, however, that for generating saving higher initial costs have to be faced. A related question is how much money we have to spend in research that might lead to those savings. A few thoughts on this will follow below (see also [12]).

In the Introduction the global value of the infrastructure stock has been estimated at € 37 trillion. Let us assume an average lifetime of these infrastructure assets of 50 years. Each year € 740 billion has then to be spent on replacement of obsolete assets. Let us further assume that through dedicated research the average lifetime can be increased by 10%, i.e. from 50 to 55 years. The yearly replacement costs would then decrease to from € 740 to € 670 billion. This is a reduction of replacement costs of € 70 billion per year. Let us assume that for saving these € 70 billion we have to invest 20% of this amount in research, i.e. € 14 billion per year. Let us further assume that 50% of the required research money, i.e. € 7 billion, has to be spent on management-oriented research and the other 50% on science-oriented research on materials and structures. A part of this science-oriented research has to be spent on ageing research. A reasonable, though conservative assumption is that 10% of science-oriented research, i.e. € 0.7 billion per year, should be spent on fundamental ageing research. This € 0.7 billion is 5% of the required research budget for realizing the savings of yearly replacement costs and only 1% of the targeted savings. Schematically this is shown in figure 4. By varying the assumptions in this exercise other values for required investments are obtained, but do not change the order of magnitude of these figures. If we judge the required research budget on ageing against the savings that can be realized the conclusion is justified that research pays off!

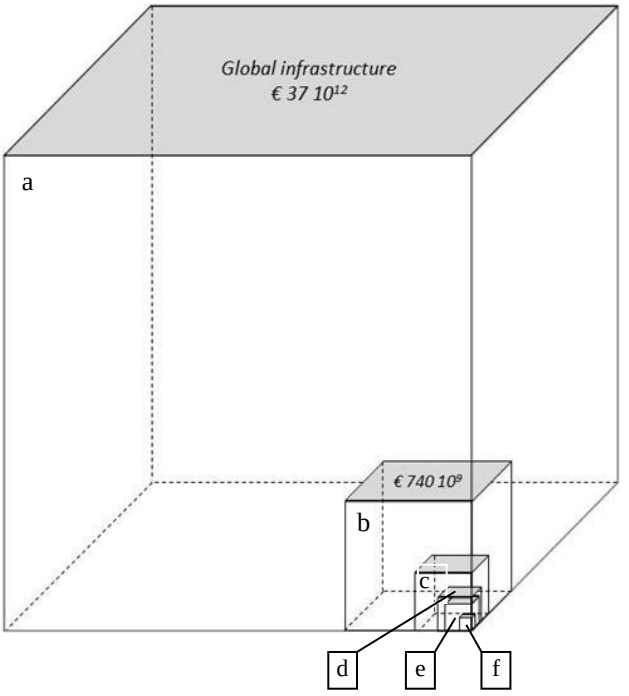

a. Value of global infrastructure:
€ 37 10^{12}

b. Annual replacement cost of assets based on mean lifetime of 50 years:
€ 740 10^{12}

c. Annual savings if service life is increased by10%:
€ 70 10^{9} /year

d. Investment in research, 20% of generated savings:
€ 14 10^{9} /year

e. Investment in fundamental materials research:
€ 7 10^{9} /year

f. 10% of materials research to be spent on ageing:
€ 0.7 10^{9} /year

Figure 4 Schematic presentation of required investment in ageing research for realizing an extension of the mean service life of infrastructure of 10%. (interest / inflation not considered). Estimated average lifetime 50 years (after Van Breugel et al [12], modified).

7. Discussion and conclusions

The world's infrastructure increases rapidly in volume and complexity. At the same time the well-functioning of a society heavily depends on proper functioning of this infrastructure. To guarantee reliable functioning of the infrastructure an integral, or holistic approach is becoming a prerequisite [29]. In such an integral approach materials aspects are inherently coupled with a variety of aspects like logistics, availability, changes in environmental awareness, aesthetics and land-use planning, to mention only a few of them. The growing complexity of the issue implies that service life design is no longer a matter of only predicting the decay rate, or ageing, of a building material. Today service life design also requires a strategy for ensuring undisturbed operation of transport systems for a predefined period of time under a set of yet unknown changes of the boundary conditions.

The total value of the world's infrastructure is estimated at € 37 trillion. This infrastructure is ageing! With the existence, growth, maintenance and replacement of ageing infrastructure a huge responsibility comes to all actors involved in planning, designing, building and operating our assets. It is a matter of *responsible stewardship* to mitigate the environmental impact that comes along with realizing and operating our infrastructure.

Increasing size and complexity of structures, systems and plants make reliable judgment of the actual state of ageing of our assets extremely difficult. The development of new building materials, today often introduced with the claim of being environmental friendly but for which long-term experience is still lacking, further complicates the whole issue. The consequences of failure of infrastructure buildings, however, can be enormous. Catastrophic accidents on large chemical plants, for example, can result in huge direct losses of life and property. Not to mention the indirect losses, which may easily reach ten times the direct losses. The indirect losses include, for example, the risk of process interruption, interruption of supply of electricity and, as a consequence of this, failing safety systems and loss of confidence in the robustness of our society. Mitigating the probability of ageing-induced failures should have, therefore, a high priority.

Ageing is an *inherent* feature of materials. Hence ageing is an inherent feature of any device, structure, system or plant, simply because they are all made of materials that age. Loss of performance due to ageing is, therefore, different from damage or failures caused by design errors, poor workmanship, production failures or inadequate maintenance. Ageing is a typical materials related issue. This means that dealing with ageing and solving ageing problems require a fundamental materials science oriented approach.

Fundamental research on ageing is recommended in order to improve the tools for accurate and reliable predictions of the long-term performance of ageing infrastructure. Monitoring the performance of old and new structures, made with traditional and new concrete mixtures and different types of cement, may explain why old structures seem to be less prone to ageing than modern structures. From these observations lessons can be learned in view of designing structures with a low susceptibility to ageing.

Like many other industries, also the building industry is under pressure. Structures have to be realised faster, but with lower environmental impact. Any product, however, realised 'under pressure', irrespective of what kind of pressure, has an inherent tendency to age (entropy principle). To cope with the risk of increasing ageing rates, in-depth knowledge of the performance of materials and structures with elapse of time is needed.

The costs associated with ageing infrastructures is a heavy financial burden for the society and a burden for the environment as well. Controlling ageing-induced degradation processes, and hence reducing costs of new-built and of maintenance of existing infrastructure, contribute to reduce this burden. For developing low-ageing concepts and models we have to invest in research. An example has been presented, illustrating how investments in research can result in savings for the society that far exceed the investments needed to generate these savings. An increase of the average service life of our infrastructure by 10% would save tens of billions of euros each year. The investment to realise these savings was estimated at 20% of these savings. Half of this amount was assumed to be needed for research on materials and structures, of which amount 10% was assumed to be needed for fundamental research on ageing phenomena at the materials level. Setting such targets for savings is not only challenging and a stimulus for research and innovation. The figures also illustrate that caring for our infrastructure finally pays off!

Since ageing is an inherent feature of all materials we know, a better understanding of ageing will potentially improve the way we use materials and how we design and produce structures and systems. In the end a more appropriate use of materials is a matter of responsible stewardship!

Acknowledgements

The Ageing Centre for Materials, Structures and Systems of the TU Delft is gratefully acknowledged for collaborating in preparing this paper.

References

[1] A.E. Long, Sustainable bridges through innovative advances. Institution of Civil Engineers, presented at Joint ICE and TRF Fellows Lecture. 23, 2007.
[2] R. Dobbs R. et al. Infrastructure productivity: How to save $ 1 trillion a year. McKinsey Global Institute, 2013, 88 p.
[3] D.M. Gann, Building innovation: Complex constructs in a changing world. London, Thomas Telford, 2000, 5 p.
[4] K. van Breugel, Caring for ageing infrastructure – Scope, strategy and responsible stewardship. Proc. 3rd. Int. Conf. on Service Life Design for Infrastructures. Zhuhai. 2014.
[5] G.C. Hoff, Integrating durability into the design process. In R.K. Dhir et al. (eds), Proc. Int. Symposium Controlling concrete degradation, Dundee, 1999, 1-14.
[6] Frontier India Strategic and Defence: News, Analysis, Opinion. $140 billion price tag to repair and modernize America's bridges. 2008, 3 p.
[7] D.A. Lange, The relevance of ageing for civil infrastructure: The profession, The politics, The Classroom. Proc. 1st. Int. Conference on Ageing of Materials & Structures, Ed. Van Breugel & Koenders, AMS 2014, Delft, 2014. pp. 17-25.
[8] ASCE "Infrastructure Report Card", http://www.infrastructurereportcard.org/grades, 2013.
[9] K. van Breugel, Global dimension of ageing of infrastructure and our responsibility. The 5th Int. Workshop on Structural Life Management of Power Structures, Korea, 2015.
[10] S. Liles, S. Liles, Our crumbling infrastructure: How the aging of America's infrastructure is a homeland security concern. 2008. 7 p.
[11] K. Li, Z., Chen, H., Lian, H., Concepts and requirements of durability design for concrete structures: an extensive review of CCES01. J. Materials & Structures. 41, 2008, 717-731
[12] K. van Breugel et al. Ageing of materials, structures and systems – An inconvenient truth. Vision document Ageing Centre. Delft. 2015.
[13] P. Horrocks, et al., Managing Ageing Plant – A summary guide. Health and Safety Executive, RR 823, 2010, 41 p.
[14] RIDDOR (abbr.) - Reporting of Injuries, Diseases and Dangerous Occurrences Regulations
[15] MARS (abbr.) European Union Major Hazard Incident Database
[16] MHIDAS (abbr.) World-wide major hazard incident database
[17] IAEA. Proactive management of ageing for nuclear power plants. Safety Report Series No. 62. International Atomic Energy Agency. 2009, 83 p.
[18] T.V. Blosser, R.C. Reid, G.W. Bond, A.B. Reynolds, L.A. Lee, T.O.P. Speidel, D.W. Vroom, M.A. Welt, (1958). A Study of the Nuclear and Physical Properties of the ORNL Graphite Reactor Shield. 1958. 40 p.
[19] C. Basyigit, I. Akkurt, R. Altindag, S. Kilincarshan, A. Akkurt, B. Mavi, R. Karaguzel, The Effect of Freezing-Thawing (F-T) Cycle on the Radiation Shielding Properties of Concretes, Building and Environment, Vol. 41, 2006, 1070-1073. Retrieved July 7, 2009, from http://bcomak.com/dosya/A6.pdf
[20] K. William, Y. Xi, D. Naus, H.L. Graves, A Review of the Effects of Radiation on Microstructure and Properties of Concretes Used in Nuclear Power Plants. U.S. Nuclear Regulatory Commission, 2013, 104 p.
[21] K. van Breugel, Multi-scale modelling: The vehicle for progress in fundamental and practice-oriented research, Proc. 2nd Int. Conf. on Nanotechnology in Construction, Bilbao, 2005.
[22] S. Pareek, Y. Suzuki, K-I. Kimura, Y. Fujikura, Y. Araki, Radiation Shielding Properties and Freeze-Thaw Durability of High-Density Concrete for Storage of Radioactive Contaminated Soil in Fukushima. Proc. 1st Int. Conf. on Ageing of Materials & Structures, Ed. Van Breugel & Koenders. AMS'14. Delft, 2014, 1-9
[23] K. van Breugel, Is there a market for self-healing cement-based materials? Proc. 1st Int. Conf. on Self-Healing Materials. Noordwijk, The Netherlands, 2007, 10 p.
[24] K. van Breugel, Self-healing material concepts as solution for aging infrastructure. Proc. 37th Conf. on Our World of Concrete & Structures, Singapore, 2012, 15 p.
[25] R. Wolfseher, Economical aspects of repair and maintenance. In P. Schweshinger et al. (eds) Proc. 5th Int. Workshop on Materials Properties and Design: Durable reinforced concrete structures. AEDIFICATIO Publishers, 1998, 33-48.
[26] P.K. Mehta, R.W. Burrows, Building durable structures in the 21st century". Indian Concrete Journal, 2001, 437-443.
[27] K. van Breugel, Ageing of old and modern concrete structures – Observations and Research. Proc. 2nd R.N. Raikar International Conference and Banthia-Basheer International Symposium on Advances in Science and Technology of Concrete. Mumbai, 2015.
[28] P.-C. Aitcin, S. Mindess, Back to the future. Concrete International. 37, 5, 2015, 37-40.
[29] N.S. Berke, M.C. Hicks, J. Malone, K.A. Rieder, Concrete Durability – A holistic approach. Concrete International, 27, 8, 2005, 63-68.

Available online at www.sciencedirect.com

ScienceDirect

Procedia Engineering 00 (2017) 000–000

Procedia Engineering

www.elsevier.com/locate/procedia

Sustainable Civil Engineering Structures and Construction Materials, SCESCM 2016

Smart graphene oxide based composite materials and their electric and magnetic stimuli-response

Shang Hao Piao[a], Hyoung Jin Choi[a,*]

[a]*Department of Polymer Science and Engineering, Inha University, Incheon 402-751, Korea*

Abstract

Compared to graphene, the functional groups of graphene oxide (GO) widen its application along with its GO-based composites in various engineering areas. Here, we briefly review their relatively new applications to the areas of both electrorheological (ER) and magnetorheological (MR) fluids under external electric or magnetic fields, respectively when they are dispersed in electrically or magnetically inert medium fluids. All the GO composites are found to exhibit improved ER characteristics compared to that of pure GO, while the GO can be adopted as either a coating layer or an additive in the carbonyl iron based MR fluids.

Peer-review under responsibility of the organizing committee of SCESCM 2016.

Keywords: Graphene oxide, GO-based composites, electrorheological, magnetorheological.

1. Introduction

Both electrorheological (ER) and magnetorheological (MR) fluids, known to be a type of the most significant smart stimuli-responsive materials, which are in general composed of electrically polarizable particles or magnetic particles dispersed in insulating liquid medium, can be controlled by an external electric field or magnetic field, respectively [1-5]. The dispersed particles in the ER fluids can become polarized under an external electric field, to be connected to the neighboring ones forming chain-like structures along the applied electric field direction [6, 7]. On the other hand, the magnetic particles dispersed in the MR fluids shows a similar behavior in the presence of the magnetic field [8, 9]. These structural changes result in the ER and MR fluids, transforming from a liquid-like to a solid-like state within a millisecond upon the applied electric or magnetic fields, and these behaviors are reversible with the fields

* Hyoung Jin Choi. Tel.: +82-32-860-7486; fax: +82-32-865-5178.
E-mail address: hjchoi@inha.ac.kr

Peer-review under responsibility of the organizing committee of SCESCM 2016.

being removed [10, 11]. As the controllable and reversible phase-transitional materials, the ER and MR fluids have been applied for a range of industrial applications in the areas of electro-mechanical or magneto-mechanical control devices such as vibration dampers, microfluidics and shock absorbers [12-17].

Concurrently, while maintaining the characteristics of graphene, graphene oxide (GO), a single-layered exfoliated graphite oxide from graphite fabricated through mechanical or chemical methods, has attracted significant interests as one of the most interesting functional materials with lower electrical conductivity, relatively high polarizability, low cost and scalable production, while maintaining the characteristics of graphene in both academia and industries [18-22]. The presence of the functional groups provides GO sheets amphiphilic with lower electrical conductivity which is appropriate for its electrorheological (ER) application [23, 24]. In addition, its good hydrophilic properties due to the presence of oxygen-functional hydrophilic groups, such as hydroxyl, carbonyl and carboxyl groups not only makes GO readily dispersible in water to form stable colloidal suspension, but also facilitates the preparation of GO-based composites in solution [25-27]. Therefore, graphene/GO-supported materials have attracted significant interest for fascinating both ER and MR effects. The illustration of the ER or MR mechanism of the chain formation in the ER and MR fluids is shown in Fig. 1.

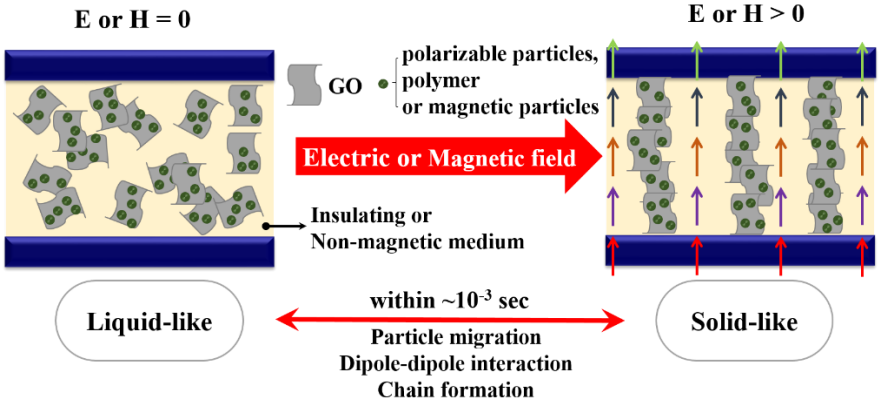

Fig. 1. (a) Schematic diagram of the GO-based composites fluid exhibiting a phase transition from a liquid-like to a solid-like state under an applied electric or magnetic field.

As for ER systems, various GO-based polymeric composites with polyaniline, copolyaniline and poly(p-phenylenediamine), along with core–shell structured polymer–GO microspherical particles with poly(methyl methacrylate), poly(glycidyl methacrylate) and polystyrene (PS) have been recently reported [28-33]. Nanocomposites of GO with various inorganic particles such as titania, silica and alumina are also attempted [34-36]. All these GO composites exhibit improved ER characteristics compared to that of pure GO. The GO was also either added as an additive into magnetic carbonyl iron (CI) particles or coated on the CI surface to improve the dispersibility and settlement problem of CI particle based MR fluids [37, 38]. Furthermore, the GO as a solid surfactant introduced into the GO/PS Pickering emulsion polymerized ER material will be also covered [39].

In this short review, we mainly focus on a variety of GO-based composite materials and their rheological performances under the electric and magnetic fields, respectively. The ER and MR properties of these materials are mainly investigated using a rotational rheometer.

2. Graphene oxide based composite materials

Fabricating a variety of GO/polymer composites as ER materials have attracted increasing attentions, because the various functional groups decorated GO lead to a good dispersion stability in aqueous or in other organic solvents [40, 21]. Among them, GO/ conducting polymer composites were known to be a type of outstanding ER materials. The GO in the composites can effectively prevent an electric short in the ER measurement due to itsrelatively low conductivity. Meanwhile, polyaniline (PANI), a typical conducting polymers, has been evaluated as a prospective

because of their facile fabrication, low cost and high thermal stability [41, 42]. Zhang et al. [28] introduced GO/PANI composite particles by synthesizing from the in situ dispersion polymerization.

On the other hand, to improve the solubility and processability, derivatives of PANI with suitable substitutes were the most promising techniques [43]. Sim et al. [29] prepared GO/poly(2-methylaniline) (P2MAN) by chemical oxidation polymerization. Zhang et al. [44] reported the GO/ ionic N-substituted copolyaniline (NCOPA) composite, which was prepared using a monomer mixture containing ionic sodium diphenylamine sulfonate and aniline, was synthesized by in situ oxidation polymerization. GO acting as a dopant in these oxidation polymerization, could reduce the conductivity of these composites. Furthermore, some other GO/ conducting polymer composites have been reported, such that Cao et al. [30] introduced poly(p-phenylenediamine)/graphene oxide nanoplatelet composites by electropolymerization, and Azman et al. [45] fabricated poly(3,4-ethylenedioxythipohene) (PEDOT)/ graphene oxide hybrid composites by in situ oxidation polymerization.

Actually, the GO based composites combined with insulating polymers can be used as good ER material because of their facile synthesis and low cost. Zhang et al. [32] reported a facile approach for fabricating core-shell structured GO-wrapped amine-modified poly(glycidyl methacrylate) (ami-PGMA) microspheres via an amine-epoxide/carboxyl chemical reaction. Kim et al. [39] prepared polystyrene (PS)–GO microspheres by Pickering emulsion polymerization method, and GO was used as a solid stabilizer.

GO/inorganic materials composites have been also assessed as suitable materials for ER materials with a range of experiments. For example, Yin et al. [34] used a GO layer as a coating shell to fabricated GO-wrapped titania dielectric microspheres via an electrostatic absorbing method and Zhang et al. [35] prepared silica-GO hybrid composite particles by the hydrolysis of tetraethyl orthosilicate (TEOS) in the presence of hydrophilic GO.

As for MR systems, due to fact that the employed magnetic particles are relatively heavier than ER materials, surface treatment or additives are normally added to alleviate the sedimentation issue. Zhang et al. [37] used 4-aminobenzoic acid (PABA) as a grafting agent, and then coated GO plate onto the carbonyl iron (CI) surface to solve the dispersion problems of CI-based MR fluids. Chen et al. [38] added GO to CI-based MR fluids and investigated the MR properties.

3. Rheological characteristics

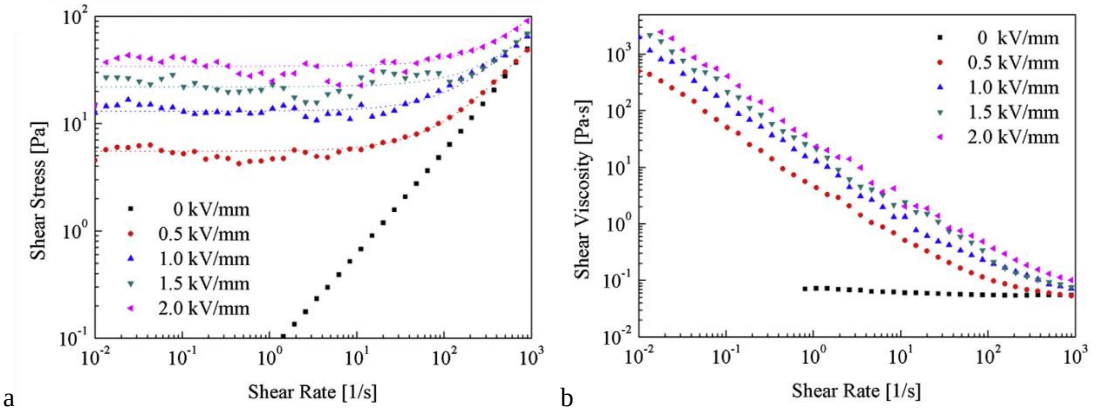

Fig. 2. (a) Shear stress vs. shear rate and (b) Viscosity vs. shear rate of GO/P2MAN composite particles-based ER fluid as a function of shear rate with increasing electric field strengths. The dotted line is generated from Equation (1). (Reprinted with permission from Ref. [29])

The GO/P2MAN composite particles (concentration of 10 vol%) were added into silicone oil (30cs) for the preparation of the ER fluid. Figure 2 shows the flow behavior of GO/P2MAN composite based ER fluid using a rotational rheometer under different electric field strengths. The relationship between shear stress and shear rate was shown in Fig. 2(a). Without an external electric field, the ER fluid exhibits a Newtonian fluid behavior, in which the shear stress increase linearly as a function of shear rate [46]. When a high electric field was applied, sudden increased

shear stress was observed and became higher with the stepwise increasing electric field strength, because the particles were polarized and form chain-like structures, which is known as Bingham fluid behavior [47].

The widely used model for ER fluids, Bingham fluid model, is given below in Eq. (1) with two simplest parameters, the yield stress (τ_y), which is related to the electric field strength and zero shear viscosity (η_0), here τ represents the shear stress, $\dot{\gamma}$ denotes the shear rate [48].

$$\tau = \tau_0 + \eta\dot{\gamma}, \quad \tau \geq \tau_0$$
$$\dot{\gamma} = 0, \quad \tau < \tau_0 \tag{1}$$

The inter-particle interaction force under an applied electric field leads to chain formation, and the chain deformation synchronously happened due to the breaking force by a hydrodynamic shear [46]. In a high shear rate region, the shear stress tends to increases were attributed to the destroyed chain particles have no to time to reform.

Together with the shear stress, the shear viscosity as a function of the shear rate, shown in Fig. 2(b). In the absence of an electric field, the shear viscosity shows Newtonian behavior, which is independent of the shear rate by showing constant shear viscosity. Under an applied electric field, the increased of shear viscosity was due to the formation of the chain structure and shear thinning behavior was observed because the aligned particle chains tended to deformation [49].

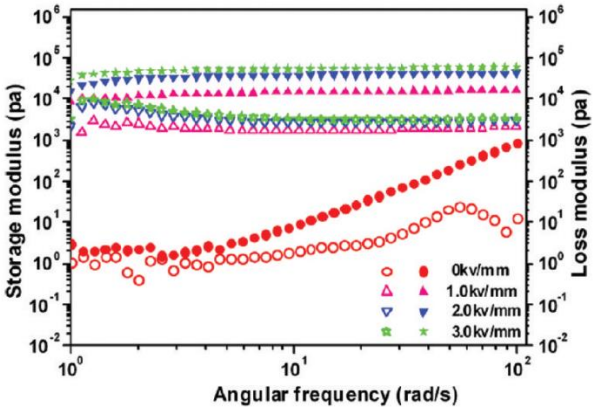

Figure 3. Frequency sweeps for Silica-GO hybrid composite based on ER fluid under different electric fields. Storage modulus: closed symbol. Loss modulus: open symbol. (Reprinted with permission from Ref. [35])

Figure 3 describes the frequency sweep test of the silica-GO hybrid composite based ER fluid under a variety of electric field strengths. The storage modulus (G') is invariably higher than the loss modulus (G") over the frequency range and both G' and G" increased when the electric field strength was increased, indicating that the solid-like property are dominant over liquid-like property in the structure of the ER fluid under the electric field. In addition, the G' or G" was approximately linear, like the liquid behavior [50].

Figure 4 illustrates the shear viscosity of the PS-GO microsphere based ER fluid measured to determine the response under voltage pulse (t = 20 s) and a constant shear rate of 1/s. In Fig. 4, as the electric field was switched on, the shear viscosity increased immediately, and decreased rapidly to a zero-field level when the electric field was switched off, indicating the PS-GO microsphere based ER fluid was quite sensitive to the external electric field [51]. The shear viscosity was in a stable state at the same electric field, and increased with increasing electric field strength.

Figure 5 shows the flow curves of the pure CI and GO/CI based MR fluid. Similar to the ER fluids, the shear stress and shear viscosity curves for both the pure CI and GO/CI particle-based MR fluids showed typical Newtonian behavior without the magnetic field applied. And the GO/CI particle-based MR fluid exhibited higher shear stress and shear viscosity value than pure CI particle-based MR fluid, can be attribute to the higher surface roughness of GO/CI increased the resistance between the adjacent particles. With the applied magnetic field, the two systems showed increased shear stress with increasing magnetic field strength (Fig. 5(a)) and the strong shear thinning behavior was also observed at a fixed magnetic field strength (Fig. 5(b)).

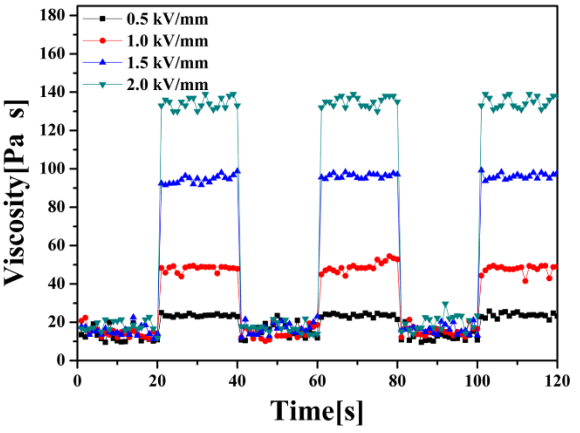

Fig. 4 Viscosity of the PS-GO microsphere based ER fluid (10 vol% particle concentration) in a range of electric field strengths. (Reprinted with permission from Ref. [39])

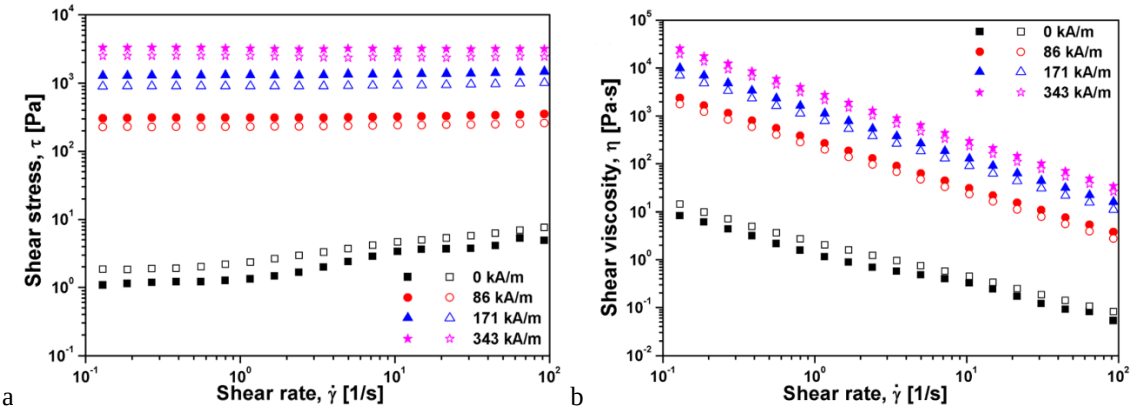

Fig. 5. (a) Shear stress and (b) shear viscosity curves of the pure CI (closed symbols) and GO/CI particle (open symbols) based MR fluids. (Reprinted with permission from Ref. [37])

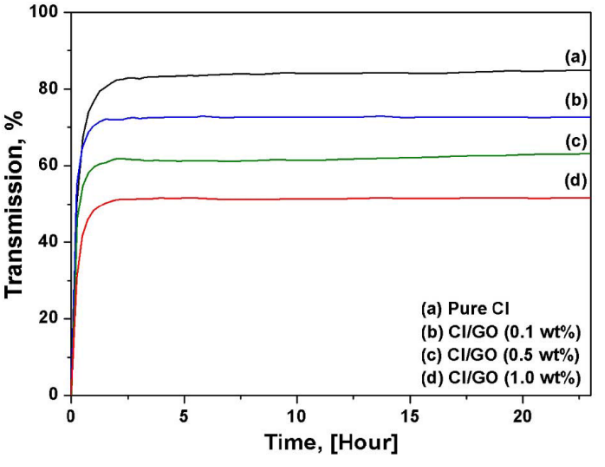

Fig. 6. Transmission as a function of time for pure CI particles and CI/GO mixture based suspensions with different weight ratios of GO. (Reprinted with permission from Ref. [52])

To confirm the dispersion stability of the MR fluid, Zhang et al. [52] performed the sedimentation test of CI based MR fluid with added different weight ratios of GO were investigated using a Turbiscan apparatus as shown in Fig. 6. Apparently, the transmission of the GO added CI based MR fluids was decreased compared to that of the pure CI based MR fluids. In other words, the dispersion stability of CI/GO mixture based MR fluid was more stable, and with more GO concentration, we could confirm the more effective role of the GO additive to reduce sedimentation.

4. Conclusions

In this short review paper, we summarize various GO-based composite materials for both ER and MR fluids, and the analysis of their rheological performances under the electric and magnetic fields, respectively. The GO sheets which are amphiphilic with lower electrical conductivity in the GO/ conducting polymer composites can effectively prevent an electric short in the ER measurement, being appropriate for its ER application. GO based composites combined with insulating polymers and GO/ inorganic materials composites have been also assessed as suitable materials for ER materials. For MR fluids, surface treatment or additives using GO are contributing positive influence to the serious dispersion problems. Thus, it could be concluded that the GO based composites can be developed for commercializing the advanced ER and MR fluids in a wide range of industries.

Acknowledgements

This work was supported by a research grant from National Research Foundation, Korea (2016).

References

[1] H.J. Choi, M.S. Jhon, Electrorheology of polymers and nanocomposites, Soft Matter, 5 (2009) 1562-1567.
[2] P. Hiamtup, A. Sirivat, A.M. Jamieson, Strain-hardening in the oscillatory shear deformation of a dedoped polyaniline electrorheological fluid, J. Mater. Sci. 45 (2010) 1972-1976.
[3] J. Jiang, Y. Tian, Y. Meng, Structure parameter of electrorheological fluids in shear flow, Langmuir, 27 (2011) 5814-5823.
[4] J.L. Goncalves, A.J.F. Bombard, D.A.W. Soares, G.B. Alcantara, Reduction of Paraffin Precipitation and Viscosity of Brazilian Crude Oil Exposed to Magnetic Fields, Energy Fuels, 24 (2010) 3144-3149.
[5] B.J. Park, F.F. Fang, H.J. Choi, Magnetorheology: Materials and application, Soft Matter, 6 (2010) 5246-5253.
[6] Y. Cheng, J. Guo, X. Liu, A. Sun, G. Xu, P. Cui, Preparation of uniform titania microspheres with good electrorheological performance and their size effect. J Mater. Chem. 21 (2011) 5051–5056.
[7] J.C. Loudet , P. Poulin , Application of an Electric Field to Colloidal Particles Suspended in a Liquid-Crystal Solvent. Phys. Rev. Lett. 87 (2001) 165503 (4PP).
[8] W.H. Li, Y. Zhou, T.F. Tiam, Viscoelastic properties of MR elastomers under harmonic loading. Rheol. Acta 49 (2010) 733-740.
[9] M. Mrlik, M. Ilcikova, V. Pavlinek, J. Mosnacek, P. Peer, P. Filip, Improved thermooxidation and sedimentation stability of covalently-coated carbonyl iron particles with cholesteryl groups and their influence on magnetorheology. J. Colloid Interface Sci. 396 (2013) 146-151.
[10] J.P. Coulter, K.D. Weiss, J.D. Carlson, Engineering applications of electrorheological materials, J. Intel. Mat. Syst. Str. 4 (1993) 248–259.
[11] Y.M. Han, S.B. Choi, Control of an ER haptic master in a virtual slave environment for minimally invasive surgery applications. Smart Mater. Struct. 17, (2008). 065012 (10pp).
[12] H. Yamaguchi, X.R. Zhang, X.D. Niu, Damping characteristics and flow behaviors of an ER fluid with a piston sine vibration in a viscous damper. Smart Mater. Struct. 19 (2010) 105032 (9PP).
[13] Y.J. Liu, R. Davidson, P. Taylor, Touch sensitive electrorheological fluid based tactile display. Smart Mater. Struct. 14 (2005) 1563-1568.
[14] M. Zhang, X. Gong, W. Wen, Manipulation of microfluidic droplets by electrorheological fluid. Electrophoresis, 30 (2009) 3116-3123.
[15] H. Yamaguchi, X.R. Zhang, X.D. Niu, K. Nishioka, Investigation of Impulse Response of an ER Fluid Viscous Damper. J. Intel. Mat. Syst. Str. 21 (2010) 423-435.
[16] T.F. Tian, W.H. Li, G. Alici, H. Du, Y.M. Deng, Microstructure and magnetorheology of graphite-based MR elastomers, Rheol. Acta, 50 (2011) 825-836.
[17] C. Gollwitzer, M. Krekhova, G. Lattermann, I. Rehberg, R. Richter, Surface instabilities and magnetic soft matter, Soft Matter, 5 (2009) 2093-2100.
[18] A.A. Alhwaige, T. Agag, H. Ishida, S. Qutubuddin, Biobased Chitosan Hybrid Aerogels with Superior Adsorption: Role of Graphene Oxide in CO2 Capture, RSC Adv. 3 (2013) 16011-16020.
[19] X. Zhou, Y. Wei, Q. He, F. Boey, Q. Zhang, H. Zhang, Reduced graphene oxide films used as matrix of MALDI-TOF-MS for detection of octachlorodibenzo-p-dioxin, Chem. Commun. 46 (2010) 6974-6976.
[20] G.Z. Sun, L.X. Zheng, Z.Y. Zhan, J.Y. Zhou, X.B. Liu, L. Li, Actuation triggered exfoliation of graphene oxide at low temperature for electrochemical capacitor applications, Carbon, 68 (2014) 748-754.
[21] D.R. Dreyer, S. Park, C.W. Bielawski, R.S. Ruoff, The chemistry of graphene oxide, Chem. Soc. Rev. 39 (2010) 228-240.
[22] H. Hu, X. Wang, J. Wang, F. Liu, M. Zhang, C. Xu, Microwave-assisted covalent modification of graphene nanosheets with chitosan and its electrorheological characteristics. Appl. Surf. Sci. 257 (2011) 2637-2642.

[23] J. Wang, H. Hu, X. Wang, C. Xu, M. Zhang, X. Shang, Preparation and mechanical and electrical properties of graphene nanosheets-poly(methyl methacrylate) nanocomposites via in situ suspension polymerization. J. Appl. Polym. Sci. 122 (2011) 1866-1871.
[24] J.Y. Hong, J. Jang, Highly stable, concentrated dispersions of graphene oxide sheets and their electro-responsive characteristics. Soft Matter, 2012, 8, 7348-7350.
[25] S. Stankovich, D.A. Dikin, G.H.B. Dommett, K.M. Kohlhaas, E J. Zimney, E.A. Stach, R.D. Piner, S.T. Nguyen, R.S. Ruoff, Graphene-based composite materials, Nature, 442 (2006) 282−286.
[26] S. Stankovich, D.A. Dikin, O.C. Compton, G.H.B. Dommett, R. S. Ruoff, S.T. Nguyen, Systematic Post-assembly Modification of Graphene Oxide Paper with Primary Alkylamines, Chem. Mater. 22 (2010) 4153−4157.
[27] J.L. Chen, X.P. Yan, A dehydration and stabilizer-free approach to production of stable water dispersions of graphene nanosheets, J. Mater. Chem. 20 (2010) 4328−4332.
[28] W.L. Zhang, Y.D. Liu, H.J. Choi, Fabrication of semiconducting graphene oxide/polyaniline composite particles and their electrorheological response under an applied electric field, CARBON, 50 (2012) 290–296.
[29] B.M. Sim, W.L. Zhang, H..J. Choi, Graphene oxide/poly(2-methylaniline) composite particle suspension and its electro-response, Mater. Chem. Phys. 153 (2015) 443-449.
[30] Y.L. Cao, H.J. Choi, W.L. Zhang, B.X. Wang, C.C. Hao, J.Q. Liu, Eco-friendly mass production of poly(p-phenylenediamine)/graphene oxide nanoplatelet composites and their electrorheological characteristics, Compos. Sci. Technol. 122 (2016) 36-41.
[31] W.L. Zhang, Y.D. Liu, H.J. Choi, Y. Seo, Core–shell structured graphene oxide-adsorbed anisotropic poly(methyl methacrylate) microparticles and their electrorheology, RSC Adv. 3 (2013) 11723–11731.
[32] W.L. Zhang, H.J. Choi, Y. Seo, Facile Fabrication of Chemically Grafted Graphene Oxide–Poly(glycidyl methacrylate) Composite Microspheres and Their Electrorheology, Macromol. Chem. Phys. 214 (2013) 1415−1422.
[33] W.L. Zhang, Y.D. Liu, H.J. Choi, Graphene oxide coated core–shell structured polystyrene microspheres and their electrorheological characteristics under applied electric field, J. Mater. Chem., 21 (2011) 6916-6921.
[34] J.B. Yin, Y.J. Shui, Y.Z. Dong X.P. Zhao, Enhanced dielectric polarization and electroresponsive characteristic of graphene oxide wrapped titania microspheres, Nanotechnology, 25 (2014) 045702 (11pp).
[35] W.L. Zhang, H.J. Choi, Silica-Graphene Oxide Hybrid Composite Particles and Their Electroresponsive Characteristics, Langmuir, 28 (2012) 7055−7062.
[36]W.L. Zhang, H.J. Choi, Y.K. Leong, Facile fabrication of graphene oxide-wrapped alumina particles and their electrorheological characteristics, Materials Chemistry and Physics 145 (2014) 151-155.
[37] W.L. Zhang, H.J. Choi, Self-assembly of graphene oxide coated soft magnetic carbonyl iron particles and their magnetorheology, J. Appl. Phys. 115 (2014) 17B508.
[38] K.K. Chen, W.L. Zhang, L. Shan, X.J. Zhang, Y.G. Meng, H.J. Choi, Y. Tian, Magnetorheology of suspensions based on graphene oxide coated or added carbonyl iron microspheres and sunflower oil, J. Appl. Phys. 116 (2014) 153508.
[39] S.D. Kim, W.L. Zhang, H.J. Choi, Pickering emulsion-fabricated polystyrene–graphene oxide microspheres and their electrorheology, Mater. Chem. C, 2 (2014) 7541-7546.
[40] D. Chen, H. Feng, J. Li, Graphene oxide: preparation, functionalization, and electrochemical applications, Chemical Reviews, 112 (2012) 6027–6053.
[41] M.S. Cho, H.J. Choi, W.S. Ahn, Enhanced electrorheology of conducting polyaniline confined in MCM-41 channels, Langmuir, 20 (2004) 202–207.
[42] A. Lengalova, V. Pavlinek, P. Saha, O. Quadrat, T. Kitano, J. Steiskal, Influence of particle concentration on the electrorheological efficiency of polyaniline suspensions. Eur. Polymer J. 39 (2003) 641–645.
[43] P.A. Basnayaka, M.K. Ram, L. Stefanakos, A. Kumar, High performance graphene poly(o-anisidine) nanocomposite for supercapacitor applicationsMater. Chem. Phys. 141 (2013) 263-271.
[44] W.L. Zhang, H.J. Choi, Fabrication and electrorheology of graphene oxide/ionic N-substituted copolyaniline composite, Colloid Polym. Sci. 291, (2013) 1401–1408.
[45] N.H.Na. Azman, H.N. Lim, Y. Sulaiman, Effect of electropolymerization potential on the preparation of PEDOT/ graphene oxide hybrid material for supercapacitor application, Electrochimica. Acta. 188 (2016) 785–792.
[46] W.H. Jang, J.W. Kim, H.J. Choi, M.S. Jhon, Synthesis and electrorheology of camphorsulfonic acid doped polyaniline suspensions, Colloid Polym. Sci. 279 (2001) 823-827.
[47] S.M. Stenicka, V. Pavlinek, P. Saha, N. Blinova, J. Stejskal, O. Quadrat, The electrorheological efficiency of polyaniline particles with various conductivities suspended in silicone oil, Colloid Polym. Sci. 287 (2009) 403-412.
[48] W.L. Zhang, S.H. Piao, H.J. Choi, J. Facile and fast synthesis of polyaniline-coated poly(glycidyl methacrylate) core–shell microspheres and their electro-responsive characteristics, Colloid Interface Sci. 402 (2013) 100-106.
[49] T.C. Halsey, J.E. Martin, D. Adolf, Rheology of electrorheological fluids. Physical Review Letters, 68 (1992) 1519-1522.
[50] J.B. Yin, X.P. Zhao, L.Q. Xiang, X. Xia, Z.S. Zhang, Enhanced electrorheology of suspensions containing sea-urchin-like hierarchical Cr-doped titania particles. Soft Matter, 5 (2009) 4687-4697.
[51] Y.D. Liu, X.M. Quan, B.R. Hwang, Y.K. Kwon, H.J. Choi, Core–shell-structured monodisperse copolymer/silica particle suspension andits electrorheological response. Langmuir, 30 (2014) 1729–1734.
[52] W.L. Zhang, S.D. Kim, H.J. Choi, Effect of Graphene Oxide on Carbonyl-Iron-Based Magnetorheological Fluid, IEEE T. MAGN. 50 (2014) 2500804 (4pp).

Available online at www.sciencedirect.com

ScienceDirect

Procedia Engineering 00 (2017) 000–000

Procedia Engineering

www.elsevier.com/locate/procedia

Sustainable Civil Engineering Structures and Construction Materials, SCESCM 2016

Effects of temperature and moisture on concrete-PCM interface performance

Ueda Tamon[a], Khuram Rashid[b], Qian Ye[c], Zhang Dawei[d,*]

[a]*Division of Engineering and Policy for Sustainable Environment, Hokkaido University, Kita 13, Nishi 8, Kita-ku, Sapporo 060-8628, Japan*
[b]*Department of Architectural Engineering & Design, University of Engineering & Technology, Lahore-54890, Pakistan*
[c]*Department of Civil Engineering and Engineering Mechanics, Columbia University, New York, NY, 10027, USA*
[d]*College Civil Engineering and Architecture, Zhejiang University, 866 Yuhangtang Road, Hangzhou 310058, China*

Abstract

There is a lack of study on effects of temperature and moisture on concrete-polymer cementitious mortar (PCM) interface mechanical properties. This paper briefly introduces the outcomes of two studies; one on effects of exposure with elevated temperature and moisture and the other with freezing and thawing temperature cycles and moisture. The former show that there are significant effects of elevated temperature on both tensile and shear bond strength and that there are small effects of moisture. The bond strength can be estimated by the proposed formula with a function of constituent material strengths after the exposure. On the other hand, the latter show that the tensile bond strength decreases with freeze thaw cycles (FTC), although PCM does not show the reduction with FTC. It is considered that the tensile bond strength reduction is caused by moisture effects on the interface.

Peer-review under responsibility of the organizing committee of SCESCM 2016.

Keywords: Concrete; PCM; interface; bond strength; temperature effect; moisture effect

1. Introduction

Cementitious materials for patching/overlaying of existing concrete structures have been widely used in the world. Generally, materials for patching/overlaying are required to be more durable and have better mechanical property than concrete substrate because of objectives of patching/overlaying. Besides, the thickness of materials is

* Corresponding author. Tel.: +81-11-706-6218; fax: +81-11-707-6582.
E-mail address: ueda@eng.hokudai.ac.jp

Peer-review under responsibility of the organizing committee of SCESCM 2016.

usually thin, meaning that better property of shielding external substances is required. Polymer cementitious mortar (PCM or polymer modified cementitious mortar) is commonly adopted for patching/overlaying due to its good properties. At the same time PCM has some drawbacks. Polymer is known as temperature sensitive material and moisture effects are known to deteriorate polymer's property. Despite those facts there are lack of studies on effects of temperature and moisture on PCM property, especially on concrete-PCM interface property. This paper presents briefly the experimental outcomes on effects of temperature and moisture exposure conditions on concrete-PCM interface properties with several types of PCM commercially used now.

2. Effects of temperature and moisture on interface between concrete and various PCM

2.1. Results of various exposure conditions with elevated temperature and moisture

Effects of temperature on PCM are generally known, however, precise information of each PCM available in actual market is quite limited. Almost no information is available for temperature and moisture effects on interface property between PCM and concrete. Therefore, experimental investigation on PCM and concrete-PCM interface properties under temperature and moisture exposure conditions using 4 different PCM commercially available in Japan and China was conducted. The results show that general tendency for the effects of temperature and moisture on bonding properties is the same among those different PCM cases as shown below.

In order to see tendency of temperature effects on interface property, tension bond tests were conducted using concrete-PCM composite prism specimens with the 1st type of PCM (see Fig. 1) [1]. Test results are shown in Fig. 2. The exposure to 60 ℃ in air reduces tensile bond strength by 30% after 1 day but does not reduce further till 30 days. The tensile bond strength measured at 20 ℃ after 60 ℃ exposure is increased from the strength tested as 60 ℃ but not fully recovered. Some strength increase takes place after 30 days due to further hydration of PCM. Adopted temperature cyclic conditions were TC1 which consists of 60 ℃ in air for 12 hours and 30 ℃ in air for 12 hours and TC2 which consists of 24 hours of 60 ℃ in air, 24 hours of 20 ℃ in water, 24 hours of 0 ℃ in air and 24 hours of 25 ℃ in air. TC1 represents a climatic change for one day, while TC2 represents a climatic change for one year. 30 and 10 cycles were applied for TC1 and TC2 respectively. The reduction in tensile bond strength is more than that under constant 60 ℃ exposure.

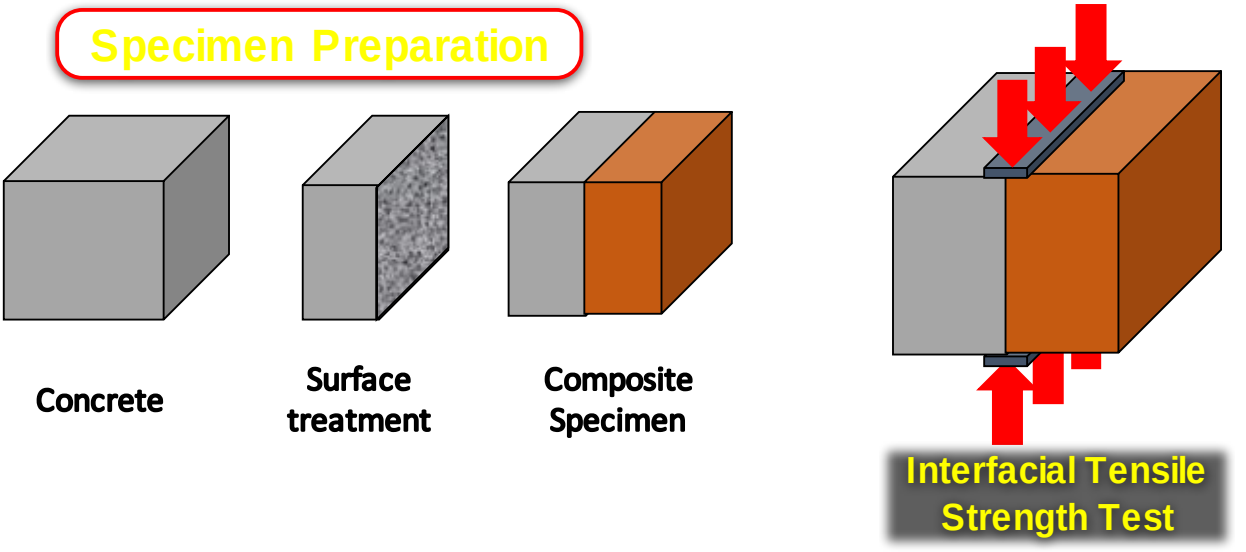

Fig. 1. Interfacial tensile strength specimen and loading condition.

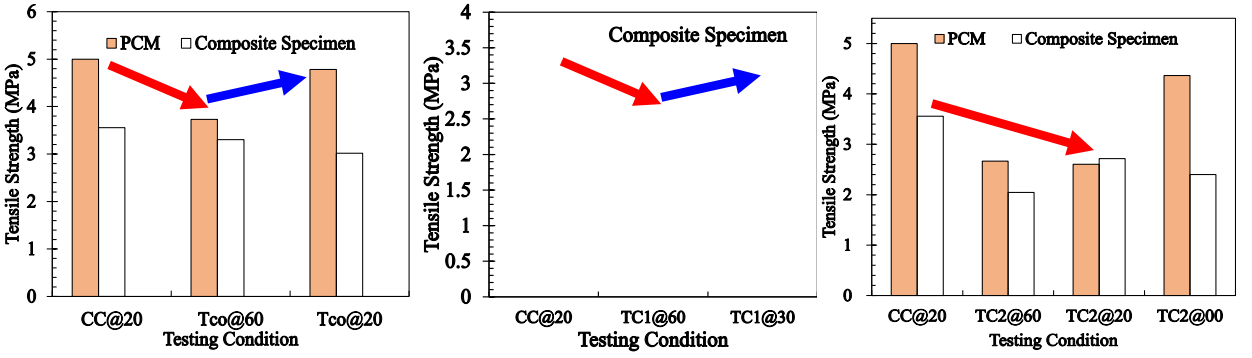

Fig. 2. Interfacial and PCM tensile strength under various temperature conditions.

The 2nd and 3rd types of PCM were used to examine combined effects of temperature and moisture on concrete-PCM interface strength. Figure 3 shows experimental outline. Tensile bond strength at concrete-PCM interface is less than tensile strength of PCM and concrete under any testing condition (see Fig. 4). However, bond strength reduction in % due to temperature increase from 20 ℃ to 60 ℃ is smaller than that of PCM. The effects of temperature on tensile bond strength are almost same between wet and dry conditions. Effects of moisture on tensile bond strength are hardly seen under wet/dry cycles and continuous immersion at 20 ℃.

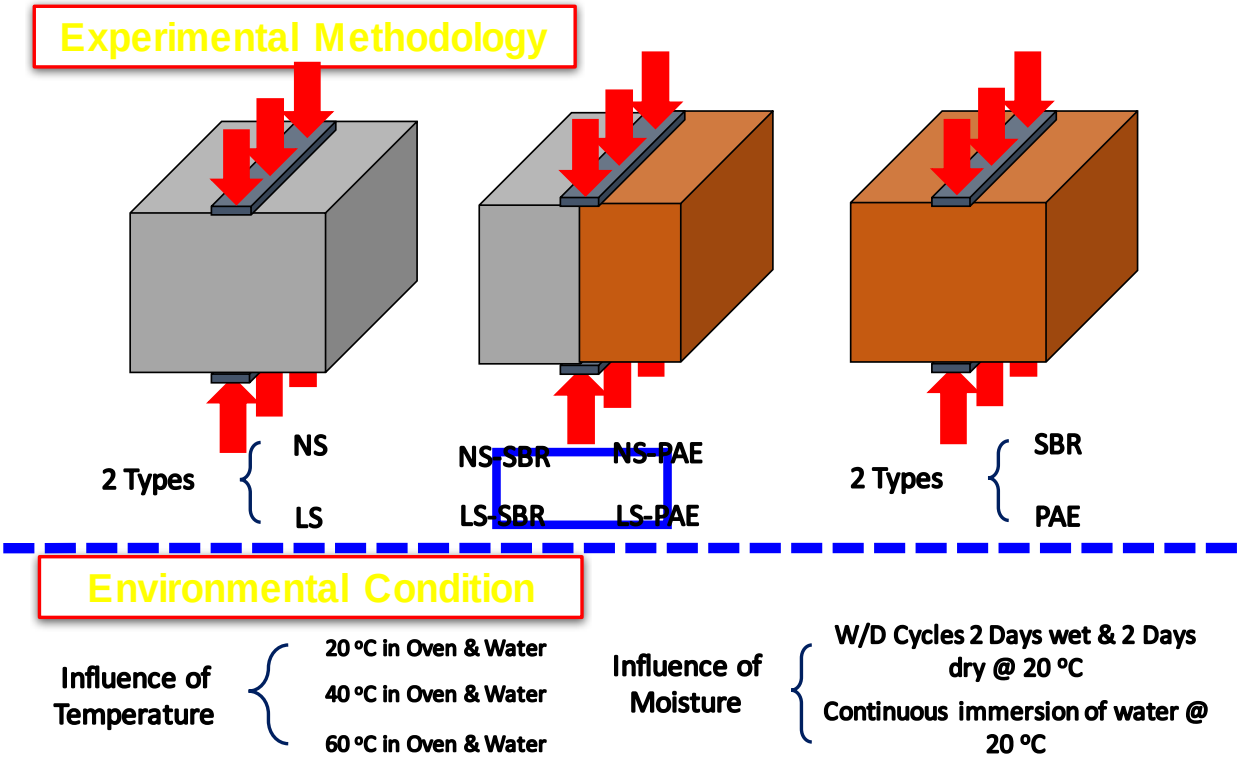

Fig. 3. Experimental outline for combined effects of temperature and moisture.

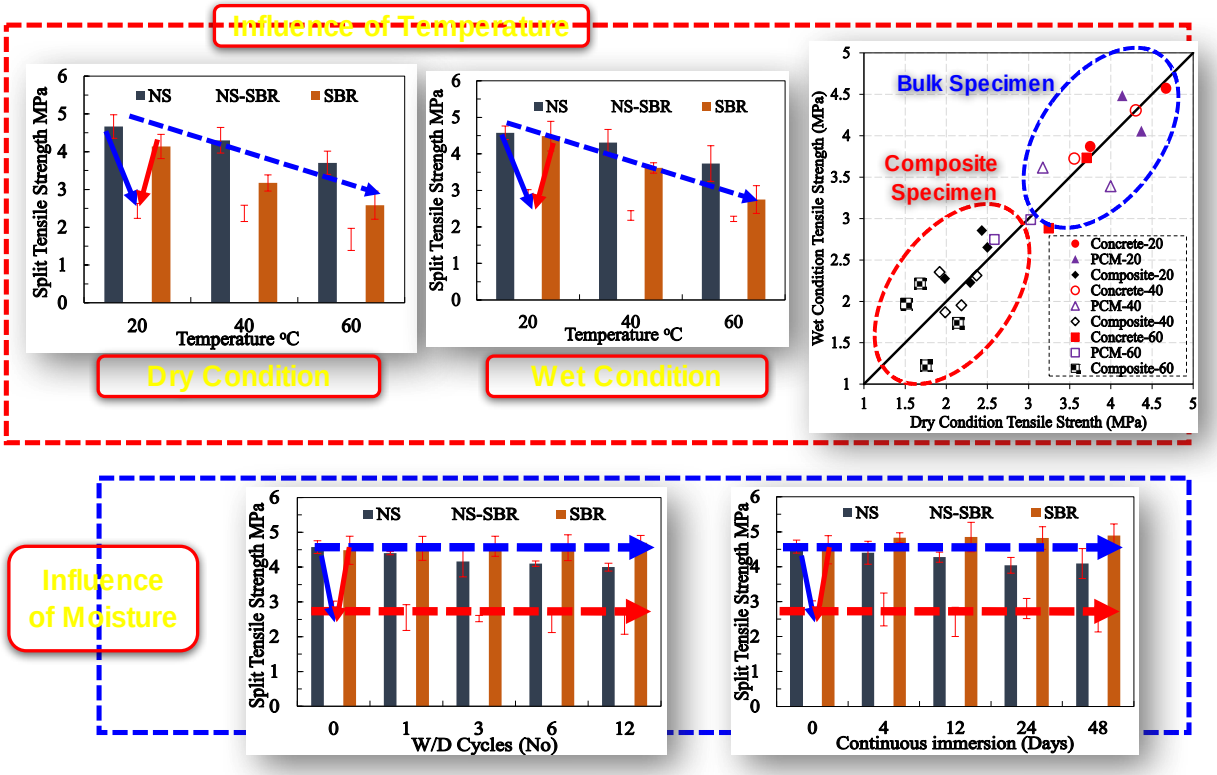

Fig. 4. Experimental results under combined effects of temperature and moisture.

The interfacial bond tests of 4th type of PCM, which was used for investigation of structural performances of beams strengthened by PCM overlaying, was conducted (see Fig. 5). There were two cases of surface treatments with and without primer. Tensile strength of the PCM is larger than the other three types of PCM and interfacial roughness is apparently higher than those for the other concrete-PCM composite specimens. Those facts are considered to be the reason why tensile bond strength is higher than those in the other concrete-PCM composite specimens. Not only tensile bond strength but also shear bond strength decreases with increase in temperature (see Fig. 6). Considering the observed relationship between strengths of constituent materials (PCM and concrete) and bond strength at their interface, the following Eqs. (1) and (4) can be proposed to estimate tensile and shear bond strength:

$$\frac{1}{f_{ITS}} = \frac{A_t}{f_{t.pcm}} + \frac{B_t}{f_{t.conc}} \tag{1}$$

where

f_{ITS} : Tensile bond strength at concerned temperature (MPa)

$f_{t,pcm}$: Tensile strength of PCM at concerned temperature (MPa)

$$= 1.2 f_{to.pcm} exp(-0.0095T) \tag{2}$$

$f_{t,conc}$: Tensile strength of concrete at concerned temperature (MPa)

$$= 1.07 f_{to,conc} exp(-0.004T) \tag{3}$$

$f_{to,pcm}$: Tensile strength of PCM after 28 days standard curing condition (MPa)
$f_{to,conc}$: Tensile strength of concrete after 28 days standard curing condition (MPa)
T : Temperature (20 ℃ < T < 60 ℃)
A_t, B_t : Experimental coefficients in tension

$$\frac{1}{\tau_{ISS}} = \frac{A_v}{\tau_{v.pcm}} + \frac{B_v}{\tau_{v.conc}} \tag{4}$$

τ_{ISS} : Shear bond strength at concerned temperature (MPa)
$\tau_{v.pcm}$: Shear strength of PCM at concerned temperature (MPa)

$$= 2\tau_{vo.pcm} exp(-0.03T) \tag{5}$$

$\tau_{v.conc}$: Shear strength of concrete at concerned temperature (MPa)

$$= 0.99\tau_{vo,conc} exp(0.0015T) \tag{6}$$

$\tau_{vo.pcm}$: Shear strength of PCM after 28 days standard curing condition (MPa)
$\tau_{vo.conc}$: Shear strength of concrete after 28 days standard curing condition (MPa)
T : Temperature (20 ℃ < T < 60 ℃)
A_v, B_v : Experimental coefficients in shear

Figure 7 shows the comparison of predicted bond strength and experimental strength for the 2nd, 3rd and 4th types of PCM. Good agreement can be seen for both cases with and without primer (–WP and –NP).

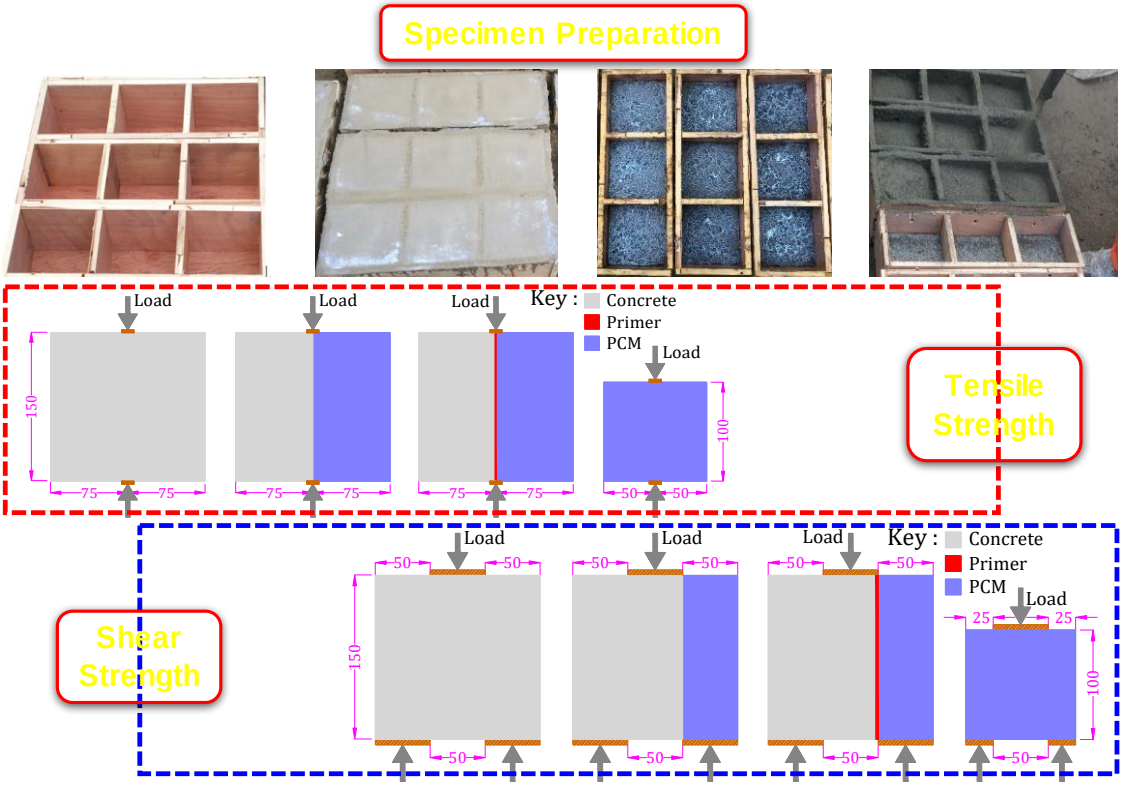

Fig. 5. Experimental outline for bond tests of interface in beam strengthened by PCM overlaying.

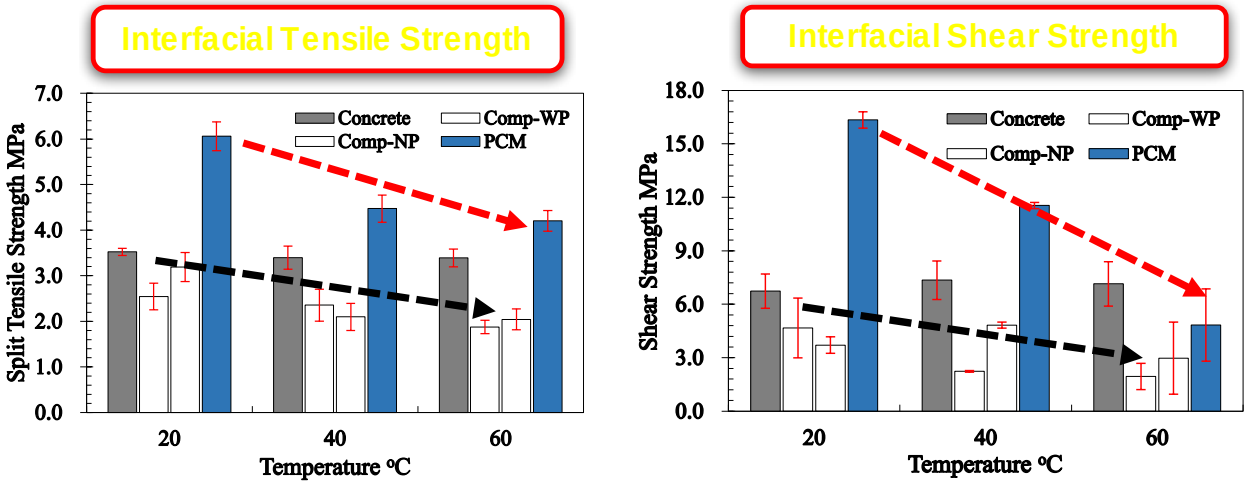

Fig. 6. Effects of temperature on both tensile and shear bond strength.

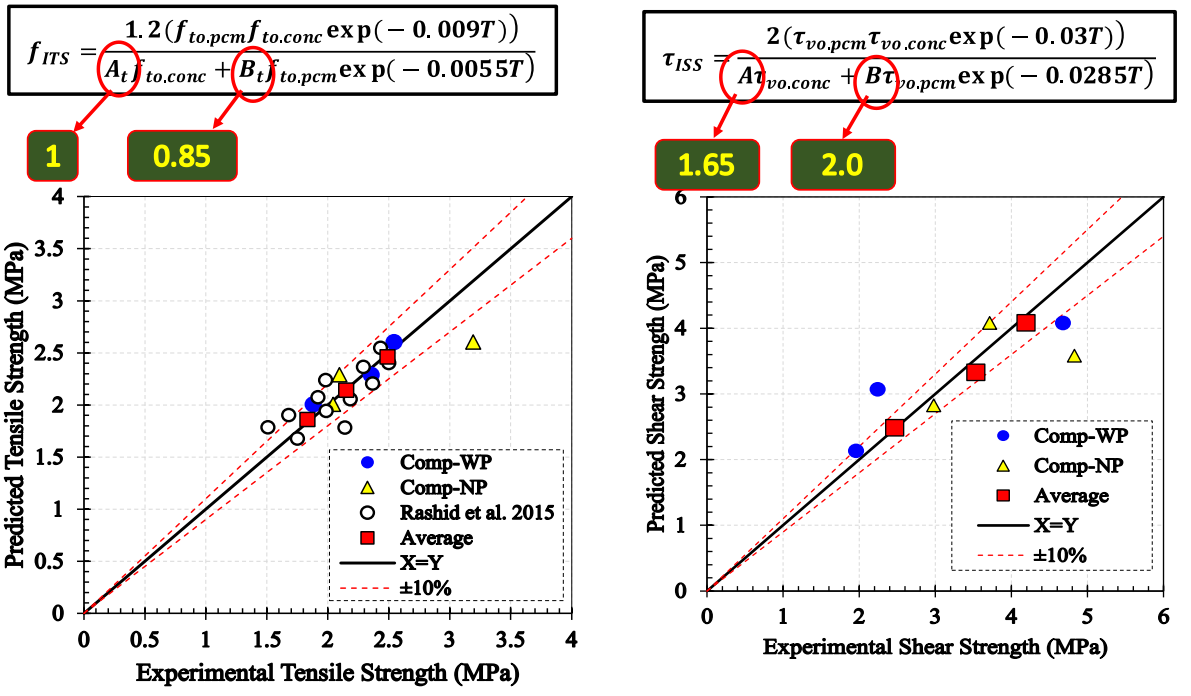

Fig. 7. Comparison between predicted and experimental tensile and shear bond strengths.

2.2. Results of exposure conditions with freeze thaw cycles and moisture

Actual climatic conditions are not only elevated temperature but also freezing temperature. Generally, polymer does not have melting point and glass transition temperature below freezing point. Freeze thaw cycles with wet condition causes frost damage in concrete and wet condition may cause degradation in polymer property. Considering those facts, 5th type of PCM was experimentally examined for mechanical properties of its own and

interface with concrete under freeze thaw cycles. For comparison, mortar with Portland cement (ordinary mortar) was also examined. The results show significant difference in the tensile bond strength (or splitting tensile strength at interface obtained as in Fig. 1) as shown below [2].

Ordinary mortar with and without air-entraining agent (MA and MX) were used for the comparison with PCM as repairing material. There were two types of substrate concrete with normal and high strength (N/NA and HA). Figure 8 shows the splitting tensile strength of concrete-ordinary mortar composite together with that of constituent materials. The ordinary mortar is with air-entraining agent (MA). It is clearly shown that the strength at interface is weaker than those of constituent materials. Although the strength reduction with freeze thaw cycles (FTC) is found for normal strength substrate concrete without air entraining agent (N), the interface strength (N-MA) did not show the strength reduction. Once the strength of constituent material (N) became less due to FTC than that of composite interface, the failure mode changed from the interface adhesive failure to the cohesion failure of the constituent material and the splitting strength of the composite showed some reduction (see Fig. 8 (c)). When the constituent material with air-entraining agent (NA, HA and MA), there is no strength reduction with FTC, thus no strength reduction of composite interface. The experimental results of concrete-ordinary mortar without air-entraining agent (MX) composite are shown in Fig. 9. The weakest strength was found with the concrete-mortar composite. The splitting strength of MX and composite were reduced with FTC. Although the substrate concrete does not show the strength reduction, the composite interface shows the strength reduction with FTC due to the strength reduction of the mortar (MX) with FTC.

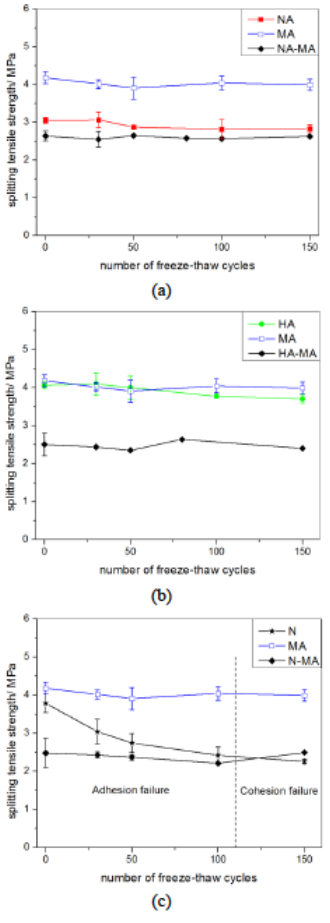

Fig. 8. Splitting tensile strength of composite specimens (concrete-ordinary mortar with air-entraining agent) and those of constituent materials

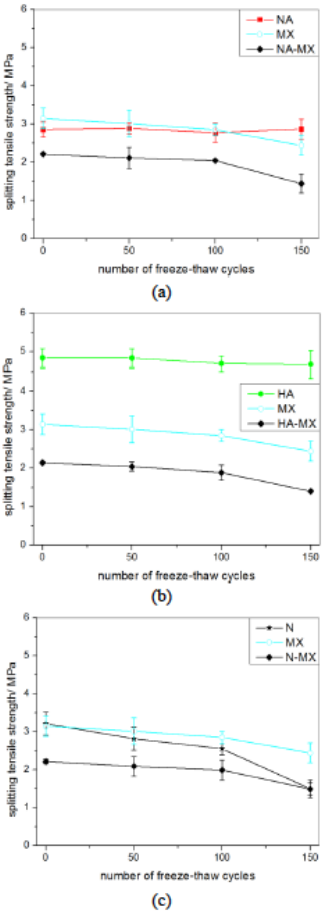

Fig. 9. Splitting tensile strength of composite specimens (concrete-ordinary mortar without air-entraining agent) and those of constituent materials

In the case of PCM the experimental results were different from the cases of ordinary mortar. It can be seen in Fig. 10 that the weakest strength is with the composite interface, and that PCM did not show the strength reduction with FTC. However, the composite interface strength always showed the strength reduction with FTC no matter how the constituent materials, including PCM itself, show the strength performance under FTC. The reason of this strength reduction was considered that there was the moisture effect on concrete-PCM interface. The moisture penetrated gradually from the edge of interface, which was not sealed, causing the bonding deterioration, which causes further moisture penetration, causing further deterioration. Some past studies also show the material degradation of PCM due to moisture. In the experiment the material deterioration was only found at interface and external surface of PCM as shown in Fig. 11.

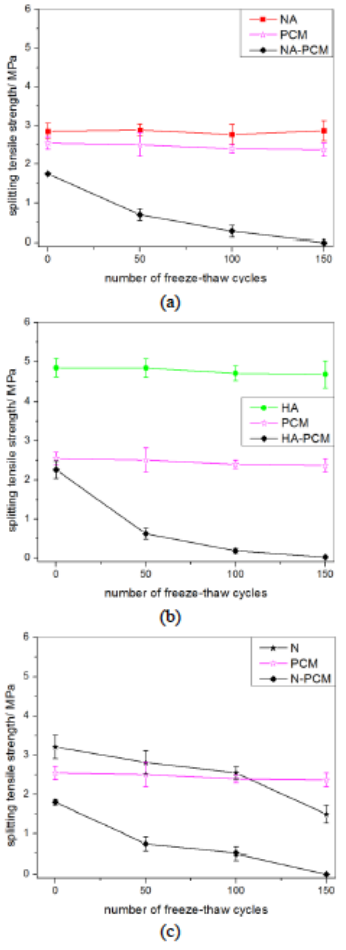

Fig. 10. Splitting tensile strength of composite specimens (concrete-PCM) and those of constituent materials

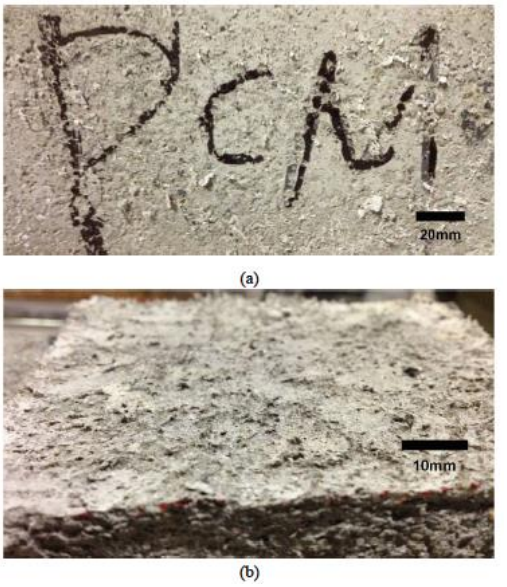

Fig. 11. PCM surface deterioration (flakes dropping) after FTC: (a) External surface, (b) Interface

3. Concluding remarks

The results of experimental investigations on effects of concrete-PCM interface performance with various PCM (1st, 2nd, 3rd, 4th and 5th type of PCM) can be concluded as follows:

3.1. Results of various exposure conditions with elevated temperature and moisture

The experimentation was conducted with four types of PCM (1st, 2nd, 3rd and 4th type of PCM). Tensile/shear bond strength of concrete-PCM interface is affected significantly by elevated temperature but less by moisture. The tensile/shear bond strength is less than tensile/shear strength of constituent materials (PCM and concrete). The reduction in tensile/shear bond strength depends on the reduction in tensile/shear strengths of PCM and concrete and then estimated by proposed equation which is a function of PCM and concrete strength.

3.2. Results of exposure conditions with freeze thaw cycles and moisture

The experiment was conducted with one type of PCM (5th type of PCM) and ordinary cement mortar. Tensile bond strength (splitting tensile strength at interface) does not decrease with freeze thaw cycles (FTC) when ordinary mortar as repairing material shows no reduction with FTC. However, it does show the reduction when ordinary mortar shows reduction. Tensile bond strength of concrete-PCM does show the strength reduction with FTC, even though PCM does not show any reduction with FTC. This reduction is observed for both cases of substrate concrete showing the reduction in its splitting strength with FTC and no reduction.

3.3. Recommendation of further study

Effects of moisture on concrete-PCM interface performance are different between elevated temperature and freezing thawing temperature cycles. Effects may be different when different PCM is applied, meaning that further study is necessary for collection of more data with various PCM. Although the case with elevated temperature does not show significant effects of moisture, further study is necessary by conducting more cycles of wet and dry.

Acknowledgements

The authors are grateful to the Grant-in-Aid for Scientific Research (A) of Japan Society of Promotion of Science (No. 26249064), the Natural Science Foundation of China (Grant Nos. 51308494) and NEXCO Group Companies' Support Fund to Disaster Prevention Measures on Expressways as the financial supports to the studies in section 2.1. The authors are also grateful to the Research and Development Grant of Japan Institute of Construction Engineering (JICE), the Express Highway Research Foundation of Japan and the open fund of state key laboratory of coastal and offshore engineering of Dalian University of Technology (LP1406) for funding the study in section 2.2.

References

[1] K. Rashid, T. Ueda, D. Zhang, K. Miyaguchi and H. Nakai, Experimental and analytical investigations on the behavior of interface between concrete and polymer cement mortar under hygrothermal conditions, Construction and Building Materials, 94 (2015) 414-425.

[2] Y. Qian, D. Zhang, T. Ueda, Interfacial tensile bond between substrate concrete and repairing mortar under freeze-thaw cycles, J. Advanced Concrete Technology, 2016 (to be printed).